



THE UNIVERSITY *of* EDINBURGH

Edinburgh Research Explorer

Small understorey trees have greater capacity than canopy trees to adjust hydraulic traits following prolonged experimental drought in a tropical forest

Citation for published version:

Giles, AL, Rowland, L, Bittencourt, PRL, Bartholomew, DC, Coughlin, I, Costa, PB, Domingues, T, Miatto, RC, Barros, FV, Ferreira, LV, Groenendijk, P, Oliveira, AAR, Da Costa, ACL, Meir, P, Mencuccini, M, Oliveira, RS & Oren, R (ed.) 2021, 'Small understorey trees have greater capacity than canopy trees to adjust hydraulic traits following prolonged experimental drought in a tropical forest', *Tree physiology*, vol. 42, no. 3, pp. 537-556. <https://doi.org/10.1093/treephys/tpab121>

Digital Object Identifier (DOI):

[10.1093/treephys/tpab121](https://doi.org/10.1093/treephys/tpab121)

Link:

[Link to publication record in Edinburgh Research Explorer](#)

Document Version:

Peer reviewed version

Published In:

Tree physiology

General rights

Copyright for the publications made accessible via the Edinburgh Research Explorer is retained by the author(s) and / or other copyright owners and it is a condition of accessing these publications that users recognise and abide by the legal requirements associated with these rights.

Take down policy

The University of Edinburgh has made every reasonable effort to ensure that Edinburgh Research Explorer content complies with UK legislation. If you believe that the public display of this file breaches copyright please contact openaccess@ed.ac.uk providing details, and we will remove access to the work immediately and investigate your claim.



Small understorey trees have greater capacity than canopy trees to adjust hydraulic traits following prolonged experimental drought in a tropical forest

Journal:	<i>Tree Physiology</i>
Manuscript ID	TP-2021-150.R1
Manuscript Type:	Research Paper
Date Submitted by the Author:	n/a
Complete List of Authors:	Giles, André; UNICAMP, Plant biology Rowland, Lucy; University of Exeter Bittencourt, Paulo Bartholomew, David Coughlin, Sarah Costa, Patricia Domingues, Tomas; Universidade de São Paulo, Departamento de Biologia; University of São Paulo Miatto, Raquel Barros, Fernanda Ferreira, Leandro Groenendijk, Peter; Plant Biology Oliveira, Alex da Costa, Antonio; Universidade Federal do Para Meir, Patrick; Australian National University Research School of Biology, Biology; University of Edinburgh School of GeoSciences, School of Geosciences Mencuccini, Maurizio; CREAM; ICREA Oliveira, Rafael; Universidade Estadual de Campinas, Departamento de Biologia Vegetal
Keywords:	Tropical Rainforest, Forest Ecophysiology, Drought, hydraulic safety, Global Climate Change, Hydraulic

1
2
3 **1 Small understorey trees have greater capacity than canopy trees to adjust hydraulic**
4 **2 traits following prolonged experimental drought in a tropical forest**

5
6 **3 Running title:** Tree size strongly controls plant hydraulic responses in a droughted tropical
7 forest
8

9 **5 Giles, A. L.^{1*}, Rowland L.², Bittencourt P. R. L.², Bartholomew, D. C.², Coughlin I.^{4,5}, Costa**
10 **6 P. B.^{1,7}, Domingues T.⁴, Miatto, R.C.⁴, Barros, F. V.², Ferreira L. V.⁶, Groenendijk, P.¹, Oliveira**
11 **7 A. A. R.⁶, da Costa A. C. L.^{6,7}, Meir P.^{5,9}, Mencuccini M.^{10,11}, Oliveira R. S.¹**
12
13
14
15
16
17
18

19 **9 *Corresponding Author:** andregiles.bio@gmail.com, ¹Instituto de Biologia, University of
20 Campinas (UNICAMP), Campinas, SP 13083-970, Brasil.
21
22
23

24
25 ¹Instituto de Biologia, University of Campinas (UNICAMP), Campinas, SP 13083-970, Brasil.

26 ²College of Life and Environmental Sciences, University of Exeter, Exeter, EX4 4RJ, UK

27 ³Biological Sciences, UWA, Perth, WA, Crawley 6009, Australia

28 ⁴Departamento de Biologia, FFCLRP, Universidade de São Paulo, Ribeirão Preto, SP 14040-
29 900, Brasil

30 ⁵Research School of Biology, Australian National University, Canberra, ACT 2601 Australia

31 ⁶Museu Paraense Emílio Goeldi, Belém, PA 66040-170, Brasil

32 ⁷ Biological Sciences, UWA, Perth, WA, Australia

33 ⁸Instituto de Geosciências, Universidade Federal do Pará, Belém, PA 66075-110, Brasil

34 ⁹School of GeoSciences, University of Edinburgh, Edinburgh, EH9 3FF, UK

35 ¹⁰CREAF, Campus UAB, Cerdanyola del Vallés, 08193 Spain

36 ¹¹ICREA, Barcelona, 08010, Spain
37
38
39
40
41
42
43
44
45
46
47
48
49
50
51
52
53
54
55
56
57
58
59
60

1
2
3 **Abstract**
4

5
6 27 Future climate change predictions for tropical forests highlight increased frequency and
7
8 28 intensity of extreme drought events. However, it remains unclear whether large and small
9
10 29 trees have differential strategies to tolerate drought due to the different niches they
11
12 30 occupy. The future of tropical forests is ultimately dependent on the capacity of small
13
14 31 trees (<10 cm in diameter) to adjust their hydraulic system to tolerate drought. To address
15
16 32 this question, we evaluated whether the drought tolerance of neotropical small trees can
17
18 33 adjust to experimental water stress and was different from tall trees. We measured
19
20 34 multiple drought resistance-related hydraulic traits across nine common neotropical
21
22 35 genera at the world's longest-running tropical forest throughfall-exclusion experiment and
23
24 36 compared their responses with surviving large canopy trees. Small understorey trees in
25
26 37 both the Control and the throughfall exclusion treatment (TFE) had lower minimum
27
28 38 stomatal conductance and maximum hydraulic leaf-specific conductivity relative to large
29
30 39 trees of the same genera, as well as greater hydraulic safety margin (HSM), percentage
31
32 40 loss of conductivity (PLC) and embolism resistance, demonstrating they occupy a distinct
33
34 41 hydraulic niche. Surprisingly, in response to the drought treatment, small trees increased
35
36 42 specific hydraulic conductivity by 56.3% and leaf:sapwood area ratio by 45.6%. The
37
38 43 greater HSM of small understorey trees relative to large canopy trees likely enabled them
39
40 44 to adjust other aspects of their hydraulic systems to increase hydraulic conductivity and
41
42 45 take advantage of increases in light availability in the understorey resulting from the
43
44 46 drought-induced mortality of canopy trees. Our results demonstrate that differences in
45
46 47 hydraulic strategies between small understorey and large canopy trees drive hydraulic
47
48 48 niche segregation. Small understorey trees can adjust their hydraulic systems in response
49
50 49 to changes in water and light availability indicating natural regeneration of tropical forests
51
52 50 following long-term drought may be possible.

51
52 **Key-words:** Long-term drought; Understorey trees; Hydraulic Safety margin; P50;
53
54 53 Maximum conductivity; Acclimation; Amazon forest.

55
56
57
58
59
60

59 Introduction

60 [Climate change](#) predictions for tropical forests comprise increased frequency and intensity
61 of extreme drought events (Aragão et al., 2018; Brodribb, Powers, Cochard, & Choat,
62 2020) and long-term reductions in soil moisture availability (Corlett 2016, Christensen et
63 al. 2017). Most studies relating to drought focus on the impacts on large trees that
64 comprise the highest proportion of forest biomass (Meir et al. 2015, Rowland, da Costa, et
65 al. 2015), often finding the effect of drought stress on a plant's hydraulic system is a key
66 driver of tree mortality (Bittencourt et al., 2020; Brodribb et al., 2020; Rowland et al.,
67 2015). However, small understorey [trees not only are responsible for up to 20% of the](#)
68 [forest carbon sink](#) (Hubau et al. 2019) [but have a fundamental role in recruitment and the](#)
69 [maintenance of tree populations](#), as they will effectively compose the future pool of large
70 tree in the forest. Thus, small trees may be critical in determining long-term drought
71 responses if there is extensive loss of large canopy trees (Rowland, da Costa, et al. 2015,
72 Esquivel-Muelbert et al. 2017).

73 Large trees occupy canopy positions (hereafter, large trees) with high light levels and high
74 vapor pressure deficit. In contrast, [small trees from the same genus](#) occupy understory
75 positions (hereafter small trees), grow slowly, generally in shaded conditions and
76 experience a lower atmospheric vapor pressure deficit (Sterck et al. 2011). The distinct
77 resource partitioning between small and large trees, (Brum et al., 2019; Poorter, Bongers,
78 Sterck, & Wöll, 2005) could cause strong differences in their water supply and demand
79 relative to large trees. Reduced water supply from the roots, alongside lower capacitance,
80 is likely to cause more negative water potentials in small trees relative to larger ones,
81 during periods of low soil moisture (Salomón et al. 2017). Large trees are more likely to

1
2
3 82 buffer periods of water deficit with greater water access by deep roots (Brum et al. 2019),
4
5 83 higher capacitance (Mcculloh et al. 2014), and elevated carbohydrate storage that allow
6
7
8 84 to maintain either [prolonged stomatal opening \(deep roots\)](#) or [prolonged stomatal closure](#)
9
10 85 [\(greater storage\)](#) (McDowell et al., 2008). These potential size-dependent variations in
11
12
13 86 structural and physiological traits suggest tree size potentially influences a tree's capacity
14
15
16 87 to acclimate in response to severe drought stress.

17
18 88 Several key traits of the hydraulic system of a plant are essential in determining the
19
20
21 89 capacity of a tree to survive prolonged drought stress. These traits are often related to
22
23 90 [preventing hydraulic failure, via emboli formation, in the xylem vessels](#) (Sperry and Tyree
24
25 91 1988), [which can lead to severe decreases in leaf water supply, photosynthesis and other](#)
26
27 92 [physiological functions](#) (Sperry et al. 2002, McDowell et al. 2008, Martinez-Vilalta et al.
28
29 93 2019). These key traits include the water potentials at which the xylem lose 50% or 88% of
30
31 94 their conductance (P50 or P88, respectively) and the hydraulic safety margin (HSM)
32
33 95 (Meinzer et al. 2009), i.e., the difference between the minimum leaf water potential that is
34
35 96 naturally experienced and P50, effectively a metric of the risk of a plant crossing a critical
36
37 97 hydraulic threshold. Following sustained periods of drought stress, a tree's capacity to
38
39 98 survive is likely to be related to its capacity to acclimate certain key drought tolerance
40
41 99 traits or to limit its demand for water, via traits such as minimum stomatal conductance,
42
43 100 thus reducing stress on its hydraulic system (Sala et al. 2010, Meir et al. 2018). Existing
44
45 101 studies on large trees show limited capacity for tropical trees to adjust plant hydraulic
46
47 102 traits in response to drought stress (Binks et al., 2016; Bittencourt et al., 2020; Powell et
48
49 103 al., 2017; Schuldt et al., 2011). Some studies have shown that the risk of embolism can be
50
51 104 reduced by increasing HSMs under drought conditions (Awad et al. 2010, Tomasella et al.
52
53 105 2018, Prendin et al. 2018). However, in a tropical forest drought experiment, large trees

1
2
3 106 were found to have limited plasticity in leaf level anatomy (Binks et al., 2016) and no
4
5 107 capacity to acclimate their hydraulic systems, especially in traits relating to embolism
6
7
8 108 resistance (Bittencourt et al., 2020; Powell et al., 2017; Rowland et al., 2015). Yet, to our
9
10 109 knowledge, no studies have evaluated whether small trees (<10 cm diameter at breast
11
12 110 height, DBH), contrary to adult trees, have the capacity to adjust their hydraulic system to
13
14 111 prolonged drought stress. Following high mortality losses in large, more drought-
15
16 112 intolerant, trees, small trees can increase photosynthetic capacity (Bartholomew et al.,
17
18 113 2020;) and lower canopy trees can increase growth rates, even following drought (Brando
19
20 114 et al., 2008; Rowland et al., 2015). This suggests that small trees can increase performance
21
22 115 in response to elevated light, despite drier conditions. Increased light availability would
23
24 116 also require these small trees to the increased atmospheric water demand, implying the
25
26 117 need to increase water supply from their hydraulic system and/or to sustain a lower xylem
27
28 118 water potential. However, these adjustments to conditions of severe drought only seem
29
30 119 to be possible if small trees have a greater drought tolerance, functioning with higher
31
32 120 levels of embolism resistance and hydraulic safety margin (HSM). Consequently,
33
34 121 consideration of ecosystem changes, such as canopy loss and shifting light availability, is
35
36 122 likely to be as important as the consideration of the direct impact of soil moisture stress
37
38 123 following long-term drought, as both factors may influence hydraulic acclimation within
39
40 124 small trees.

41
42 125 Here we take advantage of a unique drought experiment located in northeast Amazonia
43
44 126 (Meir et al. 2015, 2018) to evaluate the response of small trees to combined changes in
45
46 127 water and light availability. Previous research at this site has shown that large trees (>40
47
48 128 cm DBH) had significantly higher mortality rates, when compared to small trees and to
49
50 129 trees in adjacent control forest, leading to a 40% reduction in biomass following 14 years

1
2
3 130 of experimentally-imposed soil drought (da Costa et al., 2010; Rowland et al., 2015, Meir
4
5 131 et al. 2018). This biomass loss was almost entirely from trees reaching the upper canopy,
6
7 132 which led to increased levels of light in the understory and increased growth rates of small
8
9 133 understory trees in the wet season (da Costa et al., 2014; Metcalfe, et al., 2010; Rowland
10
11 134 et al., 2015, Meir et al. 2018). Furthermore elevated radiation loads are likely to have
12
13 135 increased leaf vapour pressure deficit and temperature, increasing the atmospheric
14
15 136 drought effect these small trees experience (Mulkey & Pearcy 1992a; Kamaluddin & Grace
16
17 137 1992; Krause, Virgo & Winter 1995). Using new data from this soil drought experiment
18
19 138 (henceforth *throughfall-exclusion experiment* – TFE), we explore how small trees adjust
20
21 139 hydraulic traits in response to increases in light availability coupled with increased drought
22
23 140 stress, specifically, if small trees are able to adjust traits to novel light conditions whilst
24
25 141 under drought stress. Thus, we test whether small trees (1-10 cm DBH) alter their plant
26
27 142 hydraulic system in response to prolonged soil moisture stress and increased canopy
28
29 143 openness, and determine how these responses vary relative to those of large trees (>20
30
31 144 cm DBH). We address the following hypotheses:

32
33
34
35
36
37
38
39
40 145 1) Considering the same genus we hope that the hydraulic systems of small trees
41
42 146 adjust to the combined soil-drought and radiation-load conditions imposed in the TFE
43
44 147 relative to the Control. We expect small trees in TFE treatment to take advantage of the
45
46 148 increased canopy openness by increasing their water transport efficiency (greater
47
48 149 hydraulic specific conductivity and leaf-sapwood ratios). At the same time, we predict that
49
50 150 small trees will have more negative water potentials resulting from drought conditions
51
52 151 and the capacity to compensate this by adjusting hydraulic traits to maintain higher
53
54 152 hydraulic safety margins to meet the elevated canopy water demands in support of
55
56 153 photosynthesis.
57
58
59
60

1
2
3 154 2) Small trees have different hydraulic strategies from large trees. Specifically, we predict
4
5 155 that, independent of the drought and radiation responses in the TFE, small trees have
6
7
8 156 greater drought tolerance, higher xylem embolism resistance and larger hydraulic safety
9
10 157 margins, relative to large trees. We therefore predict that, as a consequence of those trait
11
12
13 158 differences, small trees occupy a different hydraulic trait space from large trees.
14
15
16
17
18
19
20
21
22
23
24
25
26
27
28
29
30
31
32
33
34
35
36
37
38
39
40
41
42
43
44
45
46
47
48
49
50
51
52
53
54
55
56
57
58
59
60

For Peer Review

1
2
3 **Methods**

4
5
6 *Site and plant material*

7
8
9 Our study site is a lowland tropical rainforest located in the Caxiuanã National
10
11 Forest, state of Pará, north-east Brazil (1°43'S, 51°27 W). It has an annual rainfall of 2000-
12
13 2500mm, with a dry season (< 120 mm monthly rainfall) from July to December. A
14
15 throughfall exclusion (TFE) experiment was established in 2002, where 50% of canopy
16
17 throughfall is excluded by a plastic panel structure installed at 1-2m height over a 1 ha
18
19 area (Meir et al. 2018). The TFE plot was studied alongside a 1 ha Control plot, where no
20
21 throughfall exclusion took place. The plots have been monitored continuously since 2001
22
23 and further information on the experimental set-up can be found in earlier papers (da
24
25 Costa et al., 2010; Fisher et al., 2007; Meir et al., 2015 and Rowland et al., 2015b).
26
27
28
29

30
31 From August-September 2017, during the peak of the dry season, we sampled 74
32
33 small trees with diameters ranging from 1 to 10 cm at breast height (1.3 m). We measured
34
35 41 small trees on the Control plot and 33 on the TFE, all taken from nine genera (20
36
37 species), replicated in each plot (two to five individuals per genera per plot). While we
38
39 tried to maintain the same range of tree heights within each genus between plots, small
40
41 trees had more variable height in the TFE, with light-exposed individuals reaching over 15
42
43 meters height, whilst no individuals in the Control reached 15 metres height (See Fig. S1).
44
45 It was not possible to know the age of each sampled individual, because (destructive)
46
47 sampling for age determination (tree-ring analyses; e.g., Brien et al., 2016) was not
48
49 possible. Consequently, we must assume that our sampled trees may have strongly
50
51 varying ages (Groenendijk et al. 2014). We thus test the influence of tree stature and
52
53
54
55
56
57
58
59
60

1
2
3 181 position within the forest strata (van der Sleen et al. 2015), while assuming that most of
4
5 182 our sampled trees are likely to be young.

6
7
8
9 183 For each individual, we collected two branches from the top of the crown,
10
11 184 representing the point maximally exposed to light. The branches were third to fourth
12
13 185 order (30-55 mm of diameter), counting from the tip. We collected one set of branches
14
15
16 186 before sunrise (0400 to 0600 hours) and used these to measure embolism resistance and
17
18 187 predawn leaf water potential. We collected a second set of branches at midday (1130 to
19
20
21 188 1330 hours) and used these to measure midday leaf water potential, native embolism,
22
23 189 leaf-to-sapwood area, xylem and leaf specific conductivity, minimum leaf conductance
24
25
26 190 and wood density measurements. Immediately after collection, branches were bagged in
27
28 191 thick black plastic sacks with moist paper to humidify internal air and minimise leaf
29
30
31 192 transpiration. Branches were transported 100m from the plots to measure leaf water
32
33 193 potential, and for the remaining measurements the branches were transported to a
34
35 194 laboratory ~1km walk away.

36
37
38
39 195 We measured predawn leaf water potential (Ψ_{pd}), taken to represent the time-
40
41 196 point when transpiration is at its minimum and the water potential of the plant is closest
42
43 197 to equilibrium with that of the soil. Ψ_{pd} can be considered an integrated metric of soil
44
45
46 198 water availability across the rooting depth (Bartlett et al. 2016). We also determined
47
48 199 midday water potential (Ψ_{md}), to capture the minimum Ψ of the plant in the dry season.
49
50
51 200 This measure is affected by any cuticular or stomatal transpiration and, thus, broadly
52
53 201 captures the integrated effects of plant traits and the environment water demand on the
54
55
56 202 minimum water potential a plant reaches in natural conditions. We also measured the
57
58 203 native dry-season percentage loss of conductivity (PLC). We used the difference between
59
60

1
2
3 204 the minimum leaf water potential (Ψ_{md}) and P_{50} , to calculate the branch hydraulic safety
4
5 205 margin (HSM). These two values (native PLC and HSM) were used as indicators of the
6
7
8 206 cumulative damage from embolism.
9

10 11 207 *Predawn and midday water potential* 12

13
14 208 Predawn and midday leaf water potentials were measured in the field immediately
15
16 209 after collection, using a pressure chamber (Model 1505, PMS). Branches collected for
17
18 210 predawn water potential measures were sampled before sunrise, and for midday water
19
20 211 potential, the sampling took place between 1130 to 1330 hours. For each tree we
21
22 212 measured water potential of two leaves, or three leaves if the first two measures differed
23
24 213 substantially (>0.5 MPa difference) from one another. Measurements from multiple leaves
25
26 214 were averaged to create a single value per tree. All water potential measurements were
27
28 215 taken on the same day for small trees and across three days for large trees.
29
30
31
32

33 34 216 *Wood density, leaf to sapwood area ratio and minimum stomatal conductance* 35

36
37 217 We measured wood density (W_D) on woody sections 40 to 80 mm long with a
38
39 218 diameter of 4 to 7 mm. We debarked samples, immersed them in water for 24 hours to
40
41 219 rehydrate and measured the saturated volume using the water displacement method
42
43 220 (Pérez-Harguindeguy *et al.*, 2013). We then oven dried the samples at 60°C until they
44
45 221 were a constant mass and measured their dry weight with a precision balance to 3
46
47 222 decimal places.
48
49
50

51
52
53 223 We determined the leaf to sapwood area ratio ($A_L:A_{SW}$), on all branches by
54
55 224 measuring leaf area and calculating sapwood area from two diameter measurements of
56
57 225 the debarked basal part of the branch using precision callipers at a standardised distance
58
59 226 from the tip. To avoid overestimation we checked the absence of pith area in all branches
60

1
2
3 227 per species before the measurement. We measured leaf area by scanning all leaves on the
4
5 228 branch and quantifying their area using Image J software (version 1.6.0_20; Schneider et
6
7 229 al., 2012). We calculated the leaf area to sapwood area ratio as total branch leaf area
8
9 230 divided by its basal sapwood area. All branches had a similar size and were standardised
10
11 231 by distance to the tip (~40-70 cm). The $A_L:A_{SW}$ is a key indicator of the balance between
12
13 232 transpirative demand and water supply capacity (Mencuccini et al. 2019).

14
15
16
17
18 233 For minimum leaf conductance (G_{min}), we used the leaf conductance to water
19
20 234 vapour measured on the abaxial surface of leaves kept 30 minutes in the dark, using an
21
22 235 infrared gas analyser (Li-COR 6400, US). All measured leaves were fully formed and
23
24 236 undamaged leaves. G_{min} is a measure key indicator of residual leaf water loss and likely a
25
26 237 due to a combination of leakage stomatal conductance from partially from leakage of
27
28 238 partially closed stomata and cuticular conductance (Duursma et al. 2019, Binks et al. 2020,
29
30 239 Márquez et al. 2021)., see Rowland *et al.* (2020) and Bartholomew et al. (2020), provide
31
32 240 further details on gas exchange measurement.

33 241 *Hydraulic efficiency and native embolism*

34
35
36
37
38
39 242 We used maximum hydraulic specific conductivity (K_s) as a measure of xylem
40
41 243 hydraulic efficiency and maximum leaf specific conductivity (K_{sl}) as a measure of leaf water
42
43 244 supply capacity. We used the native percentage loss of conductivity of the collected
44
45 245 branches (PLC) as a measure of native embolism. To PLC, we measured branch xylem
46
47 246 hydraulic conductivity before ($K_{s_{nat}}$ – native conductivity) and after flushing to remove
48
49 247 emboli (K_s). We quantified the leaf area distal to each sample to obtain K_{sl} from K_l (leaf
50
51 248 conductance). Using samples from the branches collected at midday, we put the entire
52
53 249 branch underwater and discarded a 10 cm long segment from the base. After this, we cut
54
55
56
57
58
59
60

1
2
3 250 another 10-15 cm long segment from the base of each branch underwater, standard
4
5
6 251 distance from the tip of the branch and let them rehydrate for 15 min to release tension
7
8 252 and avoid artefacts (Venturas et al. 2015). Subsequently, to relax the tension in the branch
9
10 253 we cut 1-1.5 cm of branch from base to leaves underwater, in steps of ~15 cm, and used
11
12 254 the distal end of the branch for hydraulic measurements to ensure no artificially
13
14 255 embolised vessels were present in the measured sample. All samples used for hydraulic
15
16 256 measurements were second or third order branches, between 30-55 mm in length and 3-5
17
18 257 mm diameter and were recut underwater with a sharp razor blade before connecting to
19
20 258 the apparatus, to ensure all vessels were open at both ends. We then measured flow in
21
22 259 the sample using the Ventury tube method (Tyree et al. 2002, Pereira and Mazzafera
23
24 260 2013), where known resistance (PEEK capillary) is connected in series with the sample and
25
26 261 the pressure drop in the capillary is proportional to flow in the sample. K_{snat} is then
27
28 262 calculated from the pressure head applied and water flow. The samples are then flushed
29
30 263 to remove emboli and estimate K_s (Martin-StPaul et al., 2014). We used pressure
31
32 264 transducers (26PCCFA6G, Honeywell; read with a [OM-CP-VOLT101A](#) data logger, Omega
33
34 265 Engineering) to measure pressure drop in the capillary and measured the capillary
35
36 266 resistance prior to measurements using precision scales. The samples remained under-
37
38 267 water throughout the entire procedure. We calculated PLC as the ratio of K_{snat} to K_s
39
40 268 multiplied by 100. We calculated K_{s_l} as the sample hydraulic conductivity (i.e., sample
41
42 269 conductance times sample length) after flushing divided by the leaf area distal to the
43
44 270 measured sample.

45
46
47
48
49
50
51
52
53
54
55 271 *Embolism resistance and hydraulic safety*
56
57
58
59
60

1
2
3 272 As an index of xylem embolism resistance, we used P_{50} and P_{88} , the xylem water
4
5 273 potentials where, respectively, 50% and 88% of hydraulic conductivity is lost. We also used
6
7
8 274 P_{50} to calculate the hydraulic safety margin - the difference between P_{50} and Ψ_{md} , an index
9
10 275 of tree hydraulic safety. Branches collected before sunrise were rehydrated for 24 hours
11
12
13 276 and from each branch we cut two or three smaller branches of approximately 40-70 cm.
14
15 277 We measured the xylem embolism resistance of each branch using the pneumatic method
16
17
18 278 (Pereira et al. 2016, Zhang et al. 2018). With this method, the loss of hydraulic
19
20 279 conductance is estimated from the increase in air volume inside the wood caused by
21
22
23 280 embolism formation as the branch dehydrates. Air volume is estimated from the air
24
25 281 discharge from the cut end of the branch into a vacuum reservoir (~50 kPa absolute
26
27
28 282 pressure) of known volume during a given amount of time (2.5 minutes). We measured
29
30 283 initial and final pressure inside the vacuum reservoir with a pressure transducer
31
32
33 284 (163PC01D75, Honeywell) and calculated the volume of air discharged using the ideal gas
34
35 285 law. A detailed protocol is presented in (Pereira et al. 2016, Bittencourt et al. 2018) and
36
37
38 286 revised by Pereira et al. (2021). Percentage loss of conductance for each branch is
39
40 287 estimated from percentage air discharged (PAD) during its dehydration. PAD is calculated
41
42
43 288 by standardising air discharge for each branch by its minimum (fully hydrated) and
44
45 289 maximum (most dehydrated) air discharge state. We dehydrated branches using the
46
47
48 290 bench dehydration method (Sperry et al. 1988). Before each air discharge measurement,
49
50 291 branches were sealed in thick black plastic bags for one hour for leaf and wood xylem
51
52
53 292 water potential to equilibrate. Directly after the air discharge was measured, we
54
55 293 estimated wood xylem water potential by measuring the leaf water potential of one to
56
57
58 294 two leaves. Drought embolism resistance is then given by the increase in PAD with
59
60 295 decreasing xylem water potential for each tree. To calculate P_{50} , we pooled data from the

296 two-to-three branch replicates from the same tree and fitted a sigmoid curve to the data
 297 (Pammenter and Van der Willigen 1998) where P_{50} and slope (a) are the fitted parameters
 298 and P_{88} is predicted from the fit (Eqn 1):

$$PAD = 100 / (1 + \exp(a(\Psi - P_{50})))$$

299 (1)

300 **Eqn1.** Percentage air discharge equation (PAD). Ψ Water potential. P_{50} (xylem embolism
 301 resistance (MPa)

302 *Data analysis*

303 By comparing trees found on the Control and TFE experimental plots, we measure the
 304 effect of the experimental drought on our drought stress indicators (Ψ_{pd} , Ψ_{md} - midday
 305 water potential; HSM – branch hydraulic safety margin to P_{50} ; PLC – native dry season
 306 percentage loss of conductivity) and plant traits (W_D – wood density; $A_L:A_{SW}$ - leaf to
 307 sapwood area; P_{50} - xylem embolism resistance; P_{88} - xylem embolism resistance; G_{min} –
 308 minimum stomatal conductance; K_s – maximum hydraulic specific conductivity; K_{sl} -
 309 maximum hydraulic leaf -specific conductivity) in small trees. We used linear mixed effects
 310 models to test for plot (TFE vs Control) and taxonomic effects (genus and species) on
 311 hydraulics traits in small trees ($n = 66$) using the R package lme4 (Bates et al. 2015). We
 312 tested the significance of the random effect by removing it and evaluating if the model
 313 significantly worsened using log likelihood tests using the *ranova* function for *lmerTest*
 314 objects (Zuur et al. 2009). We tested sequentially for the random effect of genus on: (a)
 315 the model intercept; (b) the fixed Plot effect (drought effect, difference between plots) on
 316 slope without intercept; and (c) both intercept and plot. When either the genus effect on
 317 plot, slope or both did not show the significance, we kept the multilevel approach using

1
2
3 318 [genus as a random effect on the intercept \(1|genus\)](#), as it controls for experimental design
4
5
6 319 (Burnham and Anderson 2004). After testing the random effects, we tested the fixed TFE
7
8 320 effect on variables. When taxonomy was included as a random effect in our models, we
9
10 321 tested for both genus-only and species-nested-within-genus effects. We tested the
11
12 322 complete model (genus and species as a random effect) against a General Linear Model
13
14 323 (GLM) containing only the fixed effects. In all variables genus was significant as random
15
16 324 effect. [Therefore, linear models with genus as a random effect were used to test the](#)
17
18 325 [significance of the fixed effects](#). To quantify model goodness of fit, we considered the
19
20 326 marginal and conditional R^2 (Mulkey and Pearcy 1992b). The marginal R^2 indicates how
21
22 327 much of the model variance is explained by the fixed effects only, whereas the conditional
23
24 328 R^2 indicates how much of the model variance is explained by the complete model with
25
26 329 fixed and random effects. All the analyses were done in R (version 3.3.0; R Core Team,
27
28 330 2016)

331 *Small and large tree comparisons*

332 We tested for differences in individual tree-level responses to the TFE treatment for large
333 (n = 72) and small trees (n = 39). We use the large trees data from Bittencourt et al. (2020)
334 conducted in the same experimental plots and collected during 2017 with the same
335 methodological procedures. For this comparison we restrict the samples to those trees
336 whose genera are replicated on both plots and replicated between the large and small
337 trees, with a minimum sample size of 2 individuals per size group per plot and genus.
338 Consequently, the number of genera and individuals employed in this comparison is lower
339 than the available number of individual small trees and the full dataset published in
340 Bittencourt et al., (2020). In total we use five genera (*Eschweilera*, *Inga*, *Licania*, *Protium*,

1
2
3 341 *Swartzia*), with 15 small trees on the Control and 24 small trees on the TFE, and 35 large
4
5 342 trees on the Control and 37 large trees on the TFE. We used linear mixed-effect models to
6
7
8 343 test the effects of the tree size with two classes (large and small), and tree size on drought
9
10 344 stress indicators and hydraulic traits. Taxonomic effects were included by using genus as
11
12
13 345 random effects, following the same protocol used for the small tree analyses, presented
14
15 346 above. [Within this paper, all data presented represent the mean and standard errors of](#)
16
17 347 [the mean. A summary of available trait data by genus is presented in Table 1.](#)

18
19
20 348 To test for an overall difference in the hydraulic strategy between small and large trees,
21
22 349 we used the multivariate approach conducting non-metric multidimensional scaling
23
24 350 (NMDS) using an individual-traits matrix (McCune & Grace 2002). We construct a matrix of
25
26 351 data consisting of rows of individuals of each species and columns of traits values. We
27
28 352 standardized the individual trait values for each genus and built the similarity matrix using
29
30 353 Gower distance. NMDS searches for the best position of individuals variables on k
31
32 354 dimensions (axes) to minimize the "stress" of the resulting k-dimensional configuration.
33
34 355 We use k axes = 2 from that ordination as the initial configuration. The "stress" is obtained
35
36 356 by comparison among the pair-wise distances (differences) of each individual's variables in
37
38 357 reduced ordination space (expressed in terms of axes) and the original distance matrix
39
40 358 (Gower distance). The regression is fitted using least-squares regressions and the
41
42 359 goodness of fit is measured as the sum of squared differences between ordination-based
43
44 360 distances and the distances predicted by the regression. A goodness of fit, or stress value,
45
46 361 between 0.1 to 0.2 represent a good fit within the specified number of dimensions
47
48 362 analysed to enable points to be interpreted relative to the NMDS axes. Therefore, the axis
49
50 363 represents the data in a way that best represents their dissimilarity, points on the graph
51
52 364 that are closer together are more similar. In addition, we use MANOVA to test the

1
2
3 365 difference in multidimensional space filled by tree size (small and large groups) and by
4
5 366 plot effect (TFE and Control groups) separately (Anderson 2001). We use a MANOVA to
6
7
8 367 compare Gower distance among observations in the same group versus those in different
9
10 368 groups. We conducted a MANOVA first using small and large tree groups and then using
11
12
13 369 TFE and Control groups using both tree sizes together. The size and plot effects were
14
15 370 tested separately. Finally, we use permutations of the observations to obtain a probability
16
17
18 371 associated with the null hypothesis of no differences between groups.

21 372 **Results**

22
23
24 373 The reduced soil moisture availability and increased canopy openness caused by 15 years
25
26 374 of the TFE (Fig. S2) caused significant changes in the hydraulic traits of the small trees (Fig.
27
28
29 375 1). Maximum specific conductivity (K_s) increased significantly, by $56.3 \pm 41.5\%$, in the TFE
30
31 376 small trees relative to the Control (Fig. 1f, $p < 0.01$), similarly there was a significant
32
33 377 ($45.6 \pm 38.2\%$) increase in the leaf: sapwood area ratio ($A_L:A_{SW}$, Fig 1b.; $p < 0.001$). The TFE
34
35
36 378 also had significant effects on key physiological indicators of drought stress in small trees
37
38 379 (Fig. 1) with Ψ_{pd} 0.24 MPa lower on the TFE relative to the Control ($p < 0.001$) and Ψ_{md} 0.67
39
40
41 380 MPa lower ($p < 0.001$, Table S2). In contrast, other key hydraulic traits including xylem
42
43
44 381 embolism resistance (P_{50} and P_{88}), leaf specific conductivity (K_{sl}), minimum stomatal
45
46 382 conductance (G_{min}) and wood density (WD) showed no significant difference between the
47
48
49 383 TFE and the Control plots for small trees (Fig. 1; Table 2; Table S3).

50
51 384
52
53
54
55
56
57
58
59
60

1
2
3 385 **Taxonomic effects on hydraulic traits and their interactions with drought**

4
5 386 Using mixed-effect modelling analysis we found that the variance explained by taxonomy
6
7 387 had only a limited role in affecting the overall drought responses. When genus by genus
8
9 388 responses to the drought effect were examined separately, it was clear that there were
10
11 389 highly variable responses to the treatment among genera and sometimes these were
12
13 390 inconsistent in terms of direction, as well as magnitude. We cannot separate the
14
15 391 taxonomic effect from the residual variance because genus-specific influences on the plot
16
17 392 effect were highly variable (Fig. 2 and 3). Given the low replication (between 2 and 5 for
18
19 393 each genus on each plot treatment) and high variation within each genus, it was not
20
21 394 always statistically viable to test the plot effect within each genus (Fig. 2 and 3), however
22
23 395 where this was possible, clear statistical differences were seen for some genera but not
24
25 396 for others (Table 2 Fig. 2). For example, *Licania* showed consistent responses in P₅₀ and
26
27 397 HSM while *Ocotea* did not show differences between plots (Fig. 2 and 3). The patterns
28
29 398 described here were also maintained when we analysed the data at a species level (data
30
31 399 not shown).

32
33
34
35
36
37
38
39
40 400

401 ***Large versus small trees***

402 We compared the responses of hydraulic traits between large (>20 cm DBH) and small
403 trees (1-10 cm DBH). Except for Ψ_{pd} , the results we obtain considering only the five genera
404 that overlap between the small and large size classes, were similar to when considering all
405 nine genera of trees present in Control plot and TFE experiment (see Fig. S3
406 supplementary material and Table S3 for n values for the small to large tree comparisons).
407 Using all of the trait data for five overlapping genera, we applied NMDS ordination which
408 demonstrated that the niche space occupied by the small trees was significantly different
409 from the trait space of large trees. The traits space separated on to a clear 2-dimensional
410 axis with a stress score of 0.18, indicating a good fit between the data and an analysis
411 consisting of two axes (Fig. 4). Different associations amongst the nine hydraulic traits
412 separated the individuals in the small and large tree groups. This result was driven
413 predominantly by the first axis, which was positively related to PLC, P_{50} and P_{88} that
414 influenced small tree grouping (Fig. 4). While the first axis was negatively related to K_s , K_{sl} ,
415 G_{min} influencing large trees grouping (Fig 4, Table S4). Using the complete set of hydraulic
416 traits, we show that the hydraulic niche of small trees was significantly different from that
417 of large trees (MANOVA_(1,66); $F=7.96$; $p<0.001$; Table 1). However, there was no difference
418 in hydraulic niche space occupied by the Control and TFE groups (MANOVA_(1,64); $F=1.22$;
419 $p=0.30$), except for K_s that showed plot and tree size effects (MANOVA_(1,64); $F=3.5$; $p=0.05$).

420 In contrast to the large increase in K_s observed between small trees in Control and TFE
421 trees (Figs 1 & S2), the plot level average values of K_s were similar among large trees in
422 both Control and droughted conditions (4.82 ± 3.93 TFE and 4.86 ± 2.79 Control plot). Similar
423 to Ψ_{md} , notable plot level differences were present in small trees, but these were absent

1
2
3 424 in the large trees (-1.72 ± 0.48 MPa TFE and -1.70 ± 0.48 MPa Control treatment). However,
4
5 425 small trees had values of Ψ_{md} which were $17.12 \pm 0.03\%$ higher (values closer to 0) than the
6
7
8 426 large trees. Furthermore, for the variables which had no treatment effect amongst the
9
10 427 small trees, we find on average, across both the TFE and Control plots, the small trees had
11
12
13 428 a $38.20 \pm 32.10\%$ ($p < 0.01$) more negative P_{50} and a $68.40 \pm 58.80\%$ and $20.70 \pm 30.40\%$ lower
14
15 429 G_{min} and K_{sl} , respectively, than the large trees (Fig. 5b, 5d, 5f; $p < 0.001$). Also across the
16
17
18 430 plot we found that HSM increased by $72.97 \pm 36.34\%$ and PLC increased by $44.41 \pm 14.62\%$
19
20 431 in the small trees relative to large trees (Fig. 5g, 5i, 5j; $p < 0.01$).
21
22

23 432 We analysed the influence of genus on the combined effect of treatment and tree size
24
25 433 effect (i.e., large and small trees on the Control and TFE plot) for the five genera we could
26
27
28 434 replicate across plots and tree size classes. We found that the effects of tree size varied
29
30
31 435 substantially among genera and between traits and stress indicators (Fig. 6 and 7, table S5
32
33 436 and S6). For example, the difference in P_{50} between large trees and the small trees was
34
35 437 $61.48 \pm 52.51\%$ for *Licania* and $38.96 \pm 3.7\%$ for *Inga* (Fig. 6). In contrast, G_{min} was
36
37
38 438 significantly lower in the small trees relative to large trees across almost all genera (Fig.
39
40 439 6b). The drought-response pattern also changes when doing within-genus comparisons
41
42
43 440 between large and small trees, for example the mean P_{50} response for *Inga* was different
44
45 441 between small and large trees (Fig. 6). A difference in trait values between the Control and
46
47
48 442 TFE plots that was present either for small tree or large trees, but not for both size classes
49
50 443 simultaneously, occurred multiple times (Fig. 6 and 7), especially for the genus *Inga*.
51
52 444 Mixed effect modelling results identify a strong influence of genus on trait variation
53
54 445 between our two size classes (Table 3), yet there are limited cases where we find
55
56
57 446 significant models demonstrating trait differences between the Control and the TFE plot
58
59 447 with a significant tree size and genus effect (Table 3).
60

1
2
3 448 To test for size (small vs. large) and genus effects in each treatment (Control and TFE), we
4
5 449 created a model with both size and genus as fixed effects. In the Control plot the full
6
7
8 450 model (trait ~ genus*size) was a better predictor of variation across almost all traits,
9
10 451 except for K_s , where there was a genus only effect and G_{min} , P_{50} and P_{88} where there was a
11
12 size only effect. An interaction between size and genus was only significant for PLC (Table
13 452
14
15 453 S7). The full model was also the best predictor of trait variation in the TFE plot, although
16
17 only HSM, W_D and G_{min} showed a significant size effect. Significant interactions between
18 454
19
20 455 genus and size were found for P_{50} and P_{88} (Table S7).
21
22
23
24 456
25
26
27
28
29
30
31
32
33
34
35
36
37
38
39
40
41
42
43
44
45
46
47
48
49
50
51
52
53
54
55
56
57
58
59
60

1
2
3 457 **Discussion**
4

5 458 Our results provide the evidence that small trees can adjust their functioning in response
6
7 459 to drought, allowing them to maximize carbon gain in the higher-light levels following
8
9
10 460 mortality of large trees in the TFE. We find that small trees (1-10 cm DBH) have the
11
12 461 capacity to increase maximum specific hydraulic conductivity and leaf-sapwood area ratio
13
14 462 in response to prolonged (15 year) soil moisture deficit. Despite having significantly lower
15
16
17 463 pre-dawn and midday leaf water potentials, small trees had the capacity to adjust key
18
19
20 464 hydraulic traits to allow a positive response to a higher light environment. This suggests
21
22 465 that despite soil drought stress, small trees can still increase water transport efficiency
23
24 466 and canopy water use in response to increases in light availability, following drought-
25
26
27 467 induced mortality of large trees, potentially allowing them to maximise productivity in
28
29
30 468 periods of the year when water is available. We also show the different components of a
31
32 469 hydraulic strategy that provides niche segregation between small and large trees, with
33
34 470 small trees being more drought tolerant than large canopy trees.
35
36

37 471 Studying the effects of multiple factors (here, imposed drought and size) on the
38
39 472 physiology of hyper-diverse tropical forests is challenging. Here, we successfully addressed
40
41
42 473 this problem by using genus and species nested in genus as random factors in linear mixed
43
44 474 models and show that variability of species within genera is generally small. We
45
46
47 475 nonetheless acknowledge our sample size limitations and the possibility that greater
48
49
50 476 sampling depth may discover significant species-by-species variability in these traits.
51

52
53 477
54
55

56 478
57
58
59
60

479 **The impact of drought on the hydraulic system of small trees**

480 The substantial drought-related mortality of large trees (da Costa et al., 2010;
481 Rowland et al., 2015) in the 15 years preceding this study led to an increase in the light
482 availability in the lower canopy of the TFE, driving increases in the maximum
483 photosynthetic capacity (71.1% and 29.2% increase in J_{\max} and $V_{c_{\max}}$ respectively) and a
484 15.1% increase in the LMA of the same small trees we study here (Bartholomew et al.
485 2020). These differences in response to the prevailing light environment have also been
486 observed elsewhere in tropical tree canopies (Ruggiero et al. 2002, Domingues et al. 2010,
487 Cavaleri et al. 2010) and are indicative of plants changing their allocation strategy in
488 response to increased light availability (Poorter et al., 2009; Wright et al., 2004). Critically,
489 these allocation shifts are likely to result in a net increase in photosynthesis and growth
490 (Metcalfe, Meir, Aragão, et al. 2010, Rowland, da Costa, et al. 2015, Meir et al. 2018),
491 which require higher water supply to the canopy of each individual. The elevated soil
492 moisture stress in the TFE relative to the Control trees manifested itself as significantly
493 more negative pre-dawn and midday leaf water potential values (Figs 1h-1i), key
494 indicators of plant water stress (Bhaskar & Ackerly, 2006; Kramer, 1988; Martínez-vilalta &
495 Garcia-Forner, 2017). Interestingly however, these more negative water potentials did not
496 translate into a significant change in HSM between plots, which would imply that the small
497 trees converge to have the same vulnerability to drought (Choat et al. 2012). This could
498 occur because of a trend, albeit not statistically detectable, towards more negative P50
499 values in the TFE plot for small trees, relative to the Control trees (Fig. 1), making a
500 significant difference in HSM less likely. When examined at the genus level, five of the
501 nine genera have consistently more negative P_{50} values on the TFE relative to the Control,
502 with two remaining roughly equal and two less negative on the TFE (Fig. 2). These data

1
2
3 503 suggest that, despite operating at more negative water potentials, it is still possible for
4
5 504 small trees to adjust their hydraulic system to support the increased growth in response to
6
7
8 505 greater light availability.
9

10
11 506 Consistent with increases in photosynthetic capacity (Bartholomew et al., 2020),
12
13 507 we observe an increase in leaf area to sapwood area ratio ($A_L:A_{SW}$) in the small trees on the
14
15
16 508 TFE, relative to the Control. Combined with greater hydraulic specific conductivity, small
17
18 509 trees in the TFE are therefore able to supply water to more photosynthetic tissue without
19
20
21 510 increasing the volume of sapwood. A global study, including multiple sites from the tropics
22
23 511 showed plant hydraulic systems are highly sensitive to changes in this ratio ($A_L:A_{SW}$) and
24
25 512 may be one of the main factors controlling trade-offs in other plant hydraulic traits
26
27
28 513 (Mencuccini et al. 2019). Increasing leaf area increases the total water demand of the
29
30
31 514 tree; however, the observed increases in photosynthetic capacity (high values of $V_{c_{max}}$ and
32
33 515 J_{max} , Bartholomew et al. 2020), may allow slightly lower stomatal conductance for any
34
35 516 given CO_2 concentration (Bartholomew et al., 2020; Sperry et al., 2017). This may, in part,
36
37
38 517 compensate for the increase in demand for water that increased leaf areas could cause.
39
40
41 518 However, even with the observed increases in photosynthetic capacity, these small trees
42
43 519 probably still experience increased total water demand due to increased exposure to
44
45 520 higher temperatures and VPD, suggesting that small trees must increase maximum
46
47
48 521 hydraulic conductivity and/or tolerate reductions in water potential and therefore greater
49
50
51 522 embolism risk (Sperry et al., 2017). In our study, small trees sampled in the TFE were
52
53 523 slightly taller than the small trees in the Control plot (Fig. S1). This difference may in part-
54
55 524 contribute to the slightly elevated conductance in the branches, as taller trees can have
56
57
58 525 larger vessels at the base and greater vessel tapering from the trunk to branch tip (Olson
59
60

1
2
3 526 and Rosell 2013, Olson et al. 2020). It is, however, unlikely that these differences had a
4
5 527 large influence on our K_s results, overall, the difference in height were small and the
6
7
8 528 genera with the greatest height differences between the TFE and Control (*Protium*, *Ocotea*,
9
10 529 *Voucoupoa*, Fig. S1) showed no changes in K_s (Fig. 2).

530 **Differential hydraulic strategy between small and large trees**

531 The comparison between small trees and large trees [multidimensional hydraulic](#)
532 [trait space](#), using NMDS and MANOVA, indicate they occupy different hydraulic niche
533 [spaces, despite some overlap](#). This revealed that smaller trees do indeed have a different
534 water use strategy to larger canopy trees (Fig 3). The differences in the traits we observed
535 were far greater, and in most cases significantly so, between the large and the small trees
536 than for trees of the same size class between treatments (Fig 4). In addition, we show that
537 smaller trees across both the Control and the TFE plot have significantly more negative P_{50}
538 values and lower G_{min} values and significantly greater hydraulic safety margins (HSM),
539 midday leaf water potentials and PLC (Fig. 4). This may imply that the small trees converge
540 to the same vulnerability to drought, consistent with the results from large scale studies
541 (e.g. Choat et al., 2012). However, the HSM is 1.94 MPa more positive in the small trees
542 relative to large trees, indicative of a lack of convergence of the vulnerability of large and
543 small trees (i.e. Fig 4i), potentially suggesting vulnerability to drought is driven by the
544 ontogenetic stage of a tree. In addition, our results are consistent with the hypothesis that
545 the smaller trees are shallow rooted and compensate for the lack of access to deep water
546 through developing greater xylem embolism resistance and greater stomatal control
547 (Brum et al., 2019; Tardieu, 1996, Sperry et al. 2017). It is possible that the greater
548 hydraulic safety margin in small trees enables them to adjust more effectively to increased

1
2
3 549 light availability, despite the lower water availability in the TFE, as it enables these trees to
4
5 550 tolerate greater drought stress without passing critical thresholds.
6
7

8
9 551 The carbon gain associated with greater photosynthesis under higher light
10
11 552 environments may be translated into new xylem growth in smaller trees. This growth
12
13 553 could rapidly replace damaged tissues and is likely to be a more viable strategy for smaller
14
15
16 554 trees, relative to large trees (Damián et al. 2018, Trugman et al. 2018), which would
17
18 555 reduce the risk associated with higher PLC levels. Furthermore, small trees maintained
19
20
21 556 significantly lower G_{\min} and higher midday leaf water potentials (Fig. 5d, 5g), relative to
22
23 557 the large trees, despite having similar pre-dawn leaf water potentials, suggesting that
24
25
26 558 small trees are able to more tightly regulate water loss, during both the day and night.
27
28 559 Probably, the high regulate water loss in small tree is associate a lower water storage
29
30 560 capacity to buffer short-term variation of water availability (Goldstein et al. 1998, Meinzer
31
32 561 et al. 2003). The greater degree of control further reduces the risk of runaway embolism
33
34 562 when photosynthesising during periods with low water potential, particularly if these
35
36 563 trees can repair cavitated vessels (Nardini et al., 2011; Salleo et al., 2004; Salleo et al.,
37
38 564 1995) or grow new vessels between consecutive dry seasons (Eller *et al.* 2018). Also, small
39
40
41 565 trees also have fewer structural constraints than large trees, so small changes in hydraulic
42
43 566 traits in a small tree could have bigger effects on overall performance during drought,
44
45
46 567 because the marginal effect of each unit change is larger relative to the size of the tree
47
48 568 (Mencuccini 2002). Combined, these factors are likely to allow small trees to have greater
49
50
51 569 flexibility in terms of the strategy they use to adjust to combined changes in water and
52
53
54 570 light availability. However, as we highlight in our results, there is considerable variability
55
56
57 571 both within and between taxonomic groups with respect to how small trees may alter
58
59
60 572 their traits and their resulting drought tolerance strategy.

1
2
3 573 This study highlights the importance of forest structural changes in controlling the traits of
4
5 574 what are likely to be the next generation of trees growing up during prolonged drought
6
7
8 575 stress. We show that, relative to large trees, small trees have a larger capacity to
9
10 576 acclimate their hydraulic systems to increases in light availability following drought-
11
12
13 577 induced mortality of large canopy-dominant trees. Our results suggest that small trees are
14
15 578 able to acclimate the hydraulic conductance and leaf area to sapwood area ratio despite
16
17 579 experiencing prolonged soil moisture stress, which resulted here in lower leaf water
18
19
20 580 potentials and greater PLC. Also, our results demonstrate that there is a consistent and
21
22
23 581 larger shift in the plant hydraulic strategy of saplings relative to large trees across most of
24
25 582 Amazonia's hyper-abundant taxonomic groups. Whilst we find adjustment of traits in
26
27 583 response to the drought treatment, it remains unknown whether all small trees
28
29
30 584 community can respond in the same way or only the long-term drought surviving trees. In
31
32 585 this way, a key uncertainty that remains to be answered are relates to the long-term
33
34
35 586 development of these trees. Assuming these small trees continue to develop under the
36
37 587 experimental drought stressed conditions, it would be of interest to know if the trajectory
38
39
40 588 of change in hydraulic traits we observe can be sufficient to increase the hydraulic
41
42 589 resistance to drought of these trees as they approach full size.

43
44
45 590 Ultimately, continued acclimation of hydraulic systems throughout a the lifespan of a tree
46
47 591 may allow a more drought-resilient ecosystem to develop following the negative impacts
48
49
50 592 of drought on pre-existing larger trees. Therefore, even the current generation of trees
51
52 593 showing huge mortality rates, the next generation might be followed by a new stable
53
54
55 594 community composed of those small trees that can adapt to drought. This implies that for
56
57 595 prediction of the future of tropical ecosystems function we needs to consider trait
58
59
60 596 adjustment in the future forest instead currently forest.

1
2
3 597 **Data and Materials Availability**
4
5

6 598 We are in the process of making this data publically available through the main funding
7
8 599 bodies data centre, NERC EIDC (<https://eidc.ac.uk/>), if accepted the data will be fully
9
10 publically available on a link we will provide.
11
12

13
14 601 **Supplementary Data**
15

16
17 602 *Supplementary tables*
18

19
20 603 **Table S1.** Linear mixed effect model analysis of stress indicator variables from small tress.
21

22 604 **Table S2.** Linear mixed effect model analysis of hydraulic traits from small tress.
23

24 605 **Table S3** Numbers of individuals for small and large tree in each treatment (TFE an Control) and
25 606 mean and standard deviation of all variables measured.

26
27 607 **Table S4.** Statistics from the NMDS modelling shown in Figure 3.
28

29 608 **Table S5** Results of linear effect models of size (Size vs TFE) on the stress indicator variables on
30 609 Control plot.
31

32 610 **Table S6** Results of linear effect models of size (Size vs TFE) on the hydraulic traits variables on TFE
33 611 plot.
34

35 612 **Table S7** Results of linear effect models of size (Size vs TFE) and genus on the stress indicator and
36 613 hydraulic variables on TFE plot.
37
38

39 614
40
41
42
43
44
45
46
47
48
49
50
51
52
53
54
55
56
57
58
59
60

615

616 *Supplementary figures*

617 **Figure S1.** Height and diameter in each treatment (TFE vs. Control) and by genus for the most
618 common small tree genera in this study (9 genera)

619 **Figure S2.** Soil water content during 2016 in the Throughfall Exclusion Experiment plot and
620 in the Control plot at 10 cm and at 100 cm.

621 **Figure S3.** Comparison between the small trees and large trees from the throughfall exclusion
622 (TFE) and Control plots from grouping all 9 genera available within the large and small tree
623 groupings.

624

625 **Conflict of interest**

626 The authors have no conflict of interest to declare.

627 **Funding**

628 Funding for this work was provided by Brazilian Higher Education Co-ordination Agency
629 (CAPES- Finance Code 001 to ALG); Natural Environment Research Council (NE/N014022/1
630 to LR, NE/J011002/1 to PM and MM, and NE/L002434/1 to DCB); European Union
631 FP7(Amazalert to PM and MM);National Council for Scientific and Technological
632 Development (457914/2013-0/MCTI/CNPq/FNDCT/LBA/ESECAFLOR to ACLdC); Australian
633 Research Council (DP170104091 to PM).The São Paulo Research Foundation FAPESP
634 (grant 11/52072-0 to RSO, 2018/01847-0 to RSO and LR); Royal Society's Newton
635 International for its Fellowship to PRLB (NF170370).

636 **Acknowledgements**

637 We thank the UNICAMP postgraduate program in Ecology and the Brazilian Higher
638 Education Co-ordination Agency (CAPES). We would like to thank the entire community
639 surrounding the study area (Caxiuanã-PA northern Brazil), the climbers Joca and their

1
2
3 640 children, the workers at the scientific base "Bigode"; "Bené"; "Benézinho" and the dear
4
5 641 cook chef "Morena". We also thank "Kaká" and "Moska" for the field campaign help.
6
7

8 642 **Authors' Contributions**

9
10
11 643 ALG collected and compiled the data alongside LR, PRLB, IC, PBC, PG, LVF, DDV, JASJ, DCB
12
13 644 and ACLdC. LR designed the study with MM, ACLdC, PM, ALG and RO. ALG, MM, PRLB and
14
15 645 LR performed the statistical analysis and ALG, LR and RO wrote the paper, all authors
16
17 646 substantially contributed to revisions.
18
19
20
21

22 647 **References**

- 23 648
24
25
26 649 Anderson MJ (2001) A new method for non-parametric multivariate analysis of variance.
27 650 *Austral Ecol* 26:32–46.
28
29 651 Aragão LEOC, Anderson LO, Fonseca MG, Rosan TM, Vedovato LB, Wagner FH, Silva CVJ,
30 652 Silva Junior CHL, Arai E, Aguiar AP, Barlow J, Berenguer E, Deeter MN, Domingues LG,
31 653 Gatti L, Gloor M, Malhi Y, Marengo JA, Miller JB, Phillips OL, Saatchi S (2018) 21st
32 654 Century drought-related fires counteract the decline of Amazon deforestation carbon
33 655 emissions. *Nat Commun* 9:536. <http://dx.doi.org/10.1038/s41467-017-02771-y>
34
35
36 656 Awad H, Barigah T, Badel E, Cochard H, Herbette S (2010) Poplar vulnerability to xylem
37 657 cavitation acclimates to drier soil conditions. *Physiol Plant* 139:280–288.
38 658 <http://doi.wiley.com/10.1111/j.1399-3054.2010.01367.x>
39
40 659 B. Eller C, de V. Barros F, R.L. Bittencourt P, Rowland L, Mencuccini M, S. Oliveira R (2018)
41 660 Xylem hydraulic safety and construction costs determine tropical tree growth. *Plant*
42 661 *Cell Environ* 41:548–562. <http://doi.wiley.com/10.1111/pce.13106>
43
44 662 Bartholomew DC, Bittencourt PRL, Costa ACL, Banin LF, Britto Costa P, Coughlin SI,
45 663 Domingues TF, Ferreira L V., Giles A, Mencuccini M, Mercado L, Miatto RC, Oliveira A,
46 664 Oliveira R, Meir P, Rowland L (2020) Small tropical forest trees have a greater
47 665 capacity to adjust carbon metabolism to long-term drought than large canopy trees.
48 666 *Plant Cell Environ* 43:2380–2393.
49 667 <https://onlinelibrary.wiley.com/doi/10.1111/pce.13838>
50
51
52 668 Bates D, Mächler M, Bolker BM, Walker SC (2015) Fitting linear mixed-effects models
53 669 using lme4. *J Stat Softw* 67
54
55 670 Bhaskar R, Ackerly DD (2006) Ecological relevance of minimum seasonal water potentials.
56 671 *Physiol Plant* 127:353–359. <http://doi.wiley.com/10.1111/j.1399-3054.2006.00718.x>
57
58 672 Binks O, Coughlin I, Mencuccini M, Meir P (2020) Equivalence of foliar water uptake and
59 673 stomatal conductance? *Plant Cell Environ* 43:524–528.

- 1
2
3 674 <https://doi.org/10.1111/pce.13663>
4
5 675 Binks O, Meir P, Rowland L, Costa ACL, Vasconcelos SS, Oliveira AAR, Ferreira L,
6 676 Christoffersen B, Nardini A, Mencuccini M (2016) Plasticity in leaf-level water
7 677 relations of tropical rainforest trees in response to experimental drought. *New Phytol*
8 678 211:477–488. <https://onlinelibrary.wiley.com/doi/abs/10.1111/nph.13927>
9
10 679 Bittencourt PRL, Oliveira RS, Costa ACL, Giles AL, Coughlin I, Costa PB, Bartholomew DC,
11 680 Ferreira L V, Vasconcelos SS, Barros F V, Junior JAS, Oliveira AAR, Mencuccini M, Meir
12 681 P, Rowland L (2020) Amazonia trees have limited capacity to acclimate plant
13 682 hydraulic properties in response to long-term drought. *Glob Chang Biol* 26:3569–
14 683 3584. <https://onlinelibrary.wiley.com/doi/abs/10.1111/gcb.15040>
15
16 684 Bittencourt P, Pereira L, Oliveira R (2018) Pneumatic Method to Measure Plant Xylem
17 685 Embolism. *BIO-PROTOCOL* 8:1–14. <https://bio-protocol.org/e3059>
18
19 686 Brando PM, Nepstad DC, Davidson EA, Trumbore SE, Ray D, Camargo P (2008) Drought
20 687 effects on litterfall, wood production and belowground carbon cycling in an Amazon
21 688 forest: results of a throughfall reduction experiment. *Philos Trans R Soc B Biol Sci*
22 689 363:1839–1848. <https://royalsocietypublishing.org/doi/10.1098/rstb.2007.0031>
23
24 690 Brienen R, Schongart J, Zuidema P (2016) *Tropical Tree Physiology* Goldstein G, Santiago LS
25 691 (eds). Springer International Publishing, Cham. [http://link.springer.com/10.1007/978-](http://link.springer.com/10.1007/978-3-319-27422-5)
26 692 3-319-27422-5
27
28 693 Brodribb TJ, Powers J, Cochard H, Choat B (2020) Hanging by a thread? Forests and
29 694 drought. *Science* (80-) 368:261–266.
30 695 <https://www.sciencemag.org/lookup/doi/10.1126/science.aat7631>
31
32 696 Brum M, Vadeboncoeur MA, Ivanov V, Saleska S, Alves LF, Penha D, Asbjornsen H, Dias JD,
33 697 Aragão LEOC, Barros F, Bittencourt P, Pereira L, Oliveira RS (2019) Hydrological niche
34 698 segregation defines forest structure and drought tolerance strategies in a seasonal
35 699 Amazon forest. *J Ecol*:318–333.
36
37 700 Burnham KP, Anderson DR (2004) Multimodel Inference. *Sociol Methods Res* 33:261–304.
38 701 <http://journals.sagepub.com/doi/10.1177/0049124104268644>
39
40 702 Cavaleri MA, Oberbauer SF, Clark DB, Clark DA, Ryan MG (2010) Height is more important
41 703 than light in determining leaf morphology in a tropical forest. *Ecology* 91:1730–1739.
42 704 <http://doi.wiley.com/10.1890/09-1326.1>
43
44 705 Chadwick R, Good P, Martin G, Rowell DP (2016) Large rainfall changes consistently
45 706 projected over substantial areas of tropical land. *Nat Clim Chang* 6:177–181.
46 707 <http://www.nature.com/articles/nclimate2805>
47
48 708 Choat B, Jansen S, Brodribb TJ, Cochard H, Delzon S, Bhaskar R, Bucci SJ, Feild TS, Gleason
49 709 SM, Hacke UG, Jacobsen AL, Lens F, Maherali H, Martínez-Vilalta J, Mayr S,
50 710 Mencuccini M, Mitchell PJ, Nardini A, Pittermann J, Pratt RB, Sperry JS, Westoby M,
51 711 Wright IJ, Zanne AE (2012) Global convergence in the vulnerability of forests to
52 712 drought. *Nature* 491:752–755. <http://www.nature.com/articles/nature11688>
53
54 713 Christensen JH, Krishna Kumar K, Aldrian E, An SI, Cavalcanti, I.F.A. de C, M., Dong W,
55 714 Goswami P, Hall A, Kanyanga JK, Kitoh A, Kossin, Lau NC, Renwick J, Stephenson DB,

- 1
2
3 715 Xie SP, Zhou T (2017) Climate Phenomena and their Relevance for Future Regional
4 716 Climate Change. In: Climate Change 2013: The Physical Science Basis. Contribution of
5 717 Working Group I to the Fifth Assessment Report of the Intergovernmental Panel on
6 718 Climate Change.
- 7
8
9 719 Corlett RT (2016) The Impacts of Droughts in Tropical Forests. *Trends Plant Sci* 21:584–
10 720 593. <http://dx.doi.org/10.1016/j.tplants.2016.02.003>
- 11
12 721 da Costa ACL, Galbraith D, Almeida S, Portela BTT, da Costa M, de Athaydes Silva Junior J,
13 722 Braga AP, de Gonçalves PHL, de Oliveira AA, Fisher R, Phillips OL, Metcalfe DB, Levy P,
14 723 Meir P (2010) Effect of 7 yr of experimental drought on vegetation dynamics and
15 724 biomass storage of an eastern Amazonian rainforest. *New Phytol* 187:579–591.
16 725 <http://doi.wiley.com/10.1111/j.1469-8137.2010.03309.x>
- 17
18
19 726 da Costa ACL, Metcalfe DB, Doughty CE, de Oliveira AAR, Neto GFC, da Costa MC, Silva
20 727 Junior J de A, Aragão LEOC, Almeida S, Galbraith DR, Rowland LM, Meir P, Malhi Y
21 728 (2014) Ecosystem respiration and net primary productivity after 8–10 years of
22 729 experimental through-fall reduction in an eastern Amazon forest. *Plant Ecol Divers*
23 730 7:7–24. <http://www.tandfonline.com/doi/abs/10.1080/17550874.2013.798366>
- 24
25 731 Damián X, Fornoni J, Domínguez CA, Boege K (2018) Ontogenetic changes in the
26 732 phenotypic integration and modularity of leaf functional traits. *Funct Ecol*:234–246.
- 27
28
29 733 Domingues TF, Meir P, Feldpausch TR, Saiz G, Veenendaal EM, Schrodte F, Bird M,
30 734 Djagbletey G, Hien F, Compaore H, Diallo A, Grace J, Lloyd J (2010) Co-limitation of
31 735 photosynthetic capacity by nitrogen and phosphorus in West Africa woodlands. *Plant*,
32 736 *Cell Environ* 33:959–980.
- 33
34 737 Duffy PB, Brando P, Asner GP, Field CB (2015) Projections of future meteorological
35 738 drought and wet periods in the Amazon. *Proc Natl Acad Sci* 112:13172–13177.
36 739 <http://www.pnas.org/lookup/doi/10.1073/pnas.1421010112>
- 37
38
39 740 Duursma RA, Blackman CJ, López R, Martin-StPaul NK, Cochard H, Medlyn BE (2019) On
40 741 the minimum leaf conductance: its role in models of plant water use, and ecological
41 742 and environmental controls. *New Phytol* 221:693–705.
- 42
43 743 Esquivel-Muelbert A, Baker TR, Dexter KG, Lewis SL, ter Steege H, Lopez-Gonzalez G,
44 744 Monteagudo Mendoza A, Brienen R, Feldpausch TR, Pitman N, Alonso A, van der
45 745 Heijden G, Peña-Claros M, Ahuite M, Alexiades M, Álvarez Dávila E, Murakami AA,
46 746 Arroyo L, Aulestia M, Balslev H, Barroso J, Boot R, Cano A, Chama Moscoso V,
47 747 Comiskey JA, Cornejo F, Dallmeier F, Daly DC, Dávila N, Duivenvoorden JF, Duque
48 748 Montoya AJ, Erwin T, Di Fiore A, Fredericksen T, Fuentes A, García-Villacorta R,
49 749 Gonzales T, Guevara Andino JE, Honorio Coronado EN, Huamantupa-Chuquimaco I,
50 750 Killeen TJ, Malhi Y, Mendoza C, Mogollón H, Jørgensen PM, Montero JC, Mostacedo
51 751 B, Nauray W, Neill D, Vargas PN, Palacios S, Palacios Cuenca W, Pallqui Camacho NC,
52 752 Peacock J, Phillips JF, Pickavance G, Quesada CA, Ramírez-Angulo H, Restrepo Z,
53 753 Reynel Rodríguez C, Paredes MR, Sierra R, Silveira M, Stevenson P, Stropp J, Terborgh
54 754 J, Tirado M, Toledo M, Torres-Lezama A, Umaña MN, Urrego LE, Vasquez Martinez R,
55 755 Gamarra LV, Vela CIA, Vilanova Torre E, Vos V, von Hildebrand P, Vriesendorp C,
56 756 Wang O, Young KR, Zartman CE, Phillips OL (2017) Seasonal drought limits tree
57 757 species across the Neotropics. *Ecography (Cop)* 40:618–629.

- 1
2
3 758 <http://doi.wiley.com/10.1111/ecog.01904>
4
- 5 759 Fu R, Yin L, Li W, Arias PA, Dickinson RE, Huang L, Chakraborty S, Fernandes K, Liebmann B,
6 760 Fisher R, Myneni RB (2013) Increased dry-season length over southern Amazonia in
7 761 recent decades and its implication for future climate projection. *Proc Natl Acad Sci*
8 762 110:18110–18115. <http://www.pnas.org/cgi/doi/10.1073/pnas.1302584110>
- 9
10 763 Goldstein G, Andrade JL, Meinzer FC, Holbrook NM, Cavelier J, Jackson P, Celis A (1998)
11 764 Stem water storage and diurnal patterns of water use in tropical forest canopy trees.
12 765 *Plant, Cell Environ* 21:397–406.
- 13
14
15 766 Groenendijk P, Sass-Klaassen U, Bongers F, Zuidema PA (2014) Potential of tree-ring
16 767 analysis in a wet tropical forest: A case study on 22 commercial tree species in
17 768 Central Africa. *For Ecol Manage* 323:65–78.
18 769 <http://dx.doi.org/10.1016/j.foreco.2014.03.037>
- 19
20 770 Hubau W, De Mil T, Van den Bulcke J, Phillips OL, Angoboy Ilondea B, Van Acker J, Sullivan
21 771 MJP, Nsenga L, Toirambe B, Couralet C, Banin LF, Begne SK, Baker TR, Bourland N,
22 772 Chezeaux E, Clark CJ, Collins M, Comiskey JA, Cuni-Sanchez A, Deklerck V, Dierickx S,
23 773 Doucet J-L, Ewango CEN, Feldpausch TR, Gilpin M, Gonmadje C, Hall JS, Harris DJ,
24 774 Hardy OJ, Kamdem M-ND, Kasongo Yakusu E, Lopez-Gonzalez G, Makana J-R, Malhi Y,
25 775 Mbayu FM, Moore S, Mukinzi J, Pickavance G, Poulsen JR, Reitsma J, Rousseau M,
26 776 Sonké B, Sunderland T, Taedoumg H, Talbot J, Tshibamba Mukendi J, Umunay PM,
27 777 Vleminckx J, White LJ, Zemagho L, Lewis SL, Beeckman H (2019) The persistence of
28 778 carbon in the African forest understory. *Nat Plants* 5:133–140.
29 779 <http://www.nature.com/articles/s41477-018-0316-5>
- 30
31
32
33 780 KAMALUDDIN M, GRACE J (1992) Acclimation in Seedlings of a Tropical Tree, *Bischofia*
34 781 *javanica*, Following a Stepwise Reduction in Light. *Ann Bot* 69:557–562.
35 782 [https://academic.oup.com/aob/article-](https://academic.oup.com/aob/article-lookup/doi/10.1093/oxfordjournals.aob.a088386)
36 783 [lookup/doi/10.1093/oxfordjournals.aob.a088386](https://academic.oup.com/aob/article-lookup/doi/10.1093/oxfordjournals.aob.a088386)
- 37
38
39 784 KRAMER PJ (1988) Changing concepts regarding plant water relations. *Plant, Cell Environ*
40 785 11:565–568. <http://doi.wiley.com/10.1111/j.1365-3040.1988.tb01796.x>
- 41
42 786 Krause GH, Virgo A, Winter K (1995) High susceptibility to photoinhibition of young leaves
43 787 of tropical forest trees. *Planta* 197:583–591.
- 44
45 788 Marengo JA, Souza CM, Thonicke K, Burton C, Halladay K, Betts RA, Alves LM, Soares WR
46 789 (2018) Changes in Climate and Land Use Over the Amazon Region: Current and
47 790 Future Variability and Trends. *Front Earth Sci* 6:1–21.
48 791 <https://www.frontiersin.org/article/10.3389/feart.2018.00228/full>
- 49
50 792 Márquez DA, Stuart-Williams H, Farquhar GD (2021) An improved theory for calculating
51 793 leaf gas exchange more precisely accounting for small fluxes. *Nat Plants* 7.
52 794 <http://dx.doi.org/10.1038/s41477-021-00861-w>
- 53
54
55 795 Martin-StPaul NK, Longepierre D, Huc R, Delzon S, Burlett R, Joffre R, Rambal S, Cochard H
56 796 (2014) How reliable are methods to assess xylem vulnerability to cavitation? The
57 797 issue of ‘open vessel’ artifact in oaks. *Tree Physiol* 34:894–905.
- 58
59 798 Martinez-Vilalta J, Anderegg WRL, Sapes G, Sala A (2019) Greater focus on water pools
60

- 1
2
3 799 may improve our ability to understand and anticipate drought-induced mortality in
4 800 plants. *New Phytol* 223:22–32.
- 6 801 Martínez-Vilalta J, Garcia-Forner N (2017) Water potential regulation, stomatal behaviour
7 802 and hydraulic transport under drought: deconstructing the iso/anisohydric concept.
8 803 *Plant Cell Environ* 40:962–976.
- 10 804 Mcculloh KA, Johnson DM, Meinzer FC, Woodruff DR (2014) The dynamic pipeline:
11 805 Hydraulic capacitance and xylem hydraulic safety in four tall conifer species. *Plant,*
12 806 *Cell Environ* 37:1171–1183.
- 15 807 McDowell N, Pockman WT, Allen CD, Breshears DD, Cobb N, Kolb T, Plaut J, Sperry J, West
16 808 A, Williams DG, Yezzer EA (2008) Mechanisms of plant survival and mortality during
17 809 drought: why do some plants survive while others succumb to drought? *New Phytol*
18 810 178:719–739. <http://doi.wiley.com/10.1111/j.1469-8137.2008.02436.x>
- 21 811 Meinzer FC, James SA, Goldstein G, Woodruff D (2003) Whole-tree water transport scales
22 812 with sapwood capacitance in tropical forest canopy trees. *Plant, Cell Environ*
23 813 26:1147–1155.
- 25 814 Meinzer FC, Johnson DM, Lachenbruch B, McCulloh KA, Woodruff DR (2009) Xylem
26 815 hydraulic safety margins in woody plants: Coordination of stomatal control of xylem
27 816 tension with hydraulic capacitance. *Funct Ecol* 23:922–930.
28 817 <http://doi.wiley.com/10.1111/j.1365-2435.2009.01577.x>
- 31 818 Meir P, Mencuccini M, Binks O, Da Costa AL, Ferreira L, Rowland L (2018) Short-term
32 819 effects of drought on tropical forest do not fully predict impacts of repeated or long-
33 820 term drought: Gas exchange versus growth. *Philos Trans R Soc B Biol Sci* 373
- 35 821 Meir P, Wood TE, Galbraith DR, Brando PM, Da Costa ACL, Rowland L, Ferreira L V. (2015)
36 822 Threshold Responses to Soil Moisture Deficit by Trees and Soil in Tropical Rain
37 823 Forests: Insights from Field Experiments. *Bioscience* 65:882–892.
- 39 824 Mencuccini M (2002) Hydraulic constraints in the functional scaling of trees. *Tree Physiol*
40 825 22:553–565.
- 42 826 Mencuccini M, Rosas T, Rowland L, Choat B, Cornelissen H, Jansen S, Kramer K, Lapenis A,
43 827 Manzoni S, Niinemets Ü, Reich PB, Schrodte F, Soudzilovskaia N, Wright IJ,
44 828 Martínez-Vilalta J (2019) Leaf economics and plant hydraulics drive leaf : wood area
45 829 ratios. *New Phytol* 224:1544–1556.
46 830 <https://onlinelibrary.wiley.com/doi/abs/10.1111/nph.15998>
- 49 831 Metcalfe DB, Meir P, Aragao LEOC, Lobo-do-vale R, Galbraith D, Fisher RA, Chaves MM,
50 832 Maroco JP, Costa ACL, Almeida SS De, Braga AP, Gonc PHL (2010) Shifts in plant
51 833 respiration and carbon use efficiency at a large-scale drought experiment in the
52 834 eastern Amazon. *New Phytol*:608–621.
- 54 835 Metcalfe DB, Meir P, Aragão LEOC, Lobo-do-Vale R, Galbraith D, Fisher RA, Chaves MM,
55 836 Maroco JP, da Costa ACL, de Almeida SS, Braga AP, Gonçalves PHL, de Athaydes J, da
56 837 Costa M, Portela TTB, de Oliveira AAR, Malhi Y, Williams M (2010) Shifts in plant
57 838 respiration and carbon use efficiency at a large-scale drought experiment in the
58 839 eastern Amazon. *New Phytol* 187:608–621. <http://doi.wiley.com/10.1111/j.1469->

- 1
2
3 840 8137.2010.03319.x
4
5 841 Mulkey SS, Pearcy RW (1992a) Interactions between Acclimation and Photoinhibition of
6 842 Photosynthesis of a Tropical Forest Understorey Herb, *Alocasia macrorrhiza*, during
7 843 Simulated Canopy Gap Formation. *Funct Ecol* 6:719.
8
9 844 Mulkey SS, Pearcy RW (1992b) Interactions between Acclimation and Photoinhibition of
10 845 Photosynthesis of a Tropical Forest Understorey Herb, *Alocasia macrorrhiza*, during
11 846 Simulated Canopy Gap Formation. *Funct Ecol* 6:719.
12 847 <https://www.jstor.org/stable/2389969?origin=crossref>
13
14
15 848 Nardini A, Lo MA, Salleo S (2011) Plant Science Refilling embolized xylem conduits : Is it a
16 849 matter of phloem unloading ? *Plant Sci* 180:604–611.
17 850 <http://dx.doi.org/10.1016/j.plantsci.2010.12.011>
18
19 851 Olson ME, Anfodillo T, Gleason SM, McCulloh KA (2020) Tip-to-base xylem conduit
20 852 widening as an adaptation: causes, consequences, and empirical priorities. *New*
21 853 *Phytol:nph.16961*. <https://onlinelibrary.wiley.com/doi/10.1111/nph.16961>
22
23 854 Olson ME, Rosell JA (2013) Vessel diameter-stem diameter scaling across woody
24 855 angiosperms and the ecological causes of xylem vessel diameter variation. *New*
25 856 *Phytol* 197:1204–1213.
26
27
28 857 Pammenter NW, Van der Willigen C (1998) A mathematical and statistical analysis of the
29 858 curves illustrating vulnerability of xylem to cavitation. *Tree Physiol* 18:589–593.
30 859 [https://academic.oup.com/treephys/article-lookup/doi/10.1093/treephys/18.8-](https://academic.oup.com/treephys/article-lookup/doi/10.1093/treephys/18.8-9.589)
31 860 [9.589](https://academic.oup.com/treephys/article-lookup/doi/10.1093/treephys/18.8-9.589)
32
33 861 Pereira L, Bittencourt PRL, Oliveira RS, Junior MBM, Barros F V, Ribeiro R V, Mazzafera P
34 862 (2016) Plant pneumatics: stem air flow is related to embolism – new perspectives on
35 863 methods in plant hydraulics. *New Phytol* 211:357–370.
36 864 <https://onlinelibrary.wiley.com/doi/abs/10.1111/nph.13905>
37
38
39 865 Pereira L, Bittencourt PRL, Rowland L, Brum M, Miranda MT, Pacheco VS, Oliveira RS,
40 866 Machado EC, Jansen S, Ribeiro R V. (2021) Using the Pneumatic method to estimate
41 867 embolism resistance in species with long vessels: A commentary on the article “A
42 868 comparison of five methods to assess embolism resistance in trees”. *For Ecol Manage*
43 869 *479:2019–2021*.
44
45
46 870 Pereira L, Mazzafera P (2013) A low cost apparatus for measuring the xylem hydraulic
47 871 conductance in plants. *Bragantia* 71:583–587.
48 872 [http://www.scielo.br/scielo.php?script=sci_arttext&pid=S0006-](http://www.scielo.br/scielo.php?script=sci_arttext&pid=S0006-87052012000400017&lng=en&tlng=en)
49 873 [87052012000400017&lng=en&tlng=en](http://www.scielo.br/scielo.php?script=sci_arttext&pid=S0006-87052012000400017&lng=en&tlng=en)
50
51
52 874 Poorter L, Bongers F, Sterck FJ, Wöll H (2005) Beyond the regeneration phase:
53 875 Differentiation of height-light trajectories among tropical tree species. *J Ecol* 93:256–
54 876 267. <http://doi.wiley.com/10.1111/j.1365-2745.2004.00956.x>
55
56 877 Poorter H, Niinemets Ü, Poorter L, Wright IJ, Villar R (2009) Causes and consequences of
57 878 variation in leaf mass per area (LMA): a meta-analysis. *New Phytol* 182:565–588.
58 879 <https://onlinelibrary.wiley.com/doi/abs/10.1111/j.1469-8137.2009.02830.x>
59
60 880 Powell TL, Wheeler JK, de Oliveira AAR, da Costa ACL, Saleska SR, Meir P, Moorcroft PR

- 1
2
3 881 (2017) Differences in xylem and leaf hydraulic traits explain differences in drought
4 882 tolerance among mature Amazon rainforest trees. *Glob Chang Biol* 23:4280–4293.
5 883 <http://doi.wiley.com/10.1111/gcb.13731>
- 7 884 Prendin AL, Mayr S, Beikircher B, von Arx G, Petit G (2018) Xylem anatomical adjustments
8 885 prioritize hydraulic efficiency over safety as Norway spruce trees grow taller
9 886 Martinez-Vilalta J (ed). *Tree Physiol* 38:1088–1097.
11 887 <https://academic.oup.com/treephys/article/38/8/1088/5038975>
- 13 888 Rowland L, da Costa ACL, Galbraith DR, Oliveira RS, Binks OJ, Oliveira AAR, Pullen AM,
14 889 Doughty CE, Metcalfe DB, Vasconcelos SS, Ferreira L V, Malhi Y, Grace J, Mencuccini
15 890 M, Meir P (2015) Death from drought in tropical forests is triggered by hydraulics not
16 891 carbon starvation. *Nature* 528:119–122. <http://dx.doi.org/10.1038/nature15539>
- 18 892 Rowland L, da Costa ACL, Oliveira RS, Bittencourt PRL, Giles AL, Coughlin I, de Britto Costa
19 893 P, Bartholomew D, Domingues TF, Miatto RC, Ferreira LV, Vasconcelos SS, Junior JAS,
20 894 Oliveira AAR, Mencuccini M, Meir P (2020) The response of carbon assimilation and
21 895 storage to long-term drought in tropical trees is dependent on light availability. *Funct*
22 896 *Ecol*:1365-2435.13689. [https://onlinelibrary.wiley.com/doi/10.1111/1365-](https://onlinelibrary.wiley.com/doi/10.1111/1365-2435.13689)
23 897 [2435.13689](https://onlinelibrary.wiley.com/doi/10.1111/1365-2435.13689)
- 26 898 Rowland L, Lobo-do-Vale RL, Christoffersen BO, Melém EA, Kruijt B, Vasconcelos SS,
27 899 Domingues T, Binks OJ, Oliveira AAR, Metcalfe D, da Costa ACL, Mencuccini M, Meir P
28 900 (2015) After more than a decade of soil moisture deficit, tropical rainforest trees
29 901 maintain photosynthetic capacity, despite increased leaf respiration. *Glob Chang Biol*
30 902 21:4662–4672. <http://doi.wiley.com/10.1111/gcb.13035>
- 33 903 Ruggiero PGC, Batalha MA, Pivello VR, Meirelles ST (2002) Soil vegetation relationships in
34 904 cerrado (Brazilian savanna) and semideciduous forest, Southeastern Brazil. *Plant Ecol*
35 905 160:1–16.
- 37 906 Sala A, Piper F, Hoch G (2010) Physiological mechanisms of drought-induced tree mortality
38 907 are far from being resolved. *New Phytol* 186:274–281.
39 908 <http://doi.wiley.com/10.1111/j.1469-8137.2009.03167.x>
- 42 909 Salleo S, Lo Gullo MA, De Paoli D, Zippo M (1996) Xylem recovery from cavitation-induced
43 910 embolism in young plants of *Laurus nobilis*: A possible mechanism. *New Phytol*
44 911 132:47–56. <http://doi.wiley.com/10.1111/j.1469-8137.1996.tb04507.x>
- 46 912 Salleo S, Lo Gullo MA, Trifilò P, Nardini A (2004) New evidence for a role of vessel-
47 913 associated cells and phloem in the rapid xylem refilling of cavitated stems of *Laurus*
48 914 *nobilis* L. *Plant, Cell Environ* 27:1065–1076. [http://doi.wiley.com/10.1111/j.1365-](http://doi.wiley.com/10.1111/j.1365-3040.2004.01211.x)
49 915 [3040.2004.01211.x](http://doi.wiley.com/10.1111/j.1365-3040.2004.01211.x)
- 51 916 Salomón RL, Limousin JM, Ourcival JM, Rodríguez-Calcerrada J, Steppe K (2017) Stem
52 917 hydraulic capacitance decreases with drought stress: implications for modelling tree
53 918 hydraulics in the Mediterranean oak *Quercus ilex*. *Plant Cell Environ* 40:1379–1391.
- 56 919 Schneider CA, Rasband WS, Eliceiri KW (2012) NIH Image to ImageJ: 25 years of image
57 920 analysis. *Nat Methods* 9:671–675.
- 59 921 Schuldt B, Leuschner C, Horna V, Moser G, Köhler M, Van Straaten O, Barus H (2011)
- 60

- 1
2
3 922 Change in hydraulic properties and leaf traits in a tall rainforest tree species
4 923 subjected to long-term throughfall exclusion in the perhumid tropics. *Biogeosciences*
5 924 8:2179–2194.
- 7 925 van der Sleen P, Groenendijk P, Vlam M, Anten NPR, Boom A, Bongers F, Pons TL, Terburg
8 926 G, Zuidema PA (2015) No growth stimulation of tropical trees by 150 years of CO₂
9 927 fertilization but water-use efficiency increased. *Nat Geosci* 8:24–28.
11 928 <http://www.nature.com/articles/ngeo2313>
- 13 929 Sperry JS, Donnelly JR, Tyree MT (1988) A method for measuring hydraulic conductivity and
14 930 embolism in xylem. *Plant Cell Environ* 11:35–40.
- 16 931 Sperry JS, Hacke UG, Oren R, Comstock JP (2002) Water deficits and hydraulic limits to leaf
17 932 water supply. *Plant, Cell Environ*:251–263.
- 19 933 Sperry JS, Tyree MT (1988) Mechanism of Water Stress-Induced Xylem Embolism1. *Plant*
20 934 *Physiol* 88:581–587.
- 22 935 Sperry JS, Venturas MD, Anderegg WRL, Mencuccini M, Mackay DS, Wang Y, Love DM
23 936 (2017) Predicting stomatal responses to the environment from the optimization of
24 937 photosynthetic gain and hydraulic cost. *Plant Cell Environ* 40:816–830.
26 938 <http://doi.wiley.com/10.1111/pce.12852>
- 28 939 Sterck F, Markesteijn L, Schieving F, Poorter L (2011) Functional traits determine trade-offs
29 940 and niches in a tropical forest community. *Proc Natl Acad Sci* 108:20627–20632.
30 941 <http://www.pnas.org/cgi/doi/10.1073/pnas.1106950108>
- 32 942 Tardieu F (1996) Drought perception by plants: Do cells of draughted plants experience
33 943 water stress? *Plant Growth Regul* 20:93–104.
- 35 944 Tng DYP, Apgaua DMG, Ishida YF, Mencuccini M, Lloyd J, Laurance WF, Laurance SGW
36 945 (2018) Rainforest trees respond to drought by modifying their hydraulic architecture.
37 946 *Ecol Evol* 8:12479–12491.
- 39 947 Tomasella M, Beikircher B, Häberle KH, Hesse B, Kallenbach C, Matyssek R, Mayr S (2018)
40 948 Acclimation of branch and leaf hydraulics in adult *Fagus sylvatica* and *Picea abies* in a
41 949 forest through-fall exclusion experiment. *Tree Physiol* 38:198–211.
- 44 950 Trugman AT, Detto M, Bartlett MK, Medvigy D, Anderegg WRL, Schwalm C, Schaffer B,
45 951 Pacala SW (2018) Tree carbon allocation explains forest drought-kill and recovery
46 952 patterns. *Ecol Lett*:1552–1560.
- 48 953 Tyree MT, Vargas G, Engelbrecht BMJ, Kursar TA (2002) Drought until death do us part: A
49 954 case study of the desiccation-tolerance of a tropical moist forest seedling-tree,
50 955 *Licania platypus* (Hemsl.) Fritsch. *J Exp Bot* 53:2239–2247.
- 52 956 Venturas MD, Mackinnon ED, Jacobsen AL, Pratt RB (2015) Excising stem samples
53 957 underwater at native tension does not induce xylem cavitation. *Plant, Cell Environ*
54 958 38:1060–1068.
- 56 959 Wright IJ, Reich PB, Westoby M, Ackerly DD, Baruch Z, Bongers F, Cavender-bares J,
57 960 Chapin T, Cornelissen JHC, Diemer M, Flexas J, Garnier E, Groom PK, Gulias J (2004)
58 961 The worldwide leaf economics spectrum. *Nature* 428:821–827.

1
2
3 962 Zhang Y, Lamarque LJ, Torres-Ruiz JM, Schuldt B, Karimi Z, Li S, Qin DW, Bittencourt P,
4 963 Burlett R, Cao KF, Delzon S, Oliveira R, Pereira L, Jansen S (2018) Testing the plant
5 964 pneumatic method to estimate xylem embolism resistance in stems of temperate
6 965 trees. *Tree Physiol* 38:1016–1025.
7
8
9
10
11
12
13
14
15
16
17
18
19
20
21
22
23
24
25
26
27
28
29
30
31
32
33
34
35
36
37
38
39
40
41
42
43
44
45
46
47
48
49
50
51
52
53
54
55
56
57
58
59
60

For Peer Review

1
2
3 967 **List of Figures**
4
5

6 968 **Figure 1** Stress indicators and hydraulic traits for small trees (1-10 cm DBH) measured in dry
7 969 season oct/2017 on the Control plot and through-fall exclusion (TFE).

9 970 **Figure 2** Hydraulic traits considered by genus for small trees (1-10 cm DBH) surviving after 15 years
10 971 of throughfall exclusion (TFE) and the Control plot.

12 972 **Figure 3** Drought stress indicators and considered by genus for small trees (1-10 cm DBH) surviving
13 973 after 15 years of throughfall exclusion (TFE) and the Control plot.

15 974 **Figure 4** Non-metric multidimensional scaling (NMDS) of drought stress indicators and hydraulic
16 975 traits.

18 976 **Figure 5** Hydraulic traits comparison between small trees and large trees from the throughfall
19 977 exclusion (TFE) and Control plot.

21 978 **Figure 6** Stress indicators comparison between small trees and large trees from throughfall
22 979 exclusion (TFE) and Control plot.

24 980 **Figure 7** Hydraulic traits comparison between small trees and large trees from throughfall
25 981 exclusion (TFE) and Control plot.

27 982 **Tables**
28
29

30
31
32 983 **Table 1** – Mean and standard deviation from small trees: P_{50} - xylem embolism resistance (MPa);
33 984 P_{88} - xylem embolism resistance (MPa); G_{\min} – minimum stomatal conductance ($\text{mol m}^{-2} \text{s}^{-1}$); K_s –
34 985 maximum hydraulic specific conductivity ($\text{kg m}^{-2} \text{s}^{-1} \text{MPa}^{-1}$); K_{sl} - maximum hydraulic leaf-specific
35 986 conductivity ($\text{kg m}^{-2} \text{s}^{-1} \text{MPa}^{-1}$); $A_L:A_{SW}$ – leaf to sapwood area ratio ($\text{m}^2 \text{m}^{-2}$); W_D - Woody density;
36 987 Ψ_{pd} - predawn water potential (MPa); Ψ_{md} - midday water potential (MPa); HSM – branch hydraulic
37 988 safety margin to P_{50} (MPa); PLC – native dry season percentage loss of conductivity (%), separated
38 989 by genus and treatment.
39
40
41
42
43
44
45
46
47
48
49
50
51
52
53
54
55
56
57
58
59
60

Hydraulic traits												
Genus (n individuals)	Treatment	P ₅₀	P ₈₈	G _{min}	K _s	K _{sl}	A _L :A _{SW}	W _D	Ψ _{pd}	Ψ _{md}	HSM	PLC
<i>Eschweilera</i> (3)	Control	-2.91±0.07	-5.08±0.31	0.028±0.023	1.12±0.19	0.57±0.30	112.07±32.41	0.73±0.12	-0.32±0.23	-1.68±0.24	1.13±0.32	49.14±4.9
<i>Eschweilera</i> (3)	TFE	-3.66±2.01	-6.32±3.80	0.026±0.019	2.80±2.62	4.71±6.12	92.12±65.44	0.59±0.09	-0.52±0.24	-1.87±0.26	1.89±2.28	9.22±4.36
<i>Inga</i> (4)	Control	-4.60±1.63	-7.84±3.10	0.02±0.014	2.3±1.43	1.56±0.85	84.59±47.51	0.64±0.18	-0.37±0.26	-1.51±0.57	3.09±2.07	11.33±10.19
<i>Inga</i> (3)	TFE	-3.48±0.58	-6.22±1.62	0.02±0.006	4.56±1.68	1.93±0.73	160.81±58.68	0.63±0.08	-0.39±0.22	-1.35±0.78	2.13±0.4	19.28±13.21
<i>Licania</i> (4)	Control	-5.28±1.98	-9.62±4.40	0.025±0.014	0.15±0.04	0.12±0.07	66.15±24.41	0.76±0.062	-0.25±0.07	-1.65±0.85	3.62±2.75	38.29±28.52
<i>Licania</i> (4)	TFE	-6.18±1.59	-9.07±1.77	0.024±0.02	2.17±2.19	0.37±0.40	104.90±45.99	0.761±0.014	-0.85±0.81	-1.388±0.78	5.183±1.70	68.667±28.13
<i>Mouriri</i> (3)	Control	-4.77±0.54	-7.69±1.31	0.025±0.017	0.62±0.05	0.22±0.20	154.33±59.51	0.867±0.003	-0.24±0.09	-0.943±0.08	3.829±0.48	58.031±27.65
<i>Mouriri</i> (3)	TFE	-5.55±0.74	-7.35±2.18	0.077±0.022	3.63±3.03	1.32±0.88	143.30±92.13	0.751±0.17	-1.07±1.32	-2.583±0.95	2.972±0.77	60.769±15.83
<i>Ocotea</i> (3)	Control	-3.59±1.49	-8.72±2.63	0.007±0.003	1.63±0.81	0.84±0.17	125.38±54.22	0.638±0.05	-0.36±0.4	-0.6±0.364	2.994±1.26	36.718±18.42
<i>Ocotea</i> (3)	TFE	-5.04±2.08	-8.61±4.88	0.03±0.024	1.58±0.66	0.60±0.46	84.83±32.64	0.68±0.13	-1.44±1.17	-2.41±0.81	2.62±2.45	65.27±24.19
<i>Protium</i> (5)	Control	-2.30±0.71	-4.16±2.40	0.017±0.01	1.68±0.94	0.75±0.41	78.60±6.37	0.74±0.07	-0.31±0.3	-1.23±0.31	1.07±0.78	54.73±17.02
<i>Protium</i> (3)	TFE	-3.64±1.47	-5.65±0.73	0.013±0.01	1.10±0.07	0.44±0.07	90.57±17.71	0.72±0.049	-0.48±0.16	-1.00±0.24	2.55±1.73	49.74±11.94
<i>Swartzia</i> (3)	Control	-3.17±1.28	-5.98±1.89	0.06±0.04	1.67±0.26	0.78±0.55	72.45±18.20	0.73±0.02	-0.23±0.12	-1.57±0.16	1.60±1.36	59.73±9.94
<i>Swartzia</i> (3)	TFE	-4.34±0.57	-6.94±0.06	0.06±0.02	2.78±0.51	0.89±0.54	210.45±67.51	0.72±0.005	-0.79±0.48	-2.36±0.09	1.98±0.66	49.13±8.57
<i>Tetragastris</i> (5)	Control	-2.31±1.48	-4.34±1.81	0.03±0.01	2.22±1.66	2.29±3.12	83.86±59.38	0.64±0.05	-0.28±0.13	-1.06±0.58	1.25±1.31	22.12±15.60
<i>Tetragastris</i> (3)	TFE	-4.36±1.19	-6.52±2.90	0.016±0.01	1.33±0.62	1.04±0.45	88.10±34.28	0.58±0.04	-1.43±0.40	-2.44±0.13	1.92±1.06	43.24±6.33
<i>Vouacapoia</i> (3)	Control	-3.57±0.13	-5.37±1.45	0.015±0.003	1.00±0.16	0.95±0.64	56.71±22.69	0.69±0.13	-0.39±0.18	-1.59±0.19	1.97±0.31	43.78±11.37
<i>Vouacapoia</i> (3)	TFE	-2.22±0.79	-3.54±1.63	0.012±0.004	0.83±0.51	0.67±0.78	229.76±101.26	0.70±0.01	-0.77±0.35	-2.07±0.24	0.15±0.72	33.24±19.67

991 **Table 2** Results of linear mixed effect models of plot (Control versus TFE) on the stress indicators
 992 and hydraulic traits for small trees (1-10 cm DBH) measured in dry season (Oct/2017) on the
 993 Control plot and through-fall exclusion TFE. WD - wood density; AL:ASW - leaf to sapwood area
 994 ratio; P50 - xylem embolism resistance; P88 - xylem embolism resistance; Gmin - minimum
 995 stomatal conductance; Ks - maximum hydraulic specific conductivity; Ksl - maximum hydraulic
 996 leaf -specific conductivity; Ψ_{pd} - predawn water potential; Ψ_{md} - midday water potential. HSM -
 997 branch hydraulic safety margin to P50; PLC - native dry season percentage loss of conductivity. The
 998 table shows the least square means for the Control and TFE, and the random genus effects (see
 999 analysis section in Methods for details). The first row of each trait gives the mean and second row
 1000 gives one standard error for the fixed effects and the 95% confidence interval for genus-level
 1001 random effects. Traits for which plot had a significant effect, and species for which the random
 1002 effects were different from zero, are marked with * ($p < 0.05$), ** ($p < 0.01$) and *** ($p < 0.001$)
 1003 and ns (non-significant).

Variable	Plot-level Coefficients			Genus-level Coefficients							
	Control	TFE	Eschweilera	Inga	Licania	Mouriri	Ocotea	Protium	Swartzia	Tetragastris	Vouacapoa
P₅₀	3.56 (-4.12/-2.99)	-4.26 (-5.761/-2.79) ns	-3.29 (-4.67/-1.91) ***	0.83 (-2.56/0.90)	2.38 (-4.11/-0.65) **	1.87 (-3.65/-0.09) *	-1.03 (-2.81/0.75)	0.60 (-1.13/2.33)	-0.35 (-2.20/1.50)	0.21 (-1.48/1.90)	0.39 (-1.39/2.17)
P₈₈	6.49 (-7.45/-5.42)	-6.58 (-9.34/-4.00) ns	-5.71 (-8.18/-3.24) ***	1.44 (-4.54/1.65)	3.69 (-6.78/-0.59) *	-1.82 (-5.01/1.37)	-2.96 (-6.15/0.22)	1.11 (-1.98/4.21)	-0.66 (-3.97/2.65)	0.54 (-2.48/3.57)	1.25 (-1.94/4.43)
G_{min}	0.027 (0.02/0.03)	0.030 (0.008/0.053) ns	0.03 (0.01/0.04) ***	0.01 (-0.03/0.01)	0.00 (-0.02/0.02)	0.03 (0.01/0.05) **	-0.01 (-0.03/0.01)	-0.01 (-0.03/0.01)	0.04 (0.02/0.06) ***	0.00 (-0.02/0.02)	-0.01 (-0.03/0.01)

		1.46	2.32	1.79	1.48	-0.49	0.34	-0.19	-0.33	0.33	0.17	-0.88
	K_s	(0.95/2.00)	(0.98/3.64) *	(0.46/3.13) **	(-0.28/3.23)	(-2.24/1.26)	(-1.47/2.15)	(-2.00/1.63)	(-2.03/1.38)	(-1.56/2.22)	(-1.58/1.92)	(-2.69/0.93)
		1.00	1.22	2.23	0.51	-1.96	-1.45	-1.51	-1.59	-1.41	-0.29	-1.42
	K_{sl}	(0.45/1.55)	(0.21/2.58) ns	(0.86/3.61) **	(-2.31/1.29)	(-3.76/-0.17)	(-3.31/0.40)	(-3.37/0.35)	(-3.34/0.16)	(-3.35/0.54)	(-2.09/1.50)	(-3.28/0.44)
		90.77	131.70	104.09	13.17	-18.57	44.73	1.02	-21.00	23.56	-18.64	39.15
	A_L:A_{sw}	(69.76/110.74)	(81.14/183.50) **	(48.95/159.23) ***	(-59.03/85.37)	(-88.86/51.73)	(-29.93/119.39)	(-73.64/75.68)	(-91.29/49.29)	(-54.42/101.54)	(-88.93/51.65)	(-35.52/113.81)
		0.71	0.68	0.68	0.03	0.09	0.13	-0.01	0.06	0.05	-0.05	0.03
	W_D	(0.68/0.75)	(0.59/0.78) ns	(0.60/0.75) ***	(-0.14/0.07)	(-0.01/0.19)	(0.03/0.24) **	(-0.12/0.10)	(-0.04/0.16)	(-0.06/0.16)	(-0.15/0.06)	(-0.08/0.13)
		0.31	0.86	-0.42	0.04	0.13	0.24	0.48	-0.03	0.03	0.29	0.17
	Ψ_{pd}	(0.14/0.48)	(0.63/1.52) ***	(-0.05/0.90)	(-0.69/0.61)	(-0.50/0.76)	(-0.44/0.91)	(-0.19/1.15)	(-0.66/0.60)	(-0.67/0.74)	(-0.34/0.92)	(-0.51/0.84)
		1.29	1.93	-1.78	0.34	-0.26	-0.02	-0.27	-0.63	0.11	-0.20	0.05
	Ψ_{md}	(1.09/1.54)	(1.50/2.19) **	(1.19/2.37) ***	(-1.14/0.46)	(-1.03/0.52)	(-0.85/0.81)	(-1.10/0.56)	(-1.41/0.14)	(-0.76/0.98)	(-0.98/0.57)	(-0.78/0.88)
		2.25	2.35	1.52	1.16	2.77	1.88	1.29	-0.02	0.24	-0.02	-0.46
	HSM	(1.64/2.86)	(0.74/3.96) ns	(0.05/2.99) *	(-0.69/3.01)	(0.93/4.62) **	(-0.02/3.78)	(-0.61/3.19)	(-1.87/1.83)	(-1.74/2.21)	(-1.82/1.79)	(-2.36/1.45)
		41.315	45.82	33.18	18.44	22.47	26.22	17.82	19.68	22.31	-4.01	5.33
	PLC	(32.38/49.21)	(24.14/67.78) ns	(15.62/50.74) ***	(-41.43/4.56)	(-0.52/45.47)	(2.44/50.00) *	(-5.96/41.60)	(-2.70/42.07)	(-2.52/47.15)	(-27.79/19.77)	(-18.45/29.11)

1004

1005

Table 3. Results of linear mixed effect models of size (Large versus Small) on the stress indicators and hydraulic traits for small trees (1-10 cm DBH) and large trees (>20 cm DBH) measured in dry season (Oct/2017) on the Control plot and through-fall exclusion TFE. WD - wood density; AL:ASW - leaf to sapwood area ratio; P50 - xylem embolism resistance; P88 - xylem embolism resistance; Gmin - minimum stomatal conductance; K_s - maximum hydraulic specific conductivity; K_{sl} - maximum hydraulic leaf -specific conductivity; Ψ_{pd} - predawn water potential; Ψ_{md} - midday water potential. HSM - branch hydraulic safety margin to P50; PLC - native dry season percentage loss of conductivity. The table shows the least square means for the Control and TFE, and the random genus effects (see analysis section in Methods for details). The first row of each trait gives the mean and second row gives one standard error for the fixed effects and the 95% confidence interval for genus-level random effects. Traits for which plot had a significant effect, and species for which the random effects were different from zero, are marked with * (p < 0.05), ** (p < 0.01) and *** (p < 0.001) and ns (non-significant).

Plot-level Coefficients			Genus-level Coefficients				
Variable	Large	Small	Eschweilera	Inga	Licania	Protium	Swartzia
P ₅₀	-2.66 (-3.24/-2.08)	-4.06 (-5.20/-2.93) ***	-2.654 (-3.382/-1.926) ***	-0.824 (-1.798/0.150) ns	-1.526 (-2.540/-0.513) **	0.014 (-0.985/1.013) ns	-0.593 (-1.592/0.406) ns
P ₈₈	-4.83 (-5.87/-3.80)	-7.08 (-9.18/-5.02) ***	-4.83 (-6.16/-3.49) ***	-1.35 (-3.13/0.44) ns	-2.53 (-4.39/-0.67) **	0.21 (-1.62/2.04) ns	-1.02 (-2.85/0.81) ns
G _{min}	0.08 (0.06/0.09)	0.02 (0.007/0.06) ***	0.07482 (0.053/0.09) ***	-0.01930 (-0.049/0.010) ns	-0.02935 (-0.05941/0.00071) *	-0.03583 (-0.066/-0.005) *	0.01851 (-0.011/0.048) ns
K _s	4.60 (2.20/5.58)	2.10 (1.09/4.33) ***	3.88 (2.59/5.16) ***	1.98 (0.28/3.68) *	-2.81 (-4.69/-0.94) **	-0.90 (-2.64/0.83) ns	-0.30 (-2.11/1.52) ns
K _{sl}	6.13 (5.06/7.19)	5.00 (3.09/6.89) *	4.35 (3.42/5.28) ***	0.90 (-0.41/2.21)	1.55 (0.24/2.86) **	1.56 (0.29/2.83) **	2.98 (1.69/4.28) ***
W _D	0.70 (0.61/0.70)	0.60 (0.52/0.67) ***	0.63 (0.59/0.67) ***	0.01 (-0.04/0.06) ns	0.05 (0.00/0.11) *	-0.05 (-0.11/0.00) *	0.05 (-0.01/0.10) ns
Ψ _{pd}	-0.44 (-0.50/-0.38)	-0.44 (-0.61/-0.28) ns	-0.48 (-0.59/-0.36) ***	0.04 (-0.12/0.20) ns	0.09 (-0.07/0.25) ns	-0.05 (-0.21/0.11) ns	0.08 (-0.08/0.24) ns
Ψ _{md}	-1.75 (-2.04/-1.46)	-1.50 (-1.98/-1.02) **	-1.85 (-2.07/-1.63) ***	0.17 (-0.12 to 0.47) ns	0.54 (0.24/0.84) ***	0.41 (0.11/0.71) ***	-0.23 (-0.54/0.08) ns
HSM	0.90	2.70	0.92	0.97	1.96	0.21	0.27

1
2
3
4
5
6
7
8
9
10
11
12
13
14
15
16
17
18
19
20
21
22
23
24
25
26
27
28
29
30
31
32
33
34
35
36
37
38
39
40
41
42
43
44
45
46

	(1.09/2.32)	(1.32/3.91)***	(0.10/1.74) **	(-0.13/2.08) ns	(0.82/3.11) ***	(-0.92/1.34) ns	(-0.85/1.40) ns
PLC	19.50	42.03	19.19	-4.71	12.90(-2.14/27.94) ns	20.93	16.15
	(8.91/30.75)	(23.13/60.94)***	(8.87/29.50) ***	(-18.36/8.93) ns		(7.02/34.84) **	(1.56/ 30.74) *

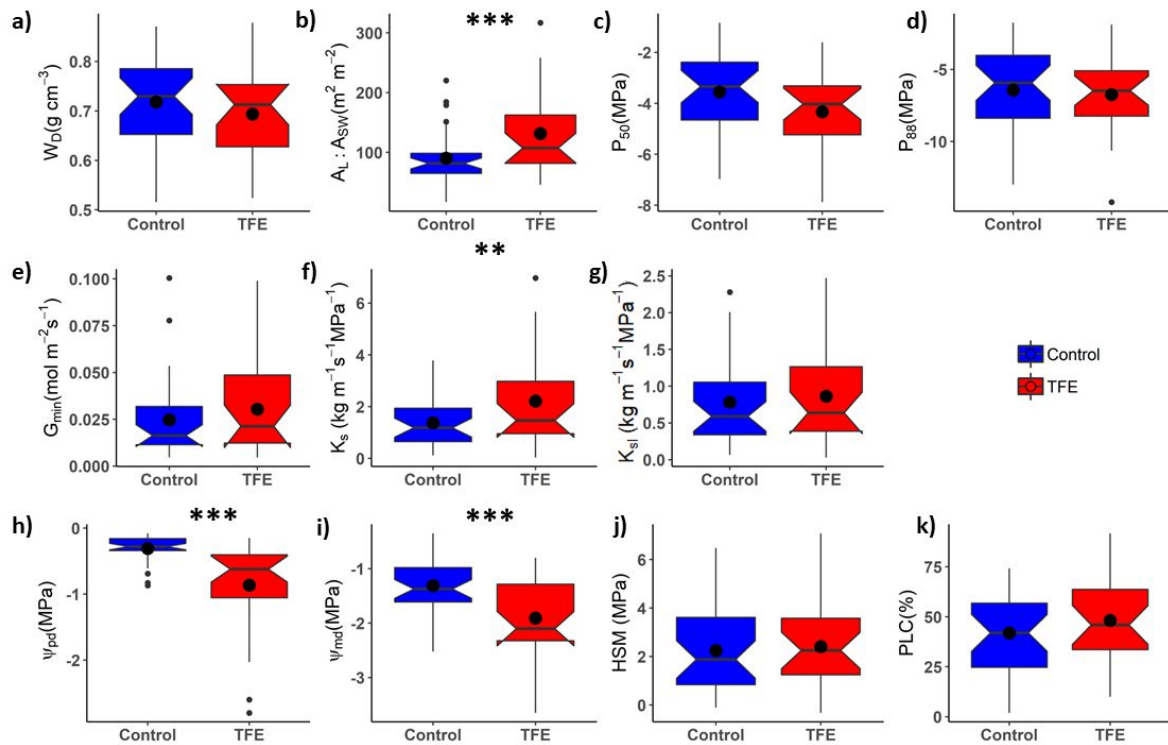
For Peer Review

1020

1021

Figures

1022



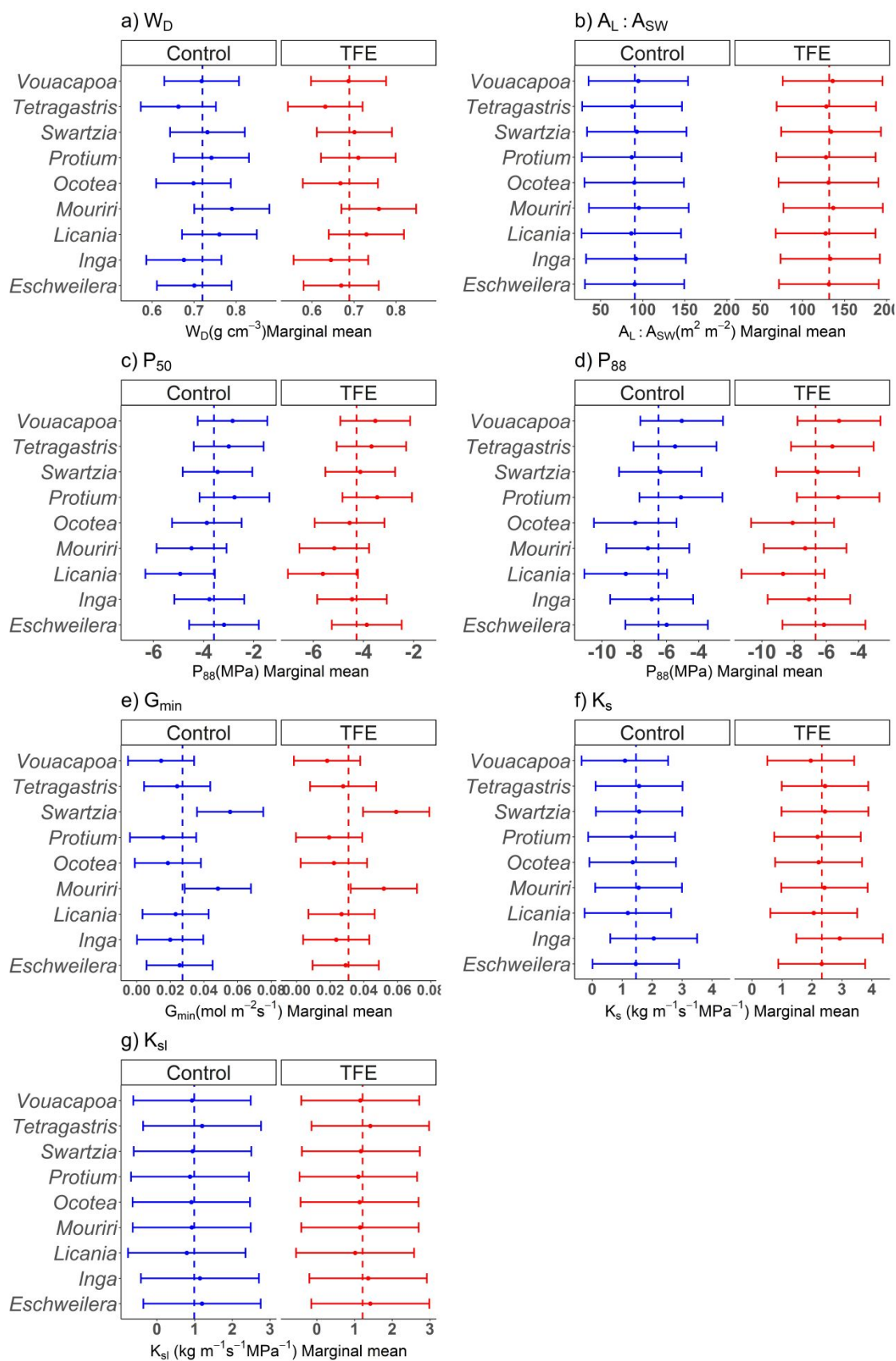
1023

1024 **Figure 1** Stress indicators and hydraulic traits for small trees (1-10 cm DBH) measured in dry season
 1025 oct/2017 on the Control plot (blue) and through-fall exclusion (TFE, red). a) W_D – wood
 1026 density b) $A_L:A_{SW}$ - leaf to sapwood area ratio c) P_{50} - xylem embolism resistance; d) P_{88} - xylem
 1027 embolism resistance; e) G_{min} – minimum stomatal conductance; f) K_s – maximum hydraulic specific
 1028 conductivity; g) K_{sl} - maximum hydraulic leaf -specific conductivity; h) Ψ_{pd} - predawn water
 1029 potential; i) Ψ_{md} - midday water potential. j) HSM – branch hydraulic safety margin to P_{50} ; l) PLC –
 1030 native dry season percentage loss of conductivity. The boxes represent quartiles 1 and 3, the
 1031 central line indicates the median and the black points the mean of each treatment. Whiskers are
 1032 either maximum value or 1.5 interquartile range above quartile 3, if outliers are present and
 1033 notches represents a confidence interval around the median represented by central line. Traits for
 1034 which plot had a significant effect are marked with * ($p < 0.05$), ** ($p < 0.01$) and *** ($p < 0.001$).
 1035 P-values are from mixed effects analysis (see Table 2 for models and analysis section in Methods

1036

1037

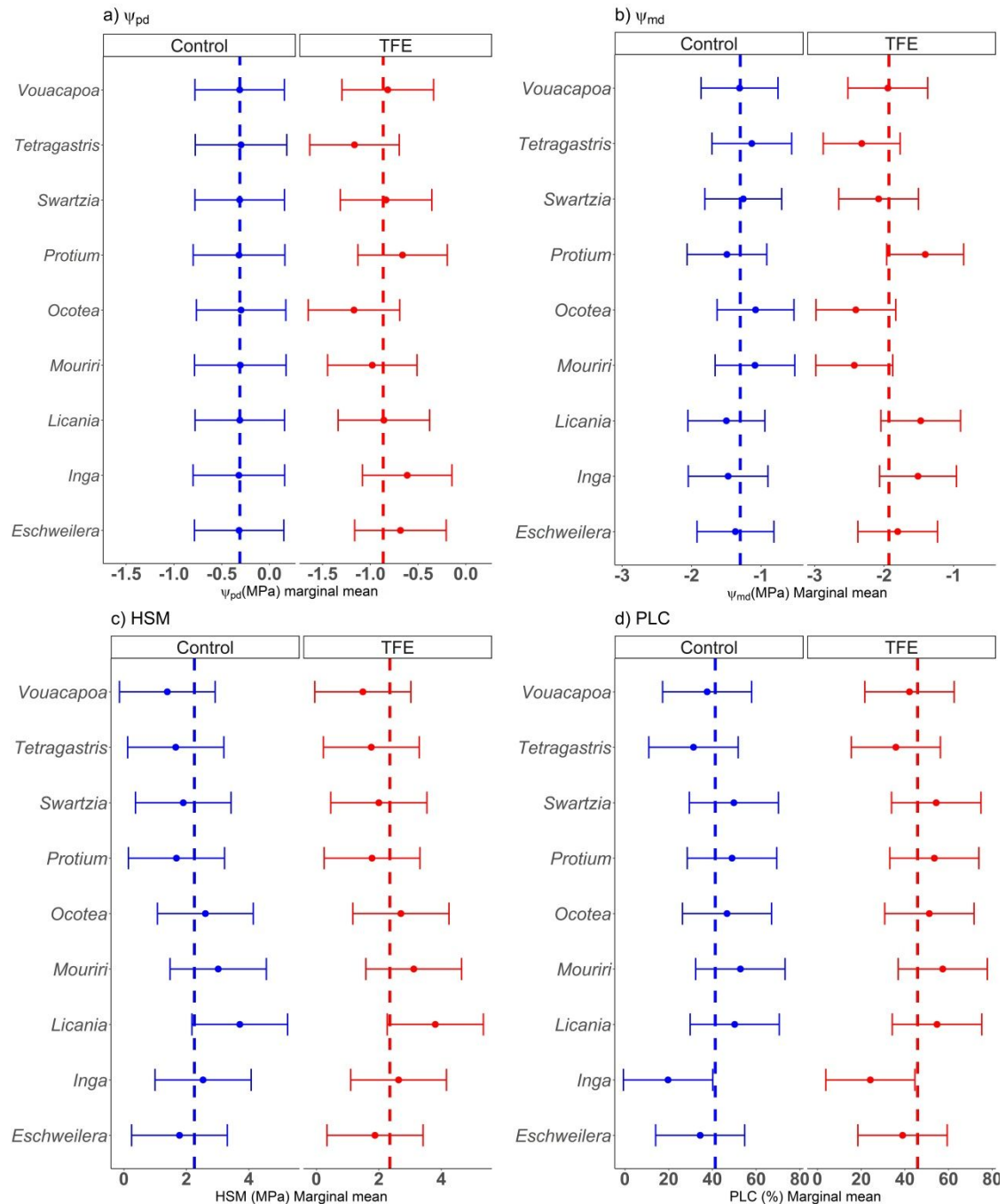
1038



1039

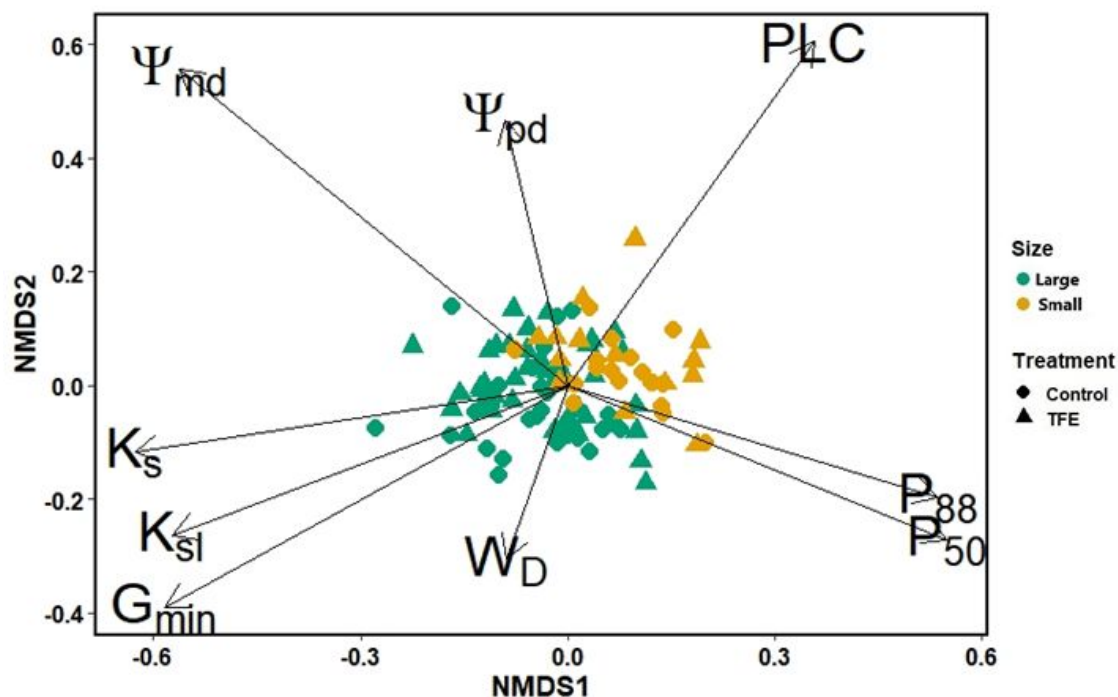
1040 **Figure 2** Hydraulic traits by genus for small trees (1-10 cm DBH) surviving after 15 years of
 1041 throughfall exclusion (TFE – red) and the Control plot (blue). a) W_D - wood density b) $A_L:A_{SW}$ - leaf
 1042 to sapwood area ratio c) P_{50} - xylem embolism resistance; d) P_{88} - xylem embolism resistance; e)

1043 G_{\min} - minimum stomatal conductance; f) K_s - maximum hydraulic specific conductivity; g) K_{sl} -
 1044 maximum hydraulic leaf -specific conductivity. The vertical dashed coloured lines represent the
 1045 marginal fixed effects for plot. The points represent random effects plus fixed effect mean by
 1046 genus and the horizontal lines represents standard error for each genus (see Table 2 for models
 1047 and analysis section in Methods).



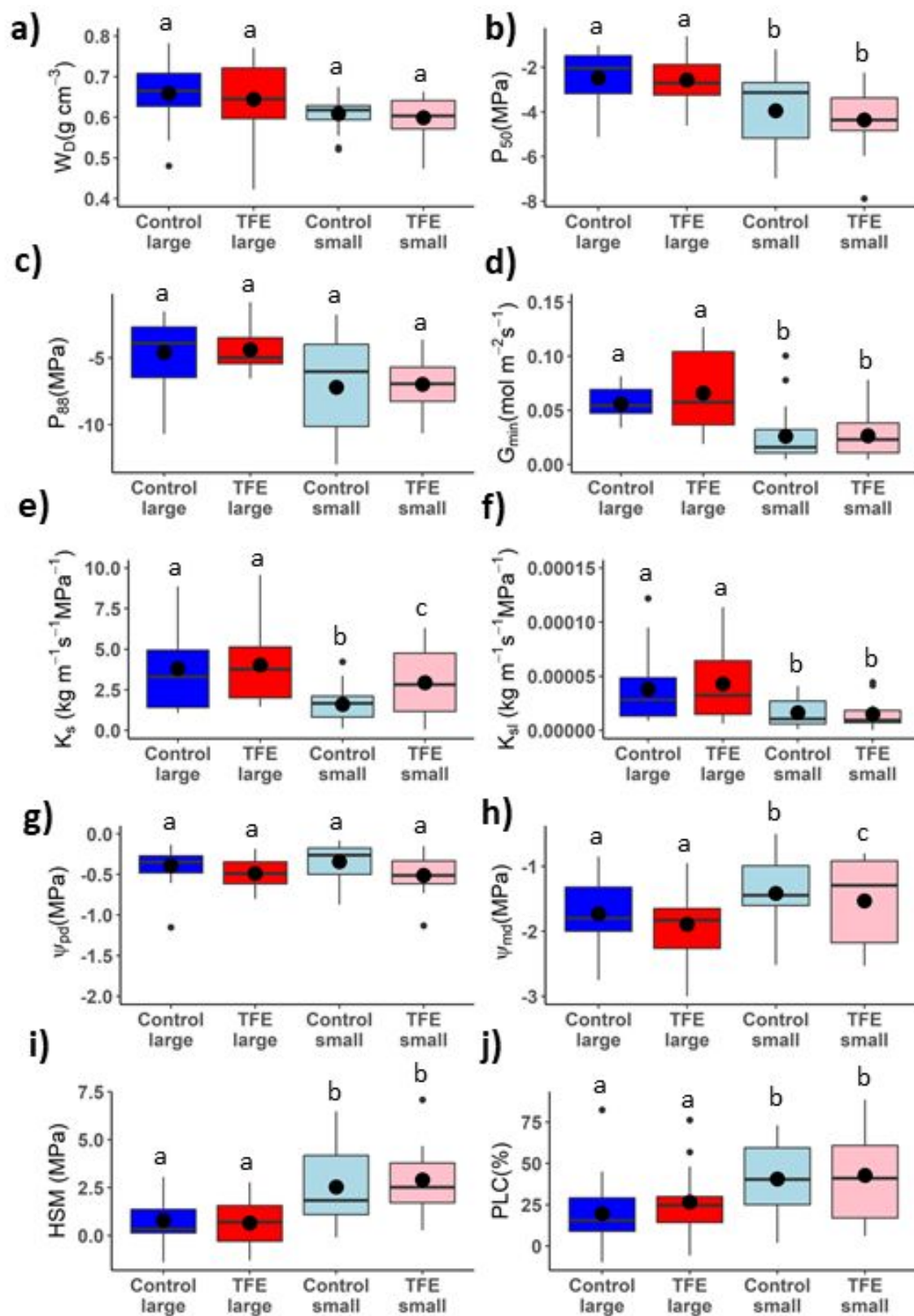
1048
 1049 **Figure 3** Drought stress indicators considered by genus for small trees (1-10 cm DBH) surviving
 1050 after 15 years of throughfall exclusion (TFE – red) and the Control plot (blue). a) Ψ_{pd} - predawn
 1051 water potential; b) Ψ_{md} - midday water potential. c) HSM – branch hydraulic safety margin to P_{50} ;
 1052 d) PLC – native dry season percentage loss of conductivity. The vertical dashed lines represents
 1053 marginal fixed effects for plot, the points represents random effects plus fixed effect mean by
 1054 genus and the horizontal lines represents standard error by genus (see Table 2 for models and
 1055 analysis section in Methods).

1056



1057

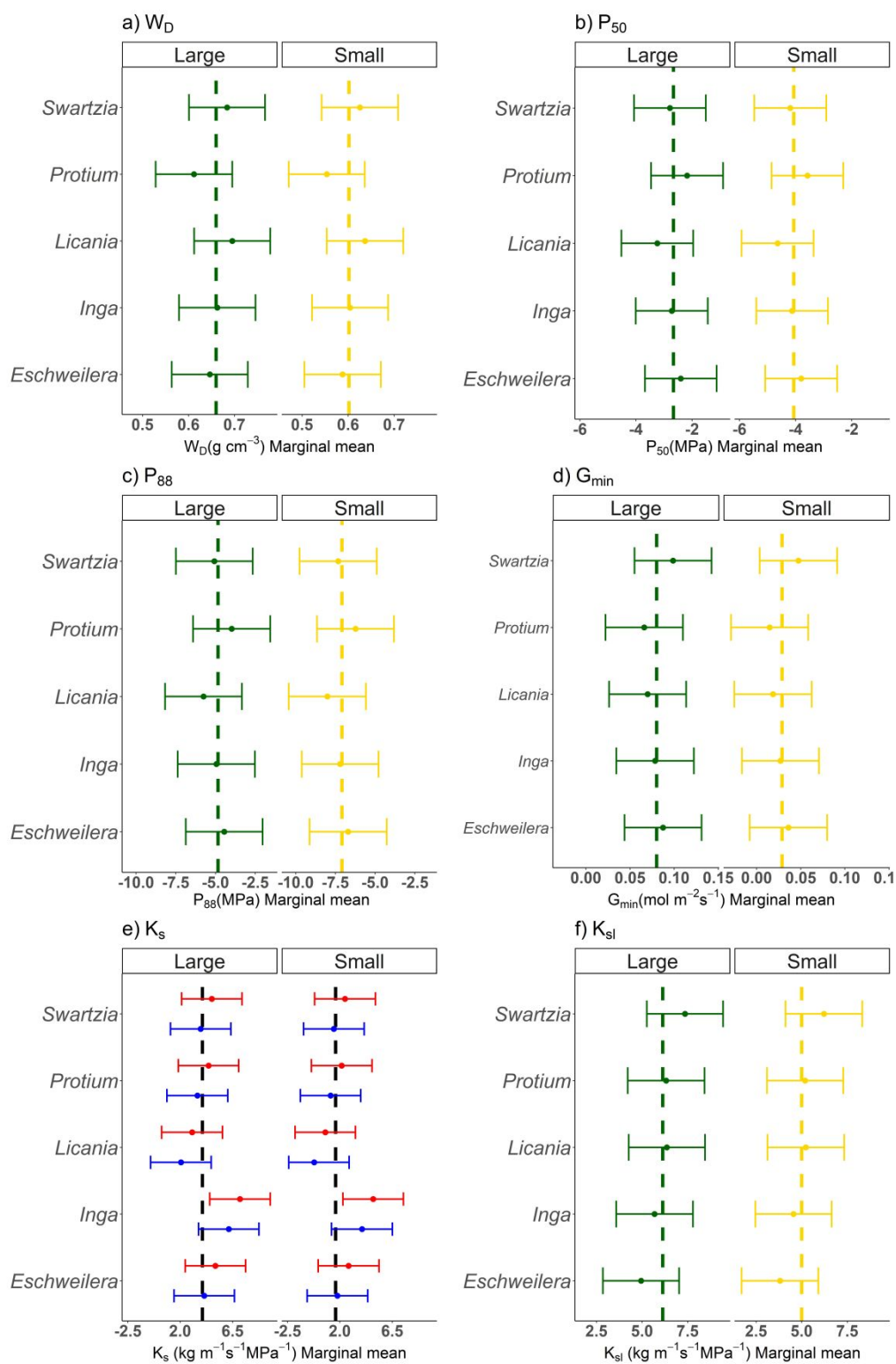
1058 **Figure 4** Non-metric multidimensional scaling (NMDS) of drought stress indicators and hydraulic
 1059 traits. Ordination showing multidimensional space filled by small (yellow) and large (green) trees
 1060 indicating distinct hydraulic ecological strategies (MANOVA; $P < 0.05$) between trees from the TFE
 1061 and Control. Hydraulic traits represented by arrows (Arrow length represent predictor "strength").
 1062 Dots represent individuals in Control and triangles individuals in TFE treatment. The green colour
 1063 represents large trees and yellow represents small trees.



1064

1065 **Figure 5** Comparison between small trees and large trees from the throughfall exclusion (TFE) and
 1066 Control plots. a) W_D – wood density; b) P_{50} - xylem embolism resistance; c) P_{88} - xylem embolism
 1067 resistance; d) G_{min} – minimum stomatal conductance; e) K_s – maximum hydraulic specific
 1068 conductivity; f) K_{sl} - maximum hydraulic leaf -specific conductivity; g) Ψ_{pd} - predawn water
 1069 potential; h) Ψ_{md} midday water potential; i) HSM – branch hydraulic safety margin to P_{50} ; j) PLC –

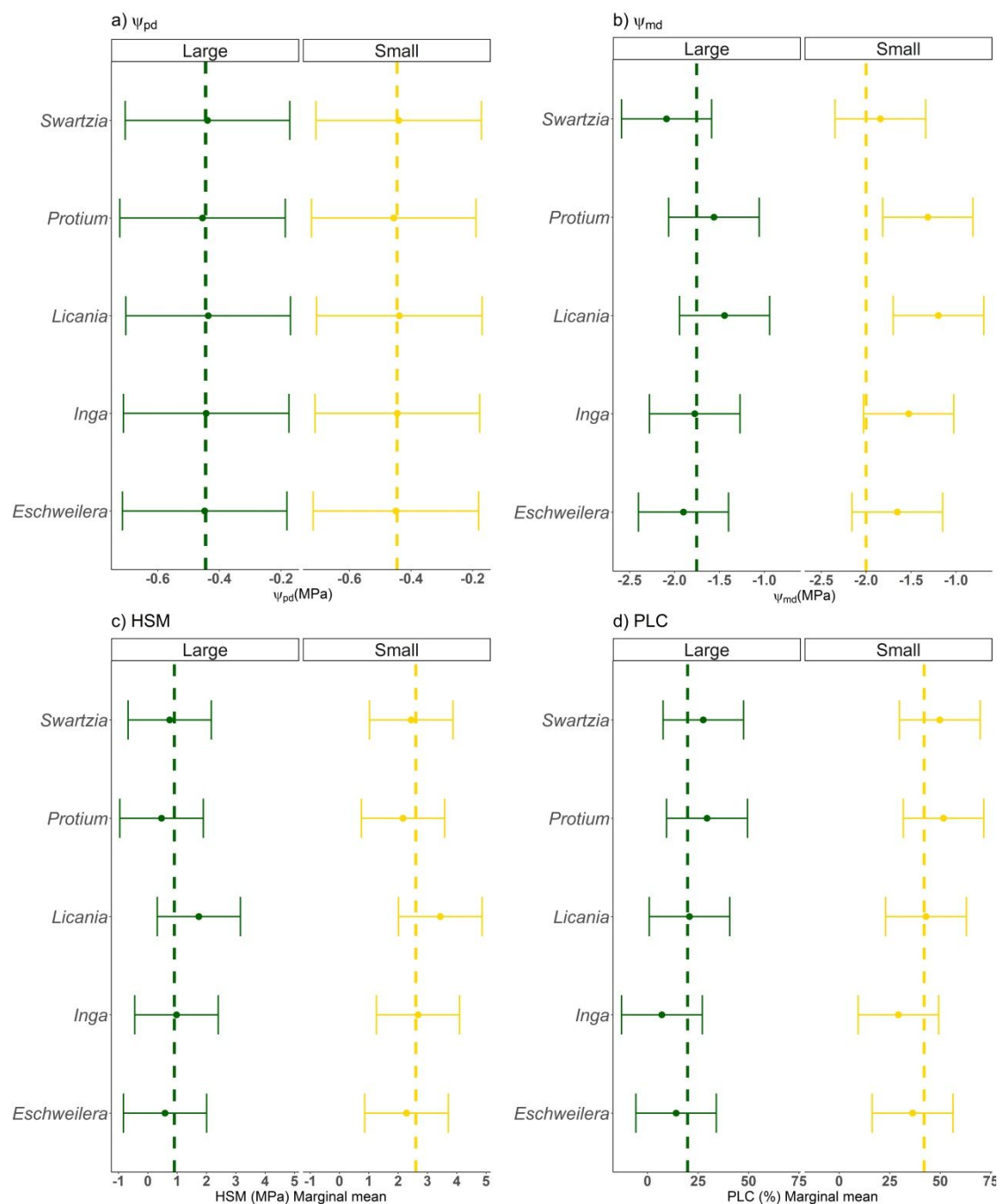
1070 native dry season percentage loss of conductivity. The boxes represent quartiles 1 and 3, the
 1071 central line indicates the median and the black points the mean of each treatment. Whiskers are
 1072 either maximum value or 1.5 interquartile range above the quartile 3, when outliers are present.
 1073 Different letters indicate significant differences within each graph, $p < 0.05$.



1074

1075 **Figure 6** Hydraulic traits comparison between small trees and large trees from throughfall
 1076 exclusion (TFE) and Control plot. a) W_D – wood density; b) P_{50} - xylem embolism resistance; c) P_{88} -
 1077 xylem embolism resistance; d) G_{min} – minimum stomatal conductance; e) K_s – maximum hydraulic

1
2
3 1078 specific conductivity; f) K_{sl} - maximum hydraulic leaf-specific conductivity. The vertical dashed lines
4 1079 represents marginal fixed effect mean, green vertical lines represents large trees and yellow
5 1080 vertical lines, the points represents random plus fixed effect mean by each level (by genus) and
6 1081 the horizontal lines represents standard error by each random effects level. The blue and red in
7 1082 horizontal lines represents Control and TFE plot, respectively and are show when a significant plot
8 1083 effect was found. All points and lines represent genus in each treatment (see Table 3 for models
9 1084 and analysis section in Methods).



1085

1086 **Figure 7** Drought stress indicators comparison between small trees and large trees from
1087 throughfall exclusion (TFE) and Control plot. a) Ψ_{pd} - predawn water potential; b) Ψ_{md} - midday
1088 water potential. c) HSM – branch hydraulic safety margin to P50; d) PLC – native dry season
1089 percentage loss of conductivity. The vertical dashed lines represents marginal fixed effect mean,
1090 the points represents random effects plus fixed effect mean by each level (by genus) and the

1
2
3 1091 horizontal lines represents standard error by each random effects level. All points and lines
4 1092 represent genus in each treatment. P-values are from mixed effects analysis (see Table 3 for
5 1093 models and analysis section in Methods).
6
7
8
9
10
11
12
13
14
15
16
17
18
19
20
21
22
23
24
25
26
27
28
29
30
31
32
33
34
35
36
37
38
39
40
41
42
43
44
45
46
47
48
49
50
51
52
53
54
55
56
57
58
59
60

For Peer Review

1
2
3
4
5
6
7
8
9
10
11
12
13
14
15
16
17
18
19
20
21
22
23
24
25
26
27
28
29
30
31
32
33
34
35
36
37
38
39
40
41
42
43
44
45
46
47
48
49
50
51
52
53
54
55
56
57
58
59
60

1 **Small understorey trees have greater capacity than canopy trees to adjust hydraulic**
2 **traits following prolonged experimental drought in a tropical forest**

3 **Running title:** Tree size strongly controls plant hydraulic responses in a droughted tropical
4 forest

5 **Giles, A. L.**^{1*}, Rowland L.², Bittencourt P. R. L.², Bartholomew, D. C.², Coughlin I.^{4,5}, Costa
6 P. B.^{1,7}, Domingues T.⁴, Miatto, R.C.⁴, Barros, F. V.², Ferreira L. V.⁶, Groenendijk, P.¹, Oliveira
7 A. A. R.⁶, da Costa A. C. L.^{6,7}, Meir P.^{5,9}, Mencuccini M.^{10,11}, Oliveira R. S.¹

8
9 *Corresponding Author: andregiles.bio@gmail.com, ¹Instituto de Biologia, University of
10 Campinas (UNICAMP), Campinas, SP 13083-970, Brasil.

11
12 ¹Instituto de Biologia, University of Campinas (UNICAMP), Campinas, SP 13083-970, Brasil.

13 ²College of Life and Environmental Sciences, University of Exeter, Exeter, EX4 4RJ, UK

14 ³Biological Sciences, UWA, Perth, WA, Crawley 6009, Australia

15 ⁴Departamento de Biologia, FFCLRP, Universidade de São Paulo, Ribeirão Preto, SP 14040-
16 900, Brasil

17 ⁵Research School of Biology, Australian National University, Canberra, ACT 2601 Australia

18 ⁶Museu Paraense Emílio Goeldi, Belém, PA 66040-170, Brasil

19 ⁷ Biological Sciences, UWA, Perth, WA, Australia

20 ⁸Instituto de Geosciências, Universidade Federal do Pará, Belém, PA 66075-110, Brasil

21 ⁹School of GeoSciences, University of Edinburgh, Edinburgh, EH9 3FF, UK

22 ¹⁰CREAF, Campus UAB, Cerdanyola del Vallés, 08193 Spain

23 ¹¹ICREA, Barcelona, 08010, Spain
24

Abstract

Future climate change predictions for tropical forests highlight increased frequency and intensity of extreme drought events. However, it remains unclear whether large and small trees have differential strategies to tolerate drought due to the different niches they occupy. The future of tropical forests is ultimately dependent on the capacity of small trees (<10 cm in diameter) to adjust their hydraulic system to tolerate drought. To address this question, we evaluated whether the drought tolerance of neotropical small trees can adjust to experimental water stress and was different from tall trees. We measured multiple drought resistance-related hydraulic traits across nine common neotropical genera at the world's longest-running tropical forest throughfall-exclusion experiment and compared their responses with surviving large canopy trees. Small understorey trees in both the Control and the throughfall exclusion treatment (TFE) had lower minimum stomatal conductance and maximum hydraulic leaf-specific conductivity relative to large trees of the same genera, as well as greater hydraulic safety margin (HSM), percentage loss of conductivity (PLC) and embolism resistance, demonstrating they occupy a distinct hydraulic niche. Surprisingly, in response to the drought treatment, small trees increased specific hydraulic conductivity by 56.3% and leaf:sapwood area ratio by 45.6%. The greater HSM of small understorey trees relative to large canopy trees likely enabled them to adjust other aspects of their hydraulic systems to increase hydraulic conductivity and take advantage of increases in light availability in the understorey resulting from the drought-induced mortality of canopy trees. Our results demonstrate that differences in hydraulic strategies between small understorey and large canopy trees drive hydraulic niche segregation. Small understorey trees can adjust their hydraulic systems in response to changes in water and light availability indicating natural regeneration of tropical forests following long-term drought may be possible.

Key-words: Long-term drought; Understorey trees; Hydraulic Safety margin; P50; Maximum conductivity; Acclimation; Amazon forest.

59 **Introduction**

60 Climate change predictions for tropical forests comprise increased frequency and intensity
61 of extreme drought events (Aragão et al., 2018; Brodribb, Powers, Cochard, & Choat,
62 2020) and long-term reductions in soil moisture availability (Corlett 2016, Christensen et
63 al. 2017). Most studies relating to drought focus on the impacts on large trees that
64 comprise the highest proportion of forest biomass (Meir et al. 2015, Rowland, da Costa, et
65 al. 2015), often finding the effect of drought stress on a plant's hydraulic system is a key
66 driver of tree mortality (Bittencourt et al., 2020; Brodribb et al., 2020; Rowland et al.,
67 2015). However, small understorey trees not only are responsible for up to 20% of the
68 forest carbon sink (Hubau et al. 2019) but have a fundamental role in recruitment and the
69 maintenance of tree populations, as they will effectively compose the future pool of large
70 tree in the forest. Thus, small trees may be critical in determining long-term drought
71 responses if there is extensive loss of large canopy trees (Rowland, da Costa, et al. 2015,
72 Esquivel-Muelbert et al. 2017).

73 Large trees occupy canopy positions (hereafter, large trees) with high light levels and high
74 vapor pressure deficit. In contrast, small trees from the same genus occupy understory
75 positions (hereafter small trees), grow slowly, generally in shaded conditions and
76 experience a lower atmospheric vapor pressure deficit (Sterck et al. 2011). The distinct
77 resource partitioning between small and large trees, (Brum et al., 2019; Poorter, Bongers,
78 Sterck, & Wöll, 2005) could cause strong differences in their water supply and demand
79 relative to large trees. Reduced water supply from the roots, alongside lower capacitance,
80 is likely to cause more negative water potentials in small trees relative to larger ones,
81 during periods of low soil moisture (Salomón et al. 2017). Large trees are more likely to

1
2
3 82 buffer periods of water deficit with greater water access by deep roots (Brum et al. 2019),
4
5 83 higher capacitance (Mcculloh et al. 2014), and elevated carbohydrate storage that allow
6
7
8 84 to maintain either prolonged stomatal opening (deep roots) or prolonged stomatal closure
9
10 85 (greater storage) (McDowell et al., 2008). These potential size-dependent variations in
11
12
13 86 structural and physiological traits suggest tree size potentially influences a tree's capacity
14
15 87 to acclimate in response to severe drought stress.

16
17
18 88 Several key traits of the hydraulic system of a plant are essential in determining the
19
20
21 89 capacity of a tree to survive prolonged drought stress. These traits are often related to
22
23 90 preventing hydraulic failure, via emboli formation, in the xylem vessels (Sperry and Tyree
24
25 91 1988), which can lead to severe decreases in leaf water supply, photosynthesis and other
26
27
28 92 physiological functions (Sperry et al. 2002, McDowell et al. 2008, Martinez-Vilalta et al.
29
30 93 2019). These key traits include the water potentials at which the xylem lose 50% or 88% of
31
32
33 94 their conductance (P50 or P88, respectively) and the hydraulic safety margin (HSM)
34
35 95 (Meinzer et al. 2009), i.e., the difference between the minimum leaf water potential that is
36
37
38 96 naturally experienced and P50, effectively a metric of the risk of a plant crossing a critical
39
40 97 hydraulic threshold. Following sustained periods of drought stress, a tree's capacity to
41
42
43 98 survive is likely to be related to its capacity to acclimate certain key drought tolerance
44
45 99 traits or to limit its demand for water, via traits such as minimum stomatal conductance,
46
47
48 100 thus reducing stress on its hydraulic system (Sala et al. 2010, Meir et al. 2018). Existing
49
50 101 studies on large trees show limited capacity for tropical trees to adjust plant hydraulic
51
52
53 102 traits in response to drought stress (Binks et al., 2016; Bittencourt et al., 2020; Powell et
54
55 103 al., 2017; Schuldt et al., 2011). Some studies have shown that the risk of embolism can be
56
57
58 104 reduced by increasing HSMs under drought conditions (Awad et al. 2010, Tomasella et al.
59
60 105 2018, Prendin et al. 2018). However, in a tropical forest drought experiment, large trees

1
2
3 106 were found to have limited plasticity in leaf level anatomy (Binks et al., 2016) and no
4
5 107 capacity to acclimate their hydraulic systems, especially in traits relating to embolism
6
7
8 108 resistance (Bittencourt et al., 2020; Powell et al., 2017; Rowland et al., 2015). Yet, to our
9
10 109 knowledge, no studies have evaluated whether small trees (<10 cm diameter at breast
11
12 110 height, DBH), contrary to adult trees, have the capacity to adjust their hydraulic system to
13
14 111 prolonged drought stress. Following high mortality losses in large, more drought-
15
16 112 intolerant, trees, small trees can increase photosynthetic capacity (Bartholomew et al.,
17
18 113 2020;) and lower canopy trees can increase growth rates, even following drought (Brando
19
20 114 et al., 2008; Rowland et al., 2015). This suggests that small trees can increase performance
21
22 115 in response to elevated light, despite drier conditions. Increased light availability would
23
24 116 also require these small trees to the increased atmospheric water demand, implying the
25
26 117 need to increase water supply from their hydraulic system and/or to sustain a lower xylem
27
28 118 water potential. However, these adjustments to conditions of severe drought only seem
29
30 119 to be possible if small trees have a greater drought tolerance, functioning with higher
31
32 120 levels of embolism resistance and hydraulic safety margin (HSM). Consequently,
33
34 121 consideration of ecosystem changes, such as canopy loss and shifting light availability, is
35
36 122 likely to be as important as the consideration of the direct impact of soil moisture stress
37
38 123 following long-term drought, as both factors may influence hydraulic acclimation within
39
40 124 small trees.

41
42 125 Here we take advantage of a unique drought experiment located in northeast Amazonia
43
44 126 (Meir et al. 2015, 2018) to evaluate the response of small trees to combined changes in
45
46 127 water and light availability. Previous research at this site has shown that large trees (>40
47
48 128 cm DBH) had significantly higher mortality rates, when compared to small trees and to
49
50 129 trees in adjacent control forest, leading to a 40% reduction in biomass following 14 years

1
2
3 130 of experimentally-imposed soil drought (da Costa et al., 2010; Rowland et al., 2015, Meir
4
5 131 et al. 2018). This biomass loss was almost entirely from trees reaching the upper canopy,
6
7
8 132 which led to increased levels of light in the understory and increased growth rates of small
9
10 133 understory trees in the wet season (da Costa et al., 2014; Metcalfe, et al., 2010; Rowland
11
12 134 et al., 2015, Meir et al. 2018). Furthermore elevated radiation loads are likely to have
13
14 135 increased leaf vapour pressure deficit and temperature, increasing the atmospheric
15
16 136 drought effect these small trees experience (Mulkey & Pearcy 1992a; Kamaluddin & Grace
17
18 137 1992; Krause, Virgo & Winter 1995). Using new data from this soil drought experiment
19
20 138 (henceforth *throughfall-exclusion experiment* – TFE), we explore how small trees adjust
21
22 139 hydraulic traits in response to increases in light availability coupled with increased drought
23
24 140 stress, specifically, if small trees are able to adjust traits to novel light conditions whilst
25
26 141 under drought stress. Thus, we test whether small trees (1-10 cm DBH) alter their plant
27
28 142 hydraulic system in response to prolonged soil moisture stress and increased canopy
29
30 143 openness, and determine how these responses vary relative to those of large trees (>20
31
32 144 cm DBH). We address the following hypotheses:

33
34
35
36
37
38
39
40 145 1) Considering the same genus we hope that the hydraulic systems of small trees
41
42 146 adjust to the combined soil-drought and radiation-load conditions imposed in the TFE
43
44 147 relative to the Control. We expect small trees in TFE treatment to take advantage of the
45
46 148 increased canopy openness by increasing their water transport efficiency (greater
47
48 149 hydraulic specific conductivity and leaf-sapwood ratios). At the same time, we predict that
49
50 150 small trees will have more negative water potentials resulting from drought conditions
51
52 151 and the capacity to compensate this by adjusting hydraulic traits to maintain higher
53
54 152 hydraulic safety margins to meet the elevated canopy water demands in support of
55
56 153 photosynthesis.
57
58
59
60

1
2
3 154 2) Small trees have different hydraulic strategies from large trees. Specifically, we predict
4
5
6 155 that, independent of the drought and radiation responses in the TFE, small trees have
7
8 156 greater drought tolerance, higher xylem embolism resistance and larger hydraulic safety
9
10 157 margins, relative to large trees. We therefore predict that, as a consequence of those trait
11
12
13 158 differences, small trees occupy a different hydraulic trait space from large trees.
14
15
16
17
18
19
20
21
22
23
24
25
26
27
28
29
30
31
32
33
34
35
36
37
38
39
40
41
42
43
44
45
46
47
48
49
50
51
52
53
54
55
56
57
58
59
60

For Peer Review

1
2
3 **Methods**

4
5
6 *Site and plant material*

7
8
9 Our study site is a lowland tropical rainforest located in the Caxiuanã National
10
11 Forest, state of Pará, north-east Brazil (1°43'S, 51°27 W). It has an annual rainfall of 2000-
12
13 2500mm, with a dry season (< 120 mm monthly rainfall) from July to December. A
14
15 throughfall exclusion (TFE) experiment was established in 2002, where 50% of canopy
16
17 throughfall is excluded by a plastic panel structure installed at 1-2m height over a 1 ha
18
19 area (Meir et al. 2018). The TFE plot was studied alongside a 1 ha Control plot, where no
20
21 throughfall exclusion took place. The plots have been monitored continuously since 2001
22
23 and further information on the experimental set-up can be found in earlier papers (da
24
25 Costa *et al.*, 2010; Fisher *et al.*, 2007; Meir *et al.*, 2015 and Rowland *et al.*, 2015b).
26
27
28
29

30
31 From August-September 2017, during the peak of the dry season, we sampled 74
32
33 small trees with diameters ranging from 1 to 10 cm at breast height (1.3 m). We measured
34
35 41 small trees on the Control plot and 33 on the TFE, all taken from nine genera (20
36
37 species), replicated in each plot (two to five individuals per genera per plot). While we
38
39 tried to maintain the same range of tree heights within each genus between plots, small
40
41 trees had more variable height in the TFE, with light-exposed individuals reaching over 15
42
43 meters height, whilst no individuals in the Control reached 15 metres height (See Fig. S1).
44
45 It was not possible to know the age of each sampled individual, because (destructive)
46
47 sampling for age determination (tree-ring analyses; e.g., Brien et al., 2016) was not
48
49 possible. Consequently, we must assume that our sampled trees may have strongly
50
51 varying ages (Groenendijk et al. 2014). We thus test the influence of tree stature and
52
53
54
55
56
57
58
59
60

1
2
3 181 position within the forest strata (van der Sleen et al. 2015), while assuming that most of
4
5 182 our sampled trees are likely to be young.

6
7
8 183 For each individual, we collected two branches from the top of the crown,
9
10 184 representing the point maximally exposed to light. The branches were third to fourth
11
12 185 order (30-55 mm of diameter), counting from the tip. We collected one set of branches
13
14 186 before sunrise (0400 to 0600 hours) and used these to measure embolism resistance and
15
16 187 predawn leaf water potential. We collected a second set of branches at midday (1130 to
17
18 188 1330 hours) and used these to measure midday leaf water potential, native embolism,
19
20 189 leaf-to-sapwood area, xylem and leaf specific conductivity, minimum leaf conductance
21
22 190 and wood density measurements. Immediately after collection, branches were bagged in
23
24 191 thick black plastic sacks with moist paper to humidify internal air and minimise leaf
25
26 192 transpiration. Branches were transported 100m from the plots to measure leaf water
27
28 193 potential, and for the remaining measurements the branches were transported to a
29
30 194 laboratory ~1km walk away.

31
32
33 195 We measured predawn leaf water potential (Ψ_{pd}), taken to represent the time-
34
35 196 point when transpiration is at its minimum and the water potential of the plant is closest
36
37 197 to equilibrium with that of the soil. Ψ_{pd} can be considered an integrated metric of soil
38
39 198 water availability across the rooting depth (Bartlett et al. 2016). We also determined
40
41 199 midday water potential (Ψ_{md}), to capture the minimum Ψ of the plant in the dry season.
42
43 200 This measure is affected by any cuticular or stomatal transpiration and, thus, broadly
44
45 201 captures the integrated effects of plant traits and the environment water demand on the
46
47 202 minimum water potential a plant reaches in natural conditions. We also measured the
48
49 203 native dry-season percentage loss of conductivity (PLC). We used the difference between
50
51
52
53
54
55
56
57
58
59
60

1
2
3 204 the minimum leaf water potential (Ψ_{md}) and P_{50} , to calculate the branch hydraulic safety
4
5 205 margin (HSM). These two values (native PLC and HSM) were used as indicators of the
6
7
8 206 cumulative damage from embolism.
9

10 11 207 *Predawn and midday water potential* 12

13
14 208 Predawn and midday leaf water potentials were measured in the field immediately
15
16 209 after collection, using a pressure chamber (Model 1505, PMS). Branches collected for
17
18 210 predawn water potential measures were sampled before sunrise, and for midday water
19
20 211 potential, the sampling took place between 1130 to 1330 hours. For each tree we
21
22 212 measured water potential of two leaves, or three leaves if the first two measures differed
23
24 213 substantially (>0.5 MPa difference) from one another. Measurements from multiple leaves
25
26 214 were averaged to create a single value per tree. All water potential measurements were
27
28 215 taken on the same day for small trees and across three days for large trees.
29
30
31
32

33 34 216 *Wood density, leaf to sapwood area ratio and minimum stomatal conductance* 35

36
37 217 We measured wood density (W_D) on woody sections 40 to 80 mm long with a
38
39 218 diameter of 4 to 7 mm. We debarked samples, immersed them in water for 24 hours to
40
41 219 rehydrate and measured the saturated volume using the water displacement method
42
43 220 (Pérez-Harguindeguy *et al.*, 2013). We then oven dried the samples at 60°C until they
44
45 221 were a constant mass and measured their dry weight with a precision balance to 3
46
47 222 decimal places.
48
49
50

51
52
53 223 We determined the leaf to sapwood area ratio ($A_L:A_{sw}$), on all branches by
54
55 224 measuring leaf area and calculating sapwood area from two diameter measurements of
56
57 225 the debarked basal part of the branch using precision callipers at a standardised distance
58
59 226 from the tip. To avoid overestimation we checked the absence of pith area in all branches
60

1
2
3 227 per species before the measurement. We measured leaf area by scanning all leaves on the
4
5 228 branch and quantifying their area using Image J software (version 1.6.0_20; Schneider et
6
7 229 al., 2012). We calculated the leaf area to sapwood area ratio as total branch leaf area
8
9 230 divided by its basal sapwood area. All branches had a similar size and were standardised
10
11 231 by distance to the tip (~40-70 cm). The $A_L:A_{SW}$ is a key indicator of the balance between
12
13 232 transpirative demand and water supply capacity (Mencuccini et al. 2019).

14
15
16
17
18 233 For minimum leaf conductance (G_{min}), we used the leaf conductance to water
19
20 234 vapour measured on the abaxial surface of leaves kept 30 minutes in the dark, using an
21
22 235 infrared gas analyser (Li-COR 6400, US). All measured leaves were fully formed and
23
24 236 undamaged leaves. G_{min} is a measure key indicator of residual leaf water loss and likely a
25
26 237 due to a combination of leakage stomatal conductance from partially from leakage of
27
28 238 partially closed stomata and cuticular conductance (Duursma et al. 2019, Binks et al. 2020,
29
30 239 Márquez et al. 2021)., see Rowland *et al.* (2020) and Bartholomew et al. (2020), provide
31
32 240 further details on gas exchange measurement.

33 34 35 36 37 38 241 *Hydraulic efficiency and native embolism*

39
40
41 242 We used maximum hydraulic specific conductivity (K_s) as a measure of xylem
42
43 243 hydraulic efficiency and maximum leaf specific conductivity (K_{sl}) as a measure of leaf water
44
45 244 supply capacity. We used the native percentage loss of conductivity of the collected
46
47 245 branches (PLC) as a measure of native embolism. To PLC, we measured branch xylem
48
49 246 hydraulic conductivity before (K_{snat} – native conductivity) and after flushing to remove
50
51 247 emboli (K_s). We quantified the leaf area distal to each sample to obtain K_{sl} from K_l (leaf
52
53 248 conductance). Using samples from the branches collected at midday, we put the entire
54
55 249 branch underwater and discarded a 10 cm long segment from the base. After this, we cut
56
57
58
59
60

1
2
3 250 another 10-15 cm long segment from the base of each branch underwater, standard
4
5
6 251 distance from the tip of the branch and let them rehydrate for 15 min to release tension
7
8 252 and avoid artefacts (Venturas et al. 2015). Subsequently, to relax the tension in the branch
9
10 253 we cut 1-1.5 cm of branch from base to leaves underwater, in steps of ~15 cm, and used
11
12 254 the distal end of the branch for hydraulic measurements to ensure no artificially
13
14 255 embolised vessels were present in the measured sample. All samples used for hydraulic
15
16 256 measurements were second or third order branches, between 30-55 mm in length and 3-5
17
18 257 mm diameter and were recut underwater with a sharp razor blade before connecting to
19
20 258 the apparatus, to ensure all vessels were open at both ends. We then measured flow in
21
22 259 the sample using the Ventury tube method (Tyree et al. 2002, Pereira and Mazzafera
23
24 260 2013), where known resistance (PEEK capillary) is connected in series with the sample and
25
26 261 the pressure drop in the capillary is proportional to flow in the sample. K_{snat} is then
27
28 262 calculated from the pressure head applied and water flow. The samples are then flushed
29
30 263 to remove emboli and estimate K_s (Martin-StPaul et al., 2014). We used pressure
31
32 264 transducers (26PCCFA6G, Honeywell; read with a OM-CP-VOLT101A data logger, Omega
33
34 265 Engineering) to measure pressure drop in the capillary and measured the capillary
35
36 266 resistance prior to measurements using precision scales. The samples remained under-
37
38 267 water throughout the entire procedure. We calculated PLC as the ratio of K_{snat} to K_s
39
40 268 multiplied by 100. We calculated K_{sl} as the sample hydraulic conductivity (i.e., sample
41
42 269 conductance times sample length) after flushing divided by the leaf area distal to the
43
44 270 measured sample.

45
46
47
48
49
50
51
52
53
54
55 271 *Embolism resistance and hydraulic safety*
56
57
58
59
60

1
2
3 272 As an index of xylem embolism resistance, we used P_{50} and P_{88} , the xylem water
4
5 273 potentials where, respectively, 50% and 88% of hydraulic conductivity is lost. We also used
6
7
8 274 P_{50} to calculate the hydraulic safety margin - the difference between P_{50} and Ψ_{md} , an index
9
10 275 of tree hydraulic safety. Branches collected before sunrise were rehydrated for 24 hours
11
12
13 276 and from each branch we cut two or three smaller branches of approximately 40-70 cm.
14
15 277 We measured the xylem embolism resistance of each branch using the pneumatic method
16
17
18 278 (Pereira et al. 2016, Zhang et al. 2018). With this method, the loss of hydraulic
19
20 279 conductance is estimated from the increase in air volume inside the wood caused by
21
22
23 280 embolism formation as the branch dehydrates. Air volume is estimated from the air
24
25 281 discharge from the cut end of the branch into a vacuum reservoir (~50 kPa absolute
26
27
28 282 pressure) of known volume during a given amount of time (2.5 minutes). We measured
29
30 283 initial and final pressure inside the vacuum reservoir with a pressure transducer
31
32
33 284 (163PC01D75, Honeywell) and calculated the volume of air discharged using the ideal gas
34
35 285 law. A detailed protocol is presented in (Pereira et al. 2016, Bittencourt et al. 2018) and
36
37
38 286 revised by Pereira et al. (2021). Percentage loss of conductance for each branch is
39
40 287 estimated from percentage air discharged (PAD) during its dehydration. PAD is calculated
41
42
43 288 by standardising air discharge for each branch by its minimum (fully hydrated) and
44
45 289 maximum (most dehydrated) air discharge state. We dehydrated branches using the
46
47
48 290 bench dehydration method (Sperry et al. 1988). Before each air discharge measurement,
49
50 291 branches were sealed in thick black plastic bags for one hour for leaf and wood xylem
51
52 292 water potential to equilibrate. Directly after the air discharge was measured, we
53
54
55 293 estimated wood xylem water potential by measuring the leaf water potential of one to
56
57 294 two leaves. Drought embolism resistance is then given by the increase in PAD with
58
59 295 decreasing xylem water potential for each tree. To calculate P_{50} , we pooled data from the
60

296 two-to-three branch replicates from the same tree and fitted a sigmoid curve to the data
 297 (Pammenter and Van der Willigen 1998) where P_{50} and slope (a) are the fitted parameters
 298 and P_{88} is predicted from the fit (Eqn 1):

$$PAD = 100 / (1 + \exp(a(\Psi - P_{50})))$$

(1)

300 **Eqn1.** Percentage air discharge equation (PAD). Ψ Water potential. P_{50} (xylem embolism
 301 resistance (MPa)

302 *Data analysis*

303 By comparing trees found on the Control and TFE experimental plots, we measure the
 304 effect of the experimental drought on our drought stress indicators (Ψ_{pd} , Ψ_{md} - midday
 305 water potential; HSM – branch hydraulic safety margin to P_{50} ; PLC – native dry season
 306 percentage loss of conductivity) and plant traits (W_D – wood density; $A_L:A_{SW}$ - leaf to
 307 sapwood area; P_{50} - xylem embolism resistance; P_{88} - xylem embolism resistance; G_{min} –
 308 minimum stomatal conductance; K_s – maximum hydraulic specific conductivity; K_{sl} -
 309 maximum hydraulic leaf -specific conductivity) in small trees. We used linear mixed effects
 310 models to test for plot (TFE vs Control) and taxonomic effects (genus and species) on
 311 hydraulics traits in small trees ($n = 66$) using the R package lme4 (Bates et al. 2015). We
 312 tested the significance of the random effect by removing it and evaluating if the model
 313 significantly worsened using log likelihood tests using the *ranova* function for *lmerTest*
 314 objects (Zuur et al. 2009). We tested sequentially for the random effect of genus on: (a)
 315 the model intercept; (b) the fixed Plot effect (drought effect, difference between plots) on
 316 slope without intercept; and (c) both intercept and plot. When either the genus effect on
 317 plot, slope or both did not show the significance, we kept the multilevel approach using

1
2
3 318 genus as a random effect on the intercept (1|genus), as it controls for experimental design
4
5 319 (Burnham and Anderson 2004). After testing the random effects, we tested the fixed TFE
6
7
8 320 effect on variables. When taxonomy was included as a random effect in our models, we
9
10
11 321 tested for both genus-only and species-nested-within-genus effects. We tested the
12
13 322 complete model (genus and species as a random effect) against a General Linear Model
14
15 323 (GLM) containing only the fixed effects. In all variables genus was significant as random
16
17
18 324 effect. Therefore, linear models with genus as a random effect were used to test the
19
20 325 significance of the fixed effects. To quantify model goodness of fit, we considered the
21
22 326 marginal and conditional R^2 (Mulkey and Pearcy 1992b). The marginal R^2 indicates how
23
24 327 much of the model variance is explained by the fixed effects only, whereas the conditional
25
26 328 R^2 indicates how much of the model variance is explained by the complete model with
27
28 329 fixed and random effects. All the analyses were done in R (version 3.3.0; R Core Team,
29
30 330 2016)

331 *Small and large tree comparisons*

332 We tested for differences in individual tree-level responses to the TFE treatment for large
333 (n = 72) and small trees (n = 39). We use the large trees data from Bittencourt et al. (2020)
334 conducted in the same experimental plots and collected during 2017 with the same
335 methodological procedures. For this comparison we restrict the samples to those trees
336 whose genera are replicated on both plots and replicated between the large and small
337 trees, with a minimum sample size of 2 individuals per size group per plot and genus.
338 Consequently, the number of genera and individuals employed in this comparison is lower
339 than the available number of individual small trees and the full dataset published in
340 Bittencourt et al., (2020). In total we use five genera (*Eschweilera*, *Inga*, *Licania*, *Protium*,

1
2
3 341 *Swartzia*), with 15 small trees on the Control and 24 small trees on the TFE, and 35 large
4
5 342 trees on the Control and 37 large trees on the TFE. We used linear mixed-effect models to
6
7
8 343 test the effects of the tree size with two classes (large and small), and tree size on drought
9
10 344 stress indicators and hydraulic traits. Taxonomic effects were included by using genus as
11
12 345 random effects, following the same protocol used for the small tree analyses, presented
13
14 346 above. Within this paper, all data presented represent the mean and standard errors of
15
16
17 347 the mean. A summary of available trait data by genus is presented in Table 1.

18
19
20 348 To test for an overall difference in the hydraulic strategy between small and large trees,
21
22 349 we used the multivariate approach conducting non-metric multidimensional scaling
23
24 350 (NMDS) using an individual-traits matrix (McCune & Grace 2002). We construct a matrix of
25
26 351 data consisting of rows of individuals of each species and columns of traits values. We
27
28 352 standardized the individual trait values for each genus and built the similarity matrix using
29
30 353 Gower distance. NMDS searches for the best position of individuals variables on k
31
32 354 dimensions (axes) to minimize the "stress" of the resulting k-dimensional configuration.
33
34 355 We use k axes = 2 from that ordination as the initial configuration. The "stress" is obtained
35
36 356 by comparison among the pair-wise distances (differences) of each individual's variables in
37
38 357 reduced ordination space (expressed in terms of axes) and the original distance matrix
39
40 358 (Gower distance). The regression is fitted using least-squares regressions and the
41
42 359 goodness of fit is measured as the sum of squared differences between ordination-based
43
44 360 distances and the distances predicted by the regression. A goodness of fit, or stress value,
45
46 361 between 0.1 to 0.2 represent a good fit within the specified number of dimensions
47
48 362 analysed to enable points to be interpreted relative to the NMDS axes. Therefore, the axis
49
50 363 represents the data in a way that best represents their dissimilarity, points on the graph
51
52 364 that are closer together are more similar. In addition, we use MANOVA to test the
53
54
55
56
57
58
59
60

1
2
3 365 difference in multidimensional space filled by tree size (small and large groups) and by
4
5 366 plot effect (TFE and Control groups) separately (Anderson 2001). We use a MANOVA to
6
7
8 367 compare Gower distance among observations in the same group versus those in different
9
10 368 groups. We conducted a MANOVA first using small and large tree groups and then using
11
12
13 369 TFE and Control groups using both tree sizes together. The size and plot effects were
14
15 370 tested separately. Finally, we use permutations of the observations to obtain a probability
16
17
18 371 associated with the null hypothesis of no differences between groups.

21 372 **Results**

22
23
24 373 The reduced soil moisture availability and increased canopy openness caused by 15 years
25
26 374 of the TFE (Fig. S2) caused significant changes in the hydraulic traits of the small trees (Fig.
27
28
29 375 1). Maximum specific conductivity (K_s) increased significantly, by $56.3 \pm 41.5\%$, in the TFE
30
31 376 small trees relative to the Control (Fig. 1f, $p < 0.01$), similarly there was a significant
32
33 377 ($45.6 \pm 38.2\%$) increase in the leaf: sapwood area ratio ($A_L:A_{SW}$, Fig 1b.; $p < 0.001$). The TFE
34
35
36 378 also had significant effects on key physiological indicators of drought stress in small trees
37
38 379 (Fig. 1) with Ψ_{pd} 0.24 MPa lower on the TFE relative to the Control ($p < 0.001$) and Ψ_{md} 0.67
39
40
41 380 MPa lower ($p < 0.001$, Table S2). In contrast, other key hydraulic traits including xylem
42
43 381 embolism resistance (P_{50} and P_{88}), leaf specific conductivity (K_{sl}), minimum stomatal
44
45
46 382 conductance (G_{min}) and wood density (WD) showed no significant difference between the
47
48
49 383 TFE and the Control plots for small trees (Fig. 1; Table 2; Table S3).

50
51 384
52
53
54
55
56
57
58
59
60

1
2
3 385 **Taxonomic effects on hydraulic traits and their interactions with drought**
4

5 386 Using mixed-effect modelling analysis we found that the variance explained by taxonomy
6
7 387 had only a limited role in affecting the overall drought responses. When genus by genus
8
9 388 responses to the drought effect were examined separately, it was clear that there were
10
11 389 highly variable responses to the treatment among genera and sometimes these were
12
13 390 inconsistent in terms of direction, as well as magnitude. We cannot separate the
14
15 391 taxonomic effect from the residual variance because genus-specific influences on the plot
16
17 392 effect were highly variable (Fig. 2 and 3). Given the low replication (between 2 and 5 for
18
19 393 each genus on each plot treatment) and high variation within each genus, it was not
20
21 394 always statistically viable to test the plot effect within each genus (Fig. 2 and 3), however
22
23 395 where this was possible, clear statistical differences were seen for some genera but not
24
25 396 for others (Table 2 Fig. 2). For example, *Licania* showed consistent responses in P₅₀ and
26
27 397 HSM while *Ocotea* did not show differences between plots (Fig. 2 and 3). The patterns
28
29 398 described here were also maintained when we analysed the data at a species level (data
30
31 399 not shown).
32
33
34
35
36
37
38
39
40
41
42
43
44
45
46
47
48
49
50
51
52
53
54
55
56
57
58
59
60

401 ***Large versus small trees***

402 We compared the responses of hydraulic traits between large (>20 cm DBH) and small
403 trees (1-10 cm DBH). Except for Ψ_{pd} , the results we obtain considering only the five genera
404 that overlap between the small and large size classes, were similar to when considering all
405 nine genera of trees present in Control plot and TFE experiment (see Fig. S3
406 supplementary material and Table S3 for n values for the small to large tree comparisons).
407 Using all of the trait data for five overlapping genera, we applied NMDS ordination which
408 demonstrated that the niche space occupied by the small trees was significantly different
409 from the trait space of large trees. The traits space separated on to a clear 2-dimensional
410 axis with a stress score of 0.18, indicating a good fit between the data and an analysis
411 consisting of two axes (Fig. 4). Different associations amongst the nine hydraulic traits
412 separated the individuals in the small and large tree groups. This result was driven
413 predominantly by the first axis, which was positively related to PLC, P_{50} and P_{88} that
414 influenced small tree grouping (Fig. 4). While the first axis was negatively related to K_s , K_{sl} ,
415 G_{min} influencing large trees grouping (Fig 4, Table S4). Using the complete set of hydraulic
416 traits, we show that the hydraulic niche of small trees was significantly different from that
417 of large trees (MANOVA_(1,66); $F=7.96$; $p<0.001$; Table 1). However, there was no difference
418 in hydraulic niche space occupied by the Control and TFE groups (MANOVA_(1,64); $F=1.22$;
419 $p=0.30$), except for K_s that showed plot and tree size effects (MANOVA_(1,64); $F=3.5$; $p=0.05$).

420 In contrast to the large increase in K_s observed between small trees in Control and TFE
421 trees (Figs 1 & S2), the plot level average values of K_s were similar among large trees in
422 both Control and droughted conditions (4.82 ± 3.93 TFE and 4.86 ± 2.79 Control plot). Similar
423 to Ψ_{md} , notable plot level differences were present in small trees, but these were absent

1
2
3 424 in the large trees (-1.72 ± 0.48 MPa TFE and -1.70 ± 0.48 MPa Control treatment). However,
4
5 425 small trees had values of Ψ_{md} which were $17.12 \pm 0.03\%$ higher (values closer to 0) than the
6
7
8 426 large trees. Furthermore, for the variables which had no treatment effect amongst the
9
10 427 small trees, we find on average, across both the TFE and Control plots, the small trees had
11
12
13 428 a $38.20 \pm 32.10\%$ ($p < 0.01$) more negative P_{50} and a $68.40 \pm 58.80\%$ and $20.70 \pm 30.40\%$ lower
14
15 429 G_{min} and K_{sl} , respectively, than the large trees (Fig. 5b, 5d, 5f; $p < 0.001$). Also across the
16
17
18 430 plot we found that HSM increased by $72.97 \pm 36.34\%$ and PLC increased by $44.41 \pm 14.62\%$
19
20 431 in the small trees relative to large trees (Fig. 5g, 5i, 5j; $p < 0.01$).
21
22

23 432 We analysed the influence of genus on the combined effect of treatment and tree size
24
25 433 effect (i.e., large and small trees on the Control and TFE plot) for the five genera we could
26
27
28 434 replicate across plots and tree size classes. We found that the effects of tree size varied
29
30
31 435 substantially among genera and between traits and stress indicators (Fig. 6 and 7, table S5
32
33 436 and S6). For example, the difference in P_{50} between large trees and the small trees was
34
35 437 $61.48 \pm 52.51\%$ for *Licania* and $38.96 \pm 3.7\%$ for *Inga* (Fig. 6). In contrast, G_{min} was
36
37
38 438 significantly lower in the small trees relative to large trees across almost all genera (Fig.
39
40
41 439 6b). The drought-response pattern also changes when doing within-genus comparisons
42
43 440 between large and small trees, for example the mean P_{50} response for *Inga* was different
44
45 441 between small and large trees (Fig. 6). A difference in trait values between the Control and
46
47
48 442 TFE plots that was present either for small tree or large trees, but not for both size classes
49
50 443 simultaneously, occurred multiple times (Fig. 6 and 7), especially for the genus *Inga*.
51
52
53 444 Mixed effect modelling results identify a strong influence of genus on trait variation
54
55 445 between our two size classes (Table 3), yet there are limited cases where we find
56
57
58 446 significant models demonstrating trait differences between the Control and the TFE plot
59
60 447 with a significant tree size and genus effect (Table 3).

1
2
3 448 To test for size (small vs. large) and genus effects in each treatment (Control and TFE), we
4
5 449 created a model with both size and genus as fixed effects. In the Control plot the full
6
7
8 450 model (trait ~ genus*size) was a better predictor of variation across almost all traits,
9
10 451 except for K_s , where there was a genus only effect and G_{min} , P_{50} and P_{88} where there was a
11
12 size only effect. An interaction between size and genus was only significant for PLC (Table
13 452
14
15 453 S7). The full model was also the best predictor of trait variation in the TFE plot, although
16
17 only HSM, W_D and G_{min} showed a significant size effect. Significant interactions between
18 454
19
20 455 genus and size were found for P_{50} and P_{88} (Table S7).
21
22
23
24 456
25
26
27
28
29
30
31
32
33
34
35
36
37
38
39
40
41
42
43
44
45
46
47
48
49
50
51
52
53
54
55
56
57
58
59
60

1
2
3 457 **Discussion**
4

5 458 Our results provide the evidence that small trees can adjust their functioning in response
6
7 459 to drought, allowing them to maximize carbon gain in the higher-light levels following
8
9
10 460 mortality of large trees in the TFE. We find that small trees (1-10 cm DBH) have the
11
12 461 capacity to increase maximum specific hydraulic conductivity and leaf-sapwood area ratio
13
14 462 in response to prolonged (15 year) soil moisture deficit. Despite having significantly lower
15
16
17 463 pre-dawn and midday leaf water potentials, small trees had the capacity to adjust key
18
19
20 464 hydraulic traits to allow a positive response to a higher light environment. This suggests
21
22 465 that despite soil drought stress, small trees can still increase water transport efficiency
23
24 466 and canopy water use in response to increases in light availability, following drought-
25
26
27 467 induced mortality of large trees, potentially allowing them to maximise productivity in
28
29 468 periods of the year when water is available. We also show the different components of a
30
31
32 469 hydraulic strategy that provides niche segregation between small and large trees, with
33
34 470 small trees being more drought tolerant than large canopy trees.

35
36
37 471 Studying the effects of multiple factors (here, imposed drought and size) on the
38
39 472 physiology of hyper-diverse tropical forests is challenging. Here, we successfully addressed
40
41
42 473 this problem by using genus and species nested in genus as random factors in linear mixed
43
44 474 models and show that variability of species within genera is generally small. We
45
46
47 475 nonetheless acknowledge our sample size limitations and the possibility that greater
48
49 476 sampling depth may discover significant species-by-species variability in these traits.

50
51
52 477

53
54
55 478
56
57
58
59
60

479 **The impact of drought on the hydraulic system of small trees**

480 The substantial drought-related mortality of large trees (da Costa et al., 2010;
481 Rowland et al., 2015) in the 15 years preceding this study led to an increase in the light
482 availability in the lower canopy of the TFE, driving increases in the maximum
483 photosynthetic capacity (71.1% and 29.2% increase in J_{\max} and $V_{c_{\max}}$ respectively) and a
484 15.1% increase in the LMA of the same small trees we study here (Bartholomew et al.
485 2020). These differences in response to the prevailing light environment have also been
486 observed elsewhere in tropical tree canopies (Ruggiero et al. 2002, Domingues et al. 2010,
487 Cavaleri et al. 2010) and are indicative of plants changing their allocation strategy in
488 response to increased light availability (Poorter et al., 2009; Wright et al., 2004). Critically,
489 these allocation shifts are likely to result in a net increase in photosynthesis and growth
490 (Metcalf, Meir, Aragão, et al. 2010, Rowland, da Costa, et al. 2015, Meir et al. 2018),
491 which require higher water supply to the canopy of each individual. The elevated soil
492 moisture stress in the TFE relative to the Control trees manifested itself as significantly
493 more negative pre-dawn and midday leaf water potential values (Figs 1h-1i), key
494 indicators of plant water stress (Bhaskar & Ackerly, 2006; Kramer, 1988; Martínez-vilalta &
495 Garcia-Forner, 2017). Interestingly however, these more negative water potentials did not
496 translate into a significant change in HSM between plots, which would imply that the small
497 trees converge to have the same vulnerability to drought (Choat et al. 2012). This could
498 occur because of a trend, albeit not statistically detectable, towards more negative P50
499 values in the TFE plot for small trees, relative to the Control trees (Fig. 1), making a
500 significant difference in HSM less likely. When examined at the genus level, five of the
501 nine genera have consistently more negative P_{50} values on the TFE relative to the Control,
502 with two remaining roughly equal and two less negative on the TFE (Fig. 2). These data

1
2
3 503 suggest that, despite operating at more negative water potentials, it is still possible for
4
5 504 small trees to adjust their hydraulic system to support the increased growth in response to
6
7
8 505 greater light availability.
9

10
11 506 Consistent with increases in photosynthetic capacity (Bartholomew et al., 2020),
12
13 507 we observe an increase in leaf area to sapwood area ratio ($A_L:A_{SW}$) in the small trees on the
14
15
16 508 TFE, relative to the Control. Combined with greater hydraulic specific conductivity, small
17
18 509 trees in the TFE are therefore able to supply water to more photosynthetic tissue without
19
20
21 510 increasing the volume of sapwood. A global study, including multiple sites from the tropics
22
23 511 showed plant hydraulic systems are highly sensitive to changes in this ratio ($A_L:A_{SW}$) and
24
25 512 may be one of the main factors controlling trade-offs in other plant hydraulic traits
26
27 513 (Mencuccini et al. 2019). Increasing leaf area increases the total water demand of the
28
29 514 tree; however, the observed increases in photosynthetic capacity (high values of $V_{c_{max}}$ and
30
31 515 J_{max} , Bartholomew et al. 2020), may allow slightly lower stomatal conductance for any
32
33 516 given CO_2 concentration (Bartholomew et al., 2020; Sperry et al., 2017). This may, in part,
34
35 517 compensate for the increase in demand for water that increased leaf areas could cause.
36
37 518 However, even with the observed increases in photosynthetic capacity, these small trees
38
39 519 probably still experience increased total water demand due to increased exposure to
40
41 520 higher temperatures and VPD, suggesting that small trees must increase maximum
42
43 521 hydraulic conductivity and/or tolerate reductions in water potential and therefore greater
44
45 522 embolism risk (Sperry et al., 2017). In our study, small trees sampled in the TFE were
46
47 523 slightly taller than the small trees in the Control plot (Fig. S1). This difference may in part-
48
49 524 contribute to the slightly elevated conductance in the branches, as taller trees can have
50
51 525 larger vessels at the base and greater vessel tapering from the trunk to branch tip (Olson
52
53
54
55
56
57
58
59
60

1
2
3 526 and Rosell 2013, Olson et al. 2020). It is, however, unlikely that these differences had a
4
5 527 large influence on our K_s results, overall, the difference in height were small and the
6
7
8 528 genera with the greatest height differences between the TFE and Control (*Protium*, *Ocotea*,
9
10 529 *Voucoupoa*, Fig. S1) showed no changes in K_s (Fig. 2).

14 530 **Differential hydraulic strategy between small and large trees**

17 531 The comparison between small trees and large trees multidimensional hydraulic
18
19 532 trait space, using NMDS and MANOVA, indicate they occupy different hydraulic niche
20
21 533 spaces, despite some overlap. This revealed that smaller trees do indeed have a different
22
23 534 water use strategy to larger canopy trees (Fig 3). The differences in the traits we observed
24
25 535 were far greater, and in most cases significantly so, between the large and the small trees
26
27 536 than for trees of the same size class between treatments (Fig 4). In addition, we show that
28
29 537 smaller trees across both the Control and the TFE plot have significantly more negative P_{50}
30
31 538 values and lower G_{min} values and significantly greater hydraulic safety margins (HSM),
32
33 539 midday leaf water potentials and PLC (Fig. 4). This may imply that the small trees converge
34
35 540 to the same vulnerability to drought, consistent with the results from large scale studies
36
37 541 (e.g. Choat et al., 2012). However, the HSM is 1.94 MPa more positive in the small trees
38
39 542 relative to large trees, indicative of a lack of convergence of the vulnerability of large and
40
41 543 small trees (i.e. Fig 4i), potentially suggesting vulnerability to drought is driven by the
42
43 544 ontogenetic stage of a tree. In addition, our results are consistent with the hypothesis that
44
45 545 the smaller trees are shallow rooted and compensate for the lack of access to deep water
46
47 546 through developing greater xylem embolism resistance and greater stomatal control
48
49 547 (Brum et al., 2019; Tardieu, 1996, Sperry et al. 2017). It is possible that the greater
50
51 548 hydraulic safety margin in small trees enables them to adjust more effectively to increased
52
53
54
55
56
57
58
59
60

1
2
3 549 light availability, despite the lower water availability in the TFE, as it enables these trees to
4
5
6 550 tolerate greater drought stress without passing critical thresholds.
7

8
9 551 The carbon gain associated with greater photosynthesis under higher light
10
11 552 environments may be translated into new xylem growth in smaller trees. This growth
12
13 553 could rapidly replace damaged tissues and is likely to be a more viable strategy for smaller
14
15
16 554 trees, relative to large trees (Damián et al. 2018, Trugman et al. 2018), which would
17
18 555 reduce the risk associated with higher PLC levels. Furthermore, small trees maintained
19
20
21 556 significantly lower G_{\min} and higher midday leaf water potentials (Fig. 5d, 5g), relative to
22
23 557 the large trees, despite having similar pre-dawn leaf water potentials, suggesting that
24
25
26 558 small trees are able to more tightly regulate water loss, during both the day and night.
27
28 559 Probably, the high regulate water loss in small tree is associate a lower water storage
29
30
31 560 capacity to buffer short-term variation of water availability (Goldstein et al. 1998, Meinzer
32
33 561 et al. 2003). The greater degree of control further reduces the risk of runaway embolism
34
35
36 562 when photosynthesising during periods with low water potential, particularly if these
37
38 563 trees can repair cavitated vessels (Nardini et al., 2011; Salleo et al., 2004; Salleo et al.,
39
40
41 564 1995) or grow new vessels between consecutive dry seasons (Eller *et al.* 2018). Also, small
42
43 565 trees also have fewer structural constraints than large trees, so small changes in hydraulic
44
45 566 traits in a small tree could have bigger effects on overall performance during drought,
46
47
48 567 because the marginal effect of each unit change is larger relative to the size of the tree
49
50
51 568 (Mencuccini 2002). Combined, these factors are likely to allow small trees to have greater
52
53 569 flexibility in terms of the strategy they use to adjust to combined changes in water and
54
55 570 light availability. However, as we highlight in our results, there is considerable variability
56
57
58 571 both within and between taxonomic groups with respect to how small trees may alter
59
60 572 their traits and their resulting drought tolerance strategy.

1
2
3 573 This study highlights the importance of forest structural changes in controlling the traits of
4
5 574 what are likely to be the next generation of trees growing up during prolonged drought
6
7
8 575 stress. We show that, relative to large trees, small trees have a larger capacity to
9
10 576 acclimate their hydraulic systems to increases in light availability following drought-
11
12
13 577 induced mortality of large canopy-dominant trees. Our results suggest that small trees are
14
15 578 able to acclimate the hydraulic conductance and leaf area to sapwood area ratio despite
16
17
18 579 experiencing prolonged soil moisture stress, which resulted here in lower leaf water
19
20 580 potentials and greater PLC. Also, our results demonstrate that there is a consistent and
21
22
23 581 larger shift in the plant hydraulic strategy of saplings relative to large trees across most of
24
25 582 Amazonia's hyper-abundant taxonomic groups. Whilst we find adjustment of traits in
26
27
28 583 response to the drought treatment, it remains unknown whether all small trees
29
30 584 community can respond in the same way or only the long-term drought surviving trees. In
31
32 585 this way, a key uncertainty that remains to be answered are relates to the long-term
33
34
35 586 development of these trees. Assuming these small trees continue to develop under the
36
37
38 587 experimental drought stressed conditions, it would be of interest to know if the trajectory
39
40 588 of change in hydraulic traits we observe can be sufficient to increase the hydraulic
41
42 589 resistance to drought of these trees as they approach full size.

43
44
45 590 Ultimately, continued acclimation of hydraulic systems throughout a the lifespan of a tree
46
47
48 591 may allow a more drought-resilient ecosystem to develop following the negative impacts
49
50 592 of drought on pre-existing larger trees. Therefore, even the current generation of trees
51
52 593 showing huge mortality rates, the next generation might be followed by a new stable
53
54
55 594 community composed of those small trees that can adapt to drought. This implies that for
56
57
58 595 prediction of the future of tropical ecosystems function we needs to consider trait
59
60 596 adjustment in the future forest instead currently forest.

1
2
3 597 **Data and Materials Availability**
4
5

6 598 We are in the process of making this data publically available through the main funding
7
8 599 bodies data centre, NERC EIDC (<https://eidc.ac.uk/>), if accepted the data will be fully
9
10 publically available on a link we will provide.
11
12

13
14 601 **Supplementary Data**
15

16
17 602 *Supplementary tables*
18

19
20 603 **Table S1.** Linear mixed effect model analysis of stress indicator variables from small tress.
21

22 604 **Table S2.** Linear mixed effect model analysis of hydraulic traits from small tress.
23

24 605 **Table S3** Numbers of individuals for small and large tree in each treatment (TFE an Control) and
25 606 mean and standard deviation of all variables measured.

26
27 607 **Table S4.** Statistics from the NMDS modelling shown in Figure 3.
28

29 608 **Table S5** Results of linear effect models of size (Size vs TFE) on the stress indicator variables on
30 609 Control plot.
31

32 610 **Table S6** Results of linear effect models of size (Size vs TFE) on the hydraulic traits variables on TFE
33 611 plot.
34

35 612 **Table S7** Results of linear effect models of size (Size vs TFE) and genus on the stress indicator and
36 613 hydraulic variables on TFE plot.
37
38

39 614
40
41
42
43
44
45
46
47
48
49
50
51
52
53
54
55
56
57
58
59
60

615

616 *Supplementary figures*

617 **Figure S1.** Height and diameter in each treatment (TFE vs. Control) and by genus for the most
618 common small tree genera in this study (9 genera)

619 **Figure S2.** Soil water content during 2016 in the Throughfall Exclusion Experiment plot and
620 in the Control plot at 10 cm and at 100 cm.

621 **Figure S3.** Comparison between the small trees and large trees from the throughfall exclusion
622 (TFE) and Control plots from grouping all 9 genera available within the large and small tree
623 groupings.

624

625 **Conflict of interest**

626 The authors have no conflict of interest to declare.

627 **Funding**

628 Funding for this work was provided by Brazilian Higher Education Co-ordination Agency
629 (CAPES- Finance Code 001 to ALG); Natural Environment Research Council (NE/N014022/1
630 to LR, NE/J011002/1 to PM and MM, and NE/L002434/1 to DCB); European Union
631 FP7(Amazalert to PM and MM);National Council for Scientific and Technological
632 Development (457914/2013-0/MCTI/CNPq/FNDCT/LBA/ESECAFLOR to ACLdC); Australian
633 Research Council (DP170104091 to PM).The São Paulo Research Foundation FAPESP
634 (grant 11/52072-0 to RSO, 2018/01847-0 to RSO and LR); Royal Society's Newton
635 International for its Fellowship to PRLB (NF170370).

636 **Acknowledgements**

637 We thank the UNICAMP postgraduate program in Ecology and the Brazilian Higher
638 Education Co-ordination Agency (CAPES). We would like to thank the entire community
639 surrounding the study area (Caxiuanã-PA northern Brazil), the climbers Joca and their

1
2
3 640 children, the workers at the scientific base "Bigode"; "Bené"; "Benézinho" and the dear
4
5 641 cook chef "Morena". We also thank "Kaká" and "Moska" for the field campaign help.
6
7

8 642 **Authors' Contributions**

9
10
11 643 ALG collected and compiled the data alongside LR, PRLB, IC, PBC, PG, LVF, DDV, JASJ, DCB
12
13 644 and ACLdC. LR designed the study with MM, ACLdC, PM, ALG and RO. ALG, MM, PRLB and
14
15 645 LR performed the statistical analysis and ALG, LR and RO wrote the paper, all authors
16
17 646 substantially contributed to revisions.
18
19
20
21

22 647 **References**

- 23 648
- 24
25
26 649 Anderson MJ (2001) A new method for non-parametric multivariate analysis of variance.
27 650 *Austral Ecol* 26:32–46.
- 28
29 651 Aragão LEOC, Anderson LO, Fonseca MG, Rosan TM, Vedovato LB, Wagner FH, Silva CVJ,
30 652 Silva Junior CHL, Arai E, Aguiar AP, Barlow J, Berenguer E, Deeter MN, Domingues LG,
31 653 Gatti L, Gloor M, Malhi Y, Marengo JA, Miller JB, Phillips OL, Saatchi S (2018) 21st
32 654 Century drought-related fires counteract the decline of Amazon deforestation carbon
33 655 emissions. *Nat Commun* 9:536. <http://dx.doi.org/10.1038/s41467-017-02771-y>
- 34
35
36 656 Awad H, Barigah T, Badel E, Cochard H, Herbette S (2010) Poplar vulnerability to xylem
37 657 cavitation acclimates to drier soil conditions. *Physiol Plant* 139:280–288.
38 658 <http://doi.wiley.com/10.1111/j.1399-3054.2010.01367.x>
- 39
40 659 B. Eller C, de V. Barros F, R.L. Bittencourt P, Rowland L, Mencuccini M, S. Oliveira R (2018)
41 660 Xylem hydraulic safety and construction costs determine tropical tree growth. *Plant*
42 661 *Cell Environ* 41:548–562. <http://doi.wiley.com/10.1111/pce.13106>
- 43
44 662 Bartholomew DC, Bittencourt PRL, Costa ACL, Banin LF, Britto Costa P, Coughlin SI,
45 663 Domingues TF, Ferreira L V., Giles A, Mencuccini M, Mercado L, Miatto RC, Oliveira A,
46 664 Oliveira R, Meir P, Rowland L (2020) Small tropical forest trees have a greater
47 665 capacity to adjust carbon metabolism to long-term drought than large canopy trees.
48 666 *Plant Cell Environ* 43:2380–2393.
49 667 <https://onlinelibrary.wiley.com/doi/10.1111/pce.13838>
- 50
51
52 668 Bates D, Mächler M, Bolker BM, Walker SC (2015) Fitting linear mixed-effects models
53 669 using lme4. *J Stat Softw* 67
- 54
55 670 Bhaskar R, Ackerly DD (2006) Ecological relevance of minimum seasonal water potentials.
56 671 *Physiol Plant* 127:353–359. <http://doi.wiley.com/10.1111/j.1399-3054.2006.00718.x>
- 57
58 672 Binks O, Coughlin I, Mencuccini M, Meir P (2020) Equivalence of foliar water uptake and
59 673 stomatal conductance? *Plant Cell Environ* 43:524–528.

- 1
2
3 674 <https://doi.org/10.1111/pce.13663>
4
5 675 Binks O, Meir P, Rowland L, Costa ACL, Vasconcelos SS, Oliveira AAR, Ferreira L,
6 676 Christoffersen B, Nardini A, Mencuccini M (2016) Plasticity in leaf-level water
7 677 relations of tropical rainforest trees in response to experimental drought. *New Phytol*
8 678 211:477–488. <https://onlinelibrary.wiley.com/doi/abs/10.1111/nph.13927>
9
10 679 Bittencourt PRL, Oliveira RS, Costa ACL, Giles AL, Coughlin I, Costa PB, Bartholomew DC,
11 680 Ferreira L V, Vasconcelos SS, Barros F V, Junior JAS, Oliveira AAR, Mencuccini M, Meir
12 681 P, Rowland L (2020) Amazonia trees have limited capacity to acclimate plant
13 682 hydraulic properties in response to long-term drought. *Glob Chang Biol* 26:3569–
14 683 3584. <https://onlinelibrary.wiley.com/doi/abs/10.1111/gcb.15040>
15
16 684 Bittencourt P, Pereira L, Oliveira R (2018) Pneumatic Method to Measure Plant Xylem
17 685 Embolism. *BIO-PROTOCOL* 8:1–14. <https://bio-protocol.org/e3059>
18
19 686 Brando PM, Nepstad DC, Davidson EA, Trumbore SE, Ray D, Camargo P (2008) Drought
20 687 effects on litterfall, wood production and belowground carbon cycling in an Amazon
21 688 forest: results of a throughfall reduction experiment. *Philos Trans R Soc B Biol Sci*
22 689 363:1839–1848. <https://royalsocietypublishing.org/doi/10.1098/rstb.2007.0031>
23
24 690 Brienen R, Schongart J, Zuidema P (2016) *Tropical Tree Physiology* Goldstein G, Santiago LS
25 691 (eds). Springer International Publishing, Cham. [http://link.springer.com/10.1007/978-](http://link.springer.com/10.1007/978-3-319-27422-5)
26 692 3-319-27422-5
27
28 693 Brodribb TJ, Powers J, Cochard H, Choat B (2020) Hanging by a thread? Forests and
29 694 drought. *Science* (80-) 368:261–266.
30 695 <https://www.sciencemag.org/lookup/doi/10.1126/science.aat7631>
31
32 696 Brum M, Vadeboncoeur MA, Ivanov V, Saleska S, Alves LF, Penha D, Asbjornsen H, Dias JD,
33 697 Aragão LEOC, Barros F, Bittencourt P, Pereira L, Oliveira RS (2019) Hydrological niche
34 698 segregation defines forest structure and drought tolerance strategies in a seasonal
35 699 Amazon forest. *J Ecol*:318–333.
36
37 700 Burnham KP, Anderson DR (2004) Multimodel Inference. *Sociol Methods Res* 33:261–304.
38 701 <http://journals.sagepub.com/doi/10.1177/0049124104268644>
39
40 702 Cavaleri MA, Oberbauer SF, Clark DB, Clark DA, Ryan MG (2010) Height is more important
41 703 than light in determining leaf morphology in a tropical forest. *Ecology* 91:1730–1739.
42 704 <http://doi.wiley.com/10.1890/09-1326.1>
43
44 705 Chadwick R, Good P, Martin G, Rowell DP (2016) Large rainfall changes consistently
45 706 projected over substantial areas of tropical land. *Nat Clim Chang* 6:177–181.
46 707 <http://www.nature.com/articles/nclimate2805>
47
48 708 Choat B, Jansen S, Brodribb TJ, Cochard H, Delzon S, Bhaskar R, Bucci SJ, Feild TS, Gleason
49 709 SM, Hacke UG, Jacobsen AL, Lens F, Maherali H, Martínez-Vilalta J, Mayr S,
50 710 Mencuccini M, Mitchell PJ, Nardini A, Pittermann J, Pratt RB, Sperry JS, Westoby M,
51 711 Wright IJ, Zanne AE (2012) Global convergence in the vulnerability of forests to
52 712 drought. *Nature* 491:752–755. <http://www.nature.com/articles/nature11688>
53
54 713 Christensen JH, Krishna Kumar K, Aldrian E, An SI, Cavalcanti, I.F.A. de C, M., Dong W,
55 714 Goswami P, Hall A, Kanyanga JK, Kitoh A, Kossin, Lau NC, Renwick J, Stephenson DB,

- 1
2
3 715 Xie SP, Zhou T (2017) Climate Phenomena and their Relevance for Future Regional
4 716 Climate Change. In: Climate Change 2013: The Physical Science Basis. Contribution of
5 717 Working Group I to the Fifth Assessment Report of the Intergovernmental Panel on
6 718 Climate Change.
- 7
8
9 719 Corlett RT (2016) The Impacts of Droughts in Tropical Forests. *Trends Plant Sci* 21:584–
10 720 593. <http://dx.doi.org/10.1016/j.tplants.2016.02.003>
- 11
12 721 da Costa ACL, Galbraith D, Almeida S, Portela BTT, da Costa M, de Athaydes Silva Junior J,
13 722 Braga AP, de Gonçalves PHL, de Oliveira AA, Fisher R, Phillips OL, Metcalfe DB, Levy P,
14 723 Meir P (2010) Effect of 7 yr of experimental drought on vegetation dynamics and
15 724 biomass storage of an eastern Amazonian rainforest. *New Phytol* 187:579–591.
16 725 <http://doi.wiley.com/10.1111/j.1469-8137.2010.03309.x>
- 17
18
19 726 da Costa ACL, Metcalfe DB, Doughty CE, de Oliveira AAR, Neto GFC, da Costa MC, Silva
20 727 Junior J de A, Aragão LEOC, Almeida S, Galbraith DR, Rowland LM, Meir P, Malhi Y
21 728 (2014) Ecosystem respiration and net primary productivity after 8–10 years of
22 729 experimental through-fall reduction in an eastern Amazon forest. *Plant Ecol Divers*
23 730 7:7–24. <http://www.tandfonline.com/doi/abs/10.1080/17550874.2013.798366>
- 24
25 731 Damián X, Fornoni J, Domínguez CA, Boege K (2018) Ontogenetic changes in the
26 732 phenotypic integration and modularity of leaf functional traits. *Funct Ecol*:234–246.
- 27
28
29 733 Domingues TF, Meir P, Feldpausch TR, Saiz G, Veenendaal EM, Schrodte F, Bird M,
30 734 Djagbletey G, Hien F, Compaore H, Diallo A, Grace J, Lloyd J (2010) Co-limitation of
31 735 photosynthetic capacity by nitrogen and phosphorus in West Africa woodlands. *Plant*,
32 736 *Cell Environ* 33:959–980.
- 33
34 737 Duffy PB, Brando P, Asner GP, Field CB (2015) Projections of future meteorological
35 738 drought and wet periods in the Amazon. *Proc Natl Acad Sci* 112:13172–13177.
36 739 <http://www.pnas.org/lookup/doi/10.1073/pnas.1421010112>
- 37
38
39 740 Duursma RA, Blackman CJ, López R, Martin-StPaul NK, Cochard H, Medlyn BE (2019) On
40 741 the minimum leaf conductance: its role in models of plant water use, and ecological
41 742 and environmental controls. *New Phytol* 221:693–705.
- 42
43 743 Esquivel-Muelbert A, Baker TR, Dexter KG, Lewis SL, ter Steege H, Lopez-Gonzalez G,
44 744 Monteagudo Mendoza A, Brienen R, Feldpausch TR, Pitman N, Alonso A, van der
45 745 Heijden G, Peña-Claros M, Ahuite M, Alexiades M, Álvarez Dávila E, Murakami AA,
46 746 Arroyo L, Aulestia M, Balslev H, Barroso J, Boot R, Cano A, Chama Moscoso V,
47 747 Comiskey JA, Cornejo F, Dallmeier F, Daly DC, Dávila N, Duivenvoorden JF, Duque
48 748 Montoya AJ, Erwin T, Di Fiore A, Fredericksen T, Fuentes A, García-Villacorta R,
49 749 Gonzales T, Guevara Andino JE, Honorio Coronado EN, Huamantupa-Chuquimaco I,
50 750 Killeen TJ, Malhi Y, Mendoza C, Mogollón H, Jørgensen PM, Montero JC, Mostacedo
51 751 B, Nauray W, Neill D, Vargas PN, Palacios S, Palacios Cuenca W, Pallqui Camacho NC,
52 752 Peacock J, Phillips JF, Pickavance G, Quesada CA, Ramírez-Angulo H, Restrepo Z,
53 753 Reynel Rodríguez C, Paredes MR, Sierra R, Silveira M, Stevenson P, Stropp J, Terborgh
54 754 J, Tirado M, Toledo M, Torres-Lezama A, Umaña MN, Urrego LE, Vasquez Martinez R,
55 755 Gamarra LV, Vela CIA, Vilanova Torre E, Vos V, von Hildebrand P, Vriesendorp C,
56 756 Wang O, Young KR, Zartman CE, Phillips OL (2017) Seasonal drought limits tree
57 757 species across the Neotropics. *Ecography (Cop)* 40:618–629.

- 1
2
3 758 <http://doi.wiley.com/10.1111/ecog.01904>
4
- 5 759 Fu R, Yin L, Li W, Arias PA, Dickinson RE, Huang L, Chakraborty S, Fernandes K, Liebmann B,
6 760 Fisher R, Myneni RB (2013) Increased dry-season length over southern Amazonia in
7 761 recent decades and its implication for future climate projection. *Proc Natl Acad Sci*
8 762 110:18110–18115. <http://www.pnas.org/cgi/doi/10.1073/pnas.1302584110>
- 9
10 763 Goldstein G, Andrade JL, Meinzer FC, Holbrook NM, Cavelier J, Jackson P, Celis A (1998)
11 764 Stem water storage and diurnal patterns of water use in tropical forest canopy trees.
12 765 *Plant, Cell Environ* 21:397–406.
- 13
14
15 766 Groenendijk P, Sass-Klaassen U, Bongers F, Zuidema PA (2014) Potential of tree-ring
16 767 analysis in a wet tropical forest: A case study on 22 commercial tree species in
17 768 Central Africa. *For Ecol Manage* 323:65–78.
18 769 <http://dx.doi.org/10.1016/j.foreco.2014.03.037>
- 19
20 770 Hubau W, De Mil T, Van den Bulcke J, Phillips OL, Angoboy Ilondea B, Van Acker J, Sullivan
21 771 MJP, Nsenga L, Toirambe B, Couralet C, Banin LF, Begne SK, Baker TR, Bourland N,
22 772 Chezeaux E, Clark CJ, Collins M, Comiskey JA, Cuni-Sanchez A, Deklerck V, Dierickx S,
23 773 Doucet J-L, Ewango CEN, Feldpausch TR, Gilpin M, Gonmadje C, Hall JS, Harris DJ,
24 774 Hardy OJ, Kamdem M-ND, Kasongo Yakusu E, Lopez-Gonzalez G, Makana J-R, Malhi Y,
25 775 Mbayu FM, Moore S, Mukinzi J, Pickavance G, Poulsen JR, Reitsma J, Rousseau M,
26 776 Sonké B, Sunderland T, Taedoumg H, Talbot J, Tshibamba Mukendi J, Umunay PM,
27 777 Vleminckx J, White LJ, Zemagho L, Lewis SL, Beeckman H (2019) The persistence of
28 778 carbon in the African forest understory. *Nat Plants* 5:133–140.
29 779 <http://www.nature.com/articles/s41477-018-0316-5>
- 30
31
32
33 780 KAMALUDDIN M, GRACE J (1992) Acclimation in Seedlings of a Tropical Tree, *Bischofia*
34 781 *javanica*, Following a Stepwise Reduction in Light. *Ann Bot* 69:557–562.
35 782 [https://academic.oup.com/aob/article-](https://academic.oup.com/aob/article-lookup/doi/10.1093/oxfordjournals.aob.a088386)
36 783 [lookup/doi/10.1093/oxfordjournals.aob.a088386](https://academic.oup.com/aob/article-lookup/doi/10.1093/oxfordjournals.aob.a088386)
- 37
38
39 784 KRAMER PJ (1988) Changing concepts regarding plant water relations. *Plant, Cell Environ*
40 785 11:565–568. <http://doi.wiley.com/10.1111/j.1365-3040.1988.tb01796.x>
- 41
42 786 Krause GH, Virgo A, Winter K (1995) High susceptibility to photoinhibition of young leaves
43 787 of tropical forest trees. *Planta* 197:583–591.
- 44
45 788 Marengo JA, Souza CM, Thonicke K, Burton C, Halladay K, Betts RA, Alves LM, Soares WR
46 789 (2018) Changes in Climate and Land Use Over the Amazon Region: Current and
47 790 Future Variability and Trends. *Front Earth Sci* 6:1–21.
48 791 <https://www.frontiersin.org/article/10.3389/feart.2018.00228/full>
- 49
50 792 Márquez DA, Stuart-Williams H, Farquhar GD (2021) An improved theory for calculating
51 793 leaf gas exchange more precisely accounting for small fluxes. *Nat Plants* 7.
52 794 <http://dx.doi.org/10.1038/s41477-021-00861-w>
- 53
54
55 795 Martin-StPaul NK, Longepierre D, Huc R, Delzon S, Burlett R, Joffre R, Rambal S, Cochard H
56 796 (2014) How reliable are methods to assess xylem vulnerability to cavitation? The
57 797 issue of ‘open vessel’ artifact in oaks. *Tree Physiol* 34:894–905.
- 58
59 798 Martinez-Vilalta J, Anderegg WRL, Sapes G, Sala A (2019) Greater focus on water pools
60

- 1
2
3 799 may improve our ability to understand and anticipate drought-induced mortality in
4 800 plants. *New Phytol* 223:22–32.
- 6 801 Martínez-Vilalta J, Garcia-Forner N (2017) Water potential regulation, stomatal behaviour
7 802 and hydraulic transport under drought: deconstructing the iso/anisohydric concept.
8 803 *Plant Cell Environ* 40:962–976.
- 10 804 Mcculloh KA, Johnson DM, Meinzer FC, Woodruff DR (2014) The dynamic pipeline:
11 805 Hydraulic capacitance and xylem hydraulic safety in four tall conifer species. *Plant,*
12 806 *Cell Environ* 37:1171–1183.
- 15 807 McDowell N, Pockman WT, Allen CD, Breshears DD, Cobb N, Kolb T, Plaut J, Sperry J, West
16 808 A, Williams DG, Yezzer EA (2008) Mechanisms of plant survival and mortality during
17 809 drought: why do some plants survive while others succumb to drought? *New Phytol*
18 810 178:719–739. <http://doi.wiley.com/10.1111/j.1469-8137.2008.02436.x>
- 21 811 Meinzer FC, James SA, Goldstein G, Woodruff D (2003) Whole-tree water transport scales
22 812 with sapwood capacitance in tropical forest canopy trees. *Plant, Cell Environ*
23 813 26:1147–1155.
- 25 814 Meinzer FC, Johnson DM, Lachenbruch B, McCulloh KA, Woodruff DR (2009) Xylem
26 815 hydraulic safety margins in woody plants: Coordination of stomatal control of xylem
27 816 tension with hydraulic capacitance. *Funct Ecol* 23:922–930.
28 817 <http://doi.wiley.com/10.1111/j.1365-2435.2009.01577.x>
- 30 818 Meir P, Mencuccini M, Binks O, Da Costa AL, Ferreira L, Rowland L (2018) Short-term
31 819 effects of drought on tropical forest do not fully predict impacts of repeated or long-
32 820 term drought: Gas exchange versus growth. *Philos Trans R Soc B Biol Sci* 373
- 35 821 Meir P, Wood TE, Galbraith DR, Brando PM, Da Costa ACL, Rowland L, Ferreira L V. (2015)
36 822 Threshold Responses to Soil Moisture Deficit by Trees and Soil in Tropical Rain
37 823 Forests: Insights from Field Experiments. *Bioscience* 65:882–892.
- 39 824 Mencuccini M (2002) Hydraulic constraints in the functional scaling of trees. *Tree Physiol*
40 825 22:553–565.
- 42 826 Mencuccini M, Rosas T, Rowland L, Choat B, Cornelissen H, Jansen S, Kramer K, Lapenis A,
43 827 Manzoni S, Niinemets Ü, Reich PB, Schrodte F, Soudzilovskaia N, Wright IJ,
44 828 Martínez-Vilalta J (2019) Leaf economics and plant hydraulics drive leaf : wood area
45 829 ratios. *New Phytol* 224:1544–1556.
46 830 <https://onlinelibrary.wiley.com/doi/abs/10.1111/nph.15998>
- 49 831 Metcalfe DB, Meir P, Aragao LEOC, Lobo-do-vale R, Galbraith D, Fisher RA, Chaves MM,
50 832 Maroco JP, Costa ACL, Almeida SS De, Braga AP, Gonc PHL (2010) Shifts in plant
51 833 respiration and carbon use efficiency at a large-scale drought experiment in the
52 834 eastern Amazon. *New Phytol*:608–621.
- 54 835 Metcalfe DB, Meir P, Aragão LEOC, Lobo-do-Vale R, Galbraith D, Fisher RA, Chaves MM,
55 836 Maroco JP, da Costa ACL, de Almeida SS, Braga AP, Gonçalves PHL, de Athaydes J, da
56 837 Costa M, Portela TTB, de Oliveira AAR, Malhi Y, Williams M (2010) Shifts in plant
57 838 respiration and carbon use efficiency at a large-scale drought experiment in the
58 839 eastern Amazon. *New Phytol* 187:608–621. <http://doi.wiley.com/10.1111/j.1469->

- 1
2
3 840 8137.2010.03319.x
4
5 841 Mulkey SS, Pearcy RW (1992a) Interactions between Acclimation and Photoinhibition of
6 842 Photosynthesis of a Tropical Forest Understorey Herb, *Alocasia macrorrhiza*, during
7 843 Simulated Canopy Gap Formation. *Funct Ecol* 6:719.
8
9 844 Mulkey SS, Pearcy RW (1992b) Interactions between Acclimation and Photoinhibition of
10 845 Photosynthesis of a Tropical Forest Understorey Herb, *Alocasia macrorrhiza*, during
11 846 Simulated Canopy Gap Formation. *Funct Ecol* 6:719.
12 847 <https://www.jstor.org/stable/2389969?origin=crossref>
13
14
15 848 Nardini A, Lo MA, Salleo S (2011) Plant Science Refilling embolized xylem conduits : Is it a
16 849 matter of phloem unloading ? *Plant Sci* 180:604–611.
17 850 <http://dx.doi.org/10.1016/j.plantsci.2010.12.011>
18
19 851 Olson ME, Anfodillo T, Gleason SM, McCulloh KA (2020) Tip-to-base xylem conduit
20 852 widening as an adaptation: causes, consequences, and empirical priorities. *New*
21 853 *Phytol:nph.16961*. <https://onlinelibrary.wiley.com/doi/10.1111/nph.16961>
22
23 854 Olson ME, Rosell JA (2013) Vessel diameter-stem diameter scaling across woody
24 855 angiosperms and the ecological causes of xylem vessel diameter variation. *New*
25 856 *Phytol* 197:1204–1213.
26
27
28 857 Pammenter NW, Van der Willigen C (1998) A mathematical and statistical analysis of the
29 858 curves illustrating vulnerability of xylem to cavitation. *Tree Physiol* 18:589–593.
30 859 [https://academic.oup.com/treephys/article-lookup/doi/10.1093/treephys/18.8-](https://academic.oup.com/treephys/article-lookup/doi/10.1093/treephys/18.8-9.589)
31 860 [9.589](https://academic.oup.com/treephys/article-lookup/doi/10.1093/treephys/18.8-9.589)
32
33 861 Pereira L, Bittencourt PRL, Oliveira RS, Junior MBM, Barros F V, Ribeiro R V, Mazzafera P
34 862 (2016) Plant pneumatics: stem air flow is related to embolism – new perspectives on
35 863 methods in plant hydraulics. *New Phytol* 211:357–370.
36 864 <https://onlinelibrary.wiley.com/doi/abs/10.1111/nph.13905>
37
38
39 865 Pereira L, Bittencourt PRL, Rowland L, Brum M, Miranda MT, Pacheco VS, Oliveira RS,
40 866 Machado EC, Jansen S, Ribeiro R V. (2021) Using the Pneumatic method to estimate
41 867 embolism resistance in species with long vessels: A commentary on the article “A
42 868 comparison of five methods to assess embolism resistance in trees”. *For Ecol Manage*
43 869 *479:2019–2021*.
44
45
46 870 Pereira L, Mazzafera P (2013) A low cost apparatus for measuring the xylem hydraulic
47 871 conductance in plants. *Bragantia* 71:583–587.
48 872 [http://www.scielo.br/scielo.php?script=sci_arttext&pid=S0006-](http://www.scielo.br/scielo.php?script=sci_arttext&pid=S0006-87052012000400017&lng=en&tlng=en)
49 873 [87052012000400017&lng=en&tlng=en](http://www.scielo.br/scielo.php?script=sci_arttext&pid=S0006-87052012000400017&lng=en&tlng=en)
50
51
52 874 Poorter L, Bongers F, Sterck FJ, Wöll H (2005) Beyond the regeneration phase:
53 875 Differentiation of height-light trajectories among tropical tree species. *J Ecol* 93:256–
54 876 267. <http://doi.wiley.com/10.1111/j.1365-2745.2004.00956.x>
55
56 877 Poorter H, Niinemets Ü, Poorter L, Wright IJ, Villar R (2009) Causes and consequences of
57 878 variation in leaf mass per area (LMA): a meta-analysis. *New Phytol* 182:565–588.
58 879 <https://onlinelibrary.wiley.com/doi/abs/10.1111/j.1469-8137.2009.02830.x>
59
60 880 Powell TL, Wheeler JK, de Oliveira AAR, da Costa ACL, Saleska SR, Meir P, Moorcroft PR

- 1
2
3 881 (2017) Differences in xylem and leaf hydraulic traits explain differences in drought
4 882 tolerance among mature Amazon rainforest trees. *Glob Chang Biol* 23:4280–4293.
5 883 <http://doi.wiley.com/10.1111/gcb.13731>
- 7 884 Prendin AL, Mayr S, Beikircher B, von Arx G, Petit G (2018) Xylem anatomical adjustments
8 885 prioritize hydraulic efficiency over safety as Norway spruce trees grow taller
9 886 Martinez-Vilalta J (ed). *Tree Physiol* 38:1088–1097.
10 887 <https://academic.oup.com/treephys/article/38/8/1088/5038975>
- 13 888 Rowland L, da Costa ACL, Galbraith DR, Oliveira RS, Binks OJ, Oliveira AAR, Pullen AM,
14 889 Doughty CE, Metcalfe DB, Vasconcelos SS, Ferreira L V, Malhi Y, Grace J, Mencuccini
15 890 M, Meir P (2015) Death from drought in tropical forests is triggered by hydraulics not
16 891 carbon starvation. *Nature* 528:119–122. <http://dx.doi.org/10.1038/nature15539>
- 19 892 Rowland L, da Costa ACL, Oliveira RS, Bittencourt PRL, Giles AL, Coughlin I, de Britto Costa
20 893 P, Bartholomew D, Domingues TF, Miatto RC, Ferreira LV, Vasconcelos SS, Junior JAS,
21 894 Oliveira AAR, Mencuccini M, Meir P (2020) The response of carbon assimilation and
22 895 storage to long-term drought in tropical trees is dependent on light availability. *Funct*
23 896 *Ecol*:1365-2435.13689. [https://onlinelibrary.wiley.com/doi/10.1111/1365-](https://onlinelibrary.wiley.com/doi/10.1111/1365-2435.13689)
24 897 [2435.13689](https://onlinelibrary.wiley.com/doi/10.1111/1365-2435.13689)
- 26 898 Rowland L, Lobo-do-Vale RL, Christoffersen BO, Melém EA, Kruijt B, Vasconcelos SS,
27 899 Domingues T, Binks OJ, Oliveira AAR, Metcalfe D, da Costa ACL, Mencuccini M, Meir P
28 900 (2015) After more than a decade of soil moisture deficit, tropical rainforest trees
29 901 maintain photosynthetic capacity, despite increased leaf respiration. *Glob Chang Biol*
30 902 21:4662–4672. <http://doi.wiley.com/10.1111/gcb.13035>
- 33 903 Ruggiero PGC, Batalha MA, Pivello VR, Meirelles ST (2002) Soil vegetation relationships in
34 904 cerrado (Brazilian savanna) and semideciduous forest, Southeastern Brazil. *Plant Ecol*
35 905 160:1–16.
- 37 906 Sala A, Piper F, Hoch G (2010) Physiological mechanisms of drought-induced tree mortality
38 907 are far from being resolved. *New Phytol* 186:274–281.
39 908 <http://doi.wiley.com/10.1111/j.1469-8137.2009.03167.x>
- 42 909 Salleo S, Lo Gullo MA, De Paoli D, Zippo M (1996) Xylem recovery from cavitation-induced
43 910 embolism in young plants of *Laurus nobilis*: A possible mechanism. *New Phytol*
44 911 132:47–56. <http://doi.wiley.com/10.1111/j.1469-8137.1996.tb04507.x>
- 46 912 Salleo S, Lo Gullo MA, Trifilò P, Nardini A (2004) New evidence for a role of vessel-
47 913 associated cells and phloem in the rapid xylem refilling of cavitated stems of *Laurus*
48 914 *nobilis* L. *Plant, Cell Environ* 27:1065–1076. [http://doi.wiley.com/10.1111/j.1365-](http://doi.wiley.com/10.1111/j.1365-3040.2004.01211.x)
49 915 [3040.2004.01211.x](http://doi.wiley.com/10.1111/j.1365-3040.2004.01211.x)
- 51 916 Salomón RL, Limousin JM, Ourcival JM, Rodríguez-Calcerrada J, Steppe K (2017) Stem
52 917 hydraulic capacitance decreases with drought stress: implications for modelling tree
53 918 hydraulics in the Mediterranean oak *Quercus ilex*. *Plant Cell Environ* 40:1379–1391.
- 56 919 Schneider CA, Rasband WS, Eliceiri KW (2012) NIH Image to ImageJ: 25 years of image
57 920 analysis. *Nat Methods* 9:671–675.
- 59 921 Schuldt B, Leuschner C, Horna V, Moser G, Köhler M, Van Straaten O, Barus H (2011)
- 60

- 1
2
3 922 Change in hydraulic properties and leaf traits in a tall rainforest tree species
4 923 subjected to long-term throughfall exclusion in the perhumid tropics. *Biogeosciences*
5 924 8:2179–2194.
- 7 925 van der Sleen P, Groenendijk P, Vlam M, Anten NPR, Boom A, Bongers F, Pons TL, Terburg
8 926 G, Zuidema PA (2015) No growth stimulation of tropical trees by 150 years of CO₂
9 927 fertilization but water-use efficiency increased. *Nat Geosci* 8:24–28.
11 928 <http://www.nature.com/articles/ngeo2313>
- 13 929 Sperry JS, Donnelly JR, Tyree MT (1988) A method for measuring hydraulic conductivity and
14 930 embolism in xylem. *Plant Cell Environ* 11:35–40.
- 16 931 Sperry JS, Hacke UG, Oren R, Comstock JP (2002) Water deficits and hydraulic limits to leaf
17 932 water supply. *Plant, Cell Environ*:251–263.
- 19 933 Sperry JS, Tyree MT (1988) Mechanism of Water Stress-Induced Xylem Embolism1. *Plant*
20 934 *Physiol* 88:581–587.
- 22 935 Sperry JS, Venturas MD, Anderegg WRL, Mencuccini M, Mackay DS, Wang Y, Love DM
23 936 (2017) Predicting stomatal responses to the environment from the optimization of
24 937 photosynthetic gain and hydraulic cost. *Plant Cell Environ* 40:816–830.
26 938 <http://doi.wiley.com/10.1111/pce.12852>
- 28 939 Sterck F, Markesteijn L, Schieving F, Poorter L (2011) Functional traits determine trade-offs
29 940 and niches in a tropical forest community. *Proc Natl Acad Sci* 108:20627–20632.
31 941 <http://www.pnas.org/cgi/doi/10.1073/pnas.1106950108>
- 32 942 Tardieu F (1996) Drought perception by plants: Do cells of draughted plants experience
33 943 water stress? *Plant Growth Regul* 20:93–104.
- 35 944 Tng DYP, Apgaua DMG, Ishida YF, Mencuccini M, Lloyd J, Laurance WF, Laurance SGW
36 945 (2018) Rainforest trees respond to drought by modifying their hydraulic architecture.
37 946 *Ecol Evol* 8:12479–12491.
- 39 947 Tomasella M, Beikircher B, Häberle KH, Hesse B, Kallenbach C, Matyssek R, Mayr S (2018)
41 948 Acclimation of branch and leaf hydraulics in adult *Fagus sylvatica* and *Picea abies* in a
42 949 forest through-fall exclusion experiment. *Tree Physiol* 38:198–211.
- 44 950 Trugman AT, Detto M, Bartlett MK, Medvigy D, Anderegg WRL, Schwalm C, Schaffer B,
45 951 Pacala SW (2018) Tree carbon allocation explains forest drought-kill and recovery
46 952 patterns. *Ecol Lett*:1552–1560.
- 48 953 Tyree MT, Vargas G, Engelbrecht BMJ, Kursar TA (2002) Drought until death do us part: A
49 954 case study of the desiccation-tolerance of a tropical moist forest seedling-tree,
51 955 *Licania platypus* (Hemsl.) Fritsch. *J Exp Bot* 53:2239–2247.
- 52 956 Venturas MD, Mackinnon ED, Jacobsen AL, Pratt RB (2015) Excising stem samples
53 957 underwater at native tension does not induce xylem cavitation. *Plant, Cell Environ*
55 958 38:1060–1068.
- 57 959 Wright IJ, Reich PB, Westoby M, Ackerly DD, Baruch Z, Bongers F, Cavender-bares J,
58 960 Chapin T, Cornelissen JHC, Diemer M, Flexas J, Garnier E, Groom PK, Gulias J (2004)
59 961 The worldwide leaf economics spectrum. *Nature* 428:821–827.

1
2
3 962 Zhang Y, Lamarque LJ, Torres-Ruiz JM, Schuldt B, Karimi Z, Li S, Qin DW, Bittencourt P,
4 963 Burlett R, Cao KF, Delzon S, Oliveira R, Pereira L, Jansen S (2018) Testing the plant
5 964 pneumatic method to estimate xylem embolism resistance in stems of temperate
6 965 trees. *Tree Physiol* 38:1016–1025.
7
8
9
10
11
12
13
14
15
16
17
18
19
20
21
22
23
24
25
26
27
28
29
30
31
32
33
34
35
36
37
38
39
40
41
42
43
44
45
46
47
48
49
50
51
52
53
54
55
56
57
58
59
60

For Peer Review

1
2
3 967 **List of Figures**
4
5

6 968 **Figure 1** Stress indicators and hydraulic traits for small trees (1-10 cm DBH) measured in dry
7 969 season oct/2017 on the Control plot and through-fall exclusion (TFE).

9 970 **Figure 2** Hydraulic traits considered by genus for small trees (1-10 cm DBH) surviving after 15 years
10 971 of throughfall exclusion (TFE) and the Control plot.

12 972 **Figure 3** Drought stress indicators and considered by genus for small trees (1-10 cm DBH) surviving
13 973 after 15 years of throughfall exclusion (TFE) and the Control plot.

15 974 **Figure 4** Non-metric multidimensional scaling (NMDS) of drought stress indicators and hydraulic
16 975 traits.

18 976 **Figure 5** Hydraulic traits comparison between small trees and large trees from the throughfall
19 977 exclusion (TFE) and Control plot.

21 978 **Figure 6** Stress indicators comparison between small trees and large trees from throughfall
22 979 exclusion (TFE) and Control plot.

24 980 **Figure 7** Hydraulic traits comparison between small trees and large trees from throughfall
25 981 exclusion (TFE) and Control plot.

27 982 **Tables**

29 983 **Table 1** – Mean and standard deviation from small trees: P_{50} - xylem embolism resistance (MPa);
30 984 P_{88} - xylem embolism resistance (MPa); G_{\min} – minimum stomatal conductance ($\text{mol m}^{-2} \text{s}^{-1}$); K_s –
31 985 maximum hydraulic specific conductivity ($\text{kg m}^{-2} \text{s}^{-1} \text{MPa}^{-1}$); K_{sl} - maximum hydraulic leaf-specific
32 986 conductivity ($\text{kg m}^{-2} \text{s}^{-1} \text{MPa}^{-1}$); $A_L:A_{SW}$ – leaf to sapwood area ratio ($\text{m}^2 \text{m}^{-2}$); W_D - Woody density;
33 987 Ψ_{pd} - predawn water potential (MPa); Ψ_{md} - midday water potential (MPa); HSM – branch hydraulic
34 988 safety margin to P_{50} (MPa); PLC – native dry season percentage loss of conductivity (%), separated
35 989 by genus and treatment.
36
37
38
39
40
41
42
43
44
45
46
47
48
49
50
51
52
53
54
55
56
57
58
59
60

Hydraulic traits												
Genus (n individuals)	Treatment	P ₅₀	P ₈₈	G _{min}	K _s	K _{sl}	A _L :A _{SW}	W _D	Ψ _{pd}	Ψ _{md}	HSM	PLC
<i>Eschweilera</i> (3)	Control	-2.91±0.07	-5.08±0.31	0.028±0.023	1.12±0.19	0.57±0.30	112.07±32.41	0.73±0.12	-0.32±0.23	-1.68±0.24	1.13±0.32	49.14±4.9
<i>Eschweilera</i> (3)	TFE	-3.66±2.01	-6.32±3.80	0.026±0.019	2.80±2.62	4.71±6.12	92.12±65.44	0.59±0.09	-0.52±0.24	-1.87±0.26	1.89±2.28	9.22±4.36
<i>Inga</i> (4)	Control	-4.60±1.63	-7.84±3.10	0.02±0.014	2.3±1.43	1.56±0.85	84.59±47.51	0.64±0.18	-0.37±0.26	-1.51±0.57	3.09±2.07	11.33±10.19
<i>Inga</i> (3)	TFE	-3.48±0.58	-6.22±1.62	0.02±0.006	4.56±1.68	1.93±0.73	160.81±58.68	0.63±0.08	-0.39±0.22	-1.35±0.78	2.13±0.4	19.28±13.21
<i>Licania</i> (4)	Control	-5.28±1.98	-9.62±4.40	0.025±0.014	0.15±0.04	0.12±0.07	66.15±24.41	0.76±0.062	-0.25±0.07	-1.65±0.85	3.62±2.75	38.29±28.52
<i>Licania</i> (4)	TFE	-6.18±1.59	-9.07±1.77	0.024±0.02	2.17±2.19	0.37±0.40	104.90±45.99	0.761±0.014	-0.85±0.81	-1.388±0.78	5.183±1.70	68.667±28.13
<i>Mouriri</i> (3)	Control	-4.77±0.54	-7.69±1.31	0.025±0.017	0.62±0.05	0.22±0.20	154.33±59.51	0.867±0.003	-0.24±0.09	-0.943±0.08	3.829±0.48	58.031±27.65
<i>Mouriri</i> (3)	TFE	-5.55±0.74	-7.35±2.18	0.077±0.022	3.63±3.03	1.32±0.88	143.30±92.13	0.751±0.17	-1.07±1.32	-2.583±0.95	2.972±0.77	60.769±15.83
<i>Ocotea</i> (3)	Control	-3.59±1.49	-8.72±2.63	0.007±0.003	1.63±0.81	0.84±0.17	125.38±54.22	0.638±0.05	-0.36±0.4	-0.6±0.364	2.994±1.26	36.718±18.42
<i>Ocotea</i> (3)	TFE	-5.04±2.08	-8.61±4.88	0.03±0.024	1.58±0.66	0.60±0.46	84.83±32.64	0.68±0.13	-1.44±1.17	-2.41±0.81	2.62±2.45	65.27±24.19
<i>Protium</i> (5)	Control	-2.30±0.71	-4.16±2.40	0.017±0.01	1.68±0.94	0.75±0.41	78.60±6.37	0.74±0.07	-0.31±0.3	-1.23±0.31	1.07±0.78	54.73±17.02
<i>Protium</i> (3)	TFE	-3.64±1.47	-5.65±0.73	0.013±0.01	1.10±0.07	0.44±0.07	90.57±17.71	0.72±0.049	-0.48±0.16	-1.00±0.24	2.55±1.73	49.74±11.94
<i>Swartzia</i> (3)	Control	-3.17±1.28	-5.98±1.89	0.06±0.04	1.67±0.26	0.78±0.55	72.45±18.20	0.73±0.02	-0.23±0.12	-1.57±0.16	1.60±1.36	59.73±9.94
<i>Swartzia</i> (3)	TFE	-4.34±0.57	-6.94±0.06	0.06±0.02	2.78±0.51	0.89±0.54	210.45±67.51	0.72±0.005	-0.79±0.48	-2.36±0.09	1.98±0.66	49.13±8.57
<i>Tetragastris</i> (5)	Control	-2.31±1.48	-4.34±1.81	0.03±0.01	2.22±1.66	2.29±3.12	83.86±59.38	0.64±0.05	-0.28±0.13	-1.06±0.58	1.25±1.31	22.12±15.60
<i>Tetragastris</i> (3)	TFE	-4.36±1.19	-6.52±2.90	0.016±0.01	1.33±0.62	1.04±0.45	88.10±34.28	0.58±0.04	-1.43±0.40	-2.44±0.13	1.92±1.06	43.24±6.33
<i>Vouacapoa</i> (3)	Control	-3.57±0.13	-5.37±1.45	0.015±0.003	1.00±0.16	0.95±0.64	56.71±22.69	0.69±0.13	-0.39±0.18	-1.59±0.19	1.97±0.31	43.78±11.37
<i>Vouacapoa</i> (3)	TFE	-2.22±0.79	-3.54±1.63	0.012±0.004	0.83±0.51	0.67±0.78	229.76±101.26	0.70±0.01	-0.77±0.35	-2.07±0.24	0.15±0.72	33.24±19.67

991 **Table 2** Results of linear mixed effect models of plot (Control versus TFE) on the stress indicators
 992 and hydraulic traits for small trees (1-10 cm DBH) measured in dry season (Oct/2017) on the
 993 Control plot and through-fall exclusion TFE. WD - wood density; AL:ASW - leaf to sapwood area
 994 ratio; P50 - xylem embolism resistance; P88 - xylem embolism resistance; Gmin - minimum
 995 stomatal conductance; Ks - maximum hydraulic specific conductivity; Ksl - maximum hydraulic
 996 leaf -specific conductivity; Ψ_{pd} - predawn water potential; Ψ_{md} - midday water potential. HSM -
 997 branch hydraulic safety margin to P50; PLC - native dry season percentage loss of conductivity. The
 998 table shows the least square means for the Control and TFE, and the random genus effects (see
 999 analysis section in Methods for details). The first row of each trait gives the mean and second row
 1000 gives one standard error for the fixed effects and the 95% confidence interval for genus-level
 1001 random effects. Traits for which plot had a significant effect, and species for which the random
 1002 effects were different from zero, are marked with * ($p < 0.05$), ** ($p < 0.01$) and *** ($p < 0.001$)
 1003 and ns (non-significant).

Variable	Plot-level Coefficients			Genus-level Coefficients							
	Control	TFE	Eschweilera	Inga	Licania	Mouriri	Ocotea	Protium	Swartzia	Tetragastris	Vouacapoa
P₅₀	3.56 (-4.12/-2.99)	-4.26 (-5.761/-2.79) ns	-3.29 (-4.67/-1.91) ***	0.83 (-2.56/0.90)	2.38 (-4.11/-0.65) **	1.87 (-3.65/-0.09) *	-1.03 (-2.81/0.75)	0.60 (-1.13/2.33)	-0.35 (-2.20/1.50)	0.21 (-1.48/1.90)	0.39 (-1.39/2.17)
P₈₈	6.49 (-7.45/-5.42)	-6.58 (-9.34/-4.00) ns	-5.71 (-8.18/-3.24) ***	1.44 (-4.54/1.65)	3.69 (-6.78/-0.59) *	-1.82 (-5.01/1.37)	-2.96 (-6.15/0.22)	1.11 (-1.98/4.21)	-0.66 (-3.97/2.65)	0.54 (-2.48/3.57)	1.25 (-1.94/4.43)
G_{min}	0.027 (0.02/0.03)	0.030 (0.008/0.053) ns	0.03 (0.01/0.04) ***	0.01 (-0.03/0.01)	0.00 (-0.02/0.02)	0.03 (0.01/0.05) **	-0.01 (-0.03/0.01)	-0.01 (-0.03/0.01)	0.04 (0.02/0.06) ***	0.00 (-0.02/0.02)	-0.01 (-0.03/0.01)

		1.46	2.32	1.79	1.48	-0.49	0.34	-0.19	-0.33	0.33	0.17	-0.88
	K_s	(0.95/2.00)	(0.98/3.64) *	(0.46/3.13) **	(-0.28/3.23)	(-2.24/1.26)	(-1.47/2.15)	(-2.00/1.63)	(-2.03/1.38)	(-1.56/2.22)	(-1.58/1.92)	(-2.69/0.93)
		1.00	1.22	2.23	0.51	-1.96	-1.45	-1.51	-1.59	-1.41	-0.29	-1.42
	K_{sl}	(0.45/1.55)	(0.21/2.58) ns	(0.86/3.61) **	(-2.31/1.29)	(-3.76/-0.17)	(-3.31/0.40)	(-3.37/0.35)	(-3.34/0.16)	(-3.35/0.54)	(-2.09/1.50)	(-3.28/0.44)
		90.77	131.70	104.09	13.17	-18.57	44.73	1.02	-21.00	23.56	-18.64	39.15
	A_L:A_{sw}	(69.76/110.74)	(81.14/183.50) **	(48.95/159.23) ***	(-59.03/85.37)	(-88.86/51.73)	(-29.93/119.39)	(-73.64/75.68)	(-91.29/49.29)	(-54.42/101.54)	(-88.93/51.65)	(-35.52/113.81)
		0.71	0.68	0.68	0.03	0.09	0.13	-0.01	0.06	0.05	-0.05	0.03
	W_D	(0.68/0.75)	(0.59/0.78) ns	(0.60/0.75) ***	(-0.14/0.07)	(-0.01/0.19)	(0.03/0.24) **	(-0.12/0.10)	(-0.04/0.16)	(-0.06/0.16)	(-0.15/0.06)	(-0.08/0.13)
		0.31	0.86	-0.42	0.04	0.13	0.24	0.48	-0.03	0.03	0.29	0.17
	Ψ_{pd}	(0.14/0.48)	(0.63/1.52) ***	(-0.05/0.90)	(-0.69/0.61)	(-0.50/0.76)	(-0.44/0.91)	(-0.19/1.15)	(-0.66/0.60)	(-0.67/0.74)	(-0.34/0.92)	(-0.51/0.84)
		1.29	1.93	-1.78	0.34	-0.26	-0.02	-0.27	-0.63	0.11	-0.20	0.05
	Ψ_{md}	(1.09/1.54)	(1.50/2.19) **	(1.19/2.37) ***	(-1.14/0.46)	(-1.03/0.52)	(-0.85/0.81)	(-1.10/0.56)	(-1.41/0.14)	(-0.76/0.98)	(-0.98/0.57)	(-0.78/0.88)
		2.25	2.35	1.52	1.16	2.77	1.88	1.29	-0.02	0.24	-0.02	-0.46
	HSM	(1.64/2.86)	(0.74/3.96) ns	(0.05/2.99) *	(-0.69/3.01)	(0.93/4.62) **	(-0.02/3.78)	(-0.61/3.19)	(-1.87/1.83)	(-1.74/2.21)	(-1.82/1.79)	(-2.36/1.45)
		41.315	45.82	33.18	18.44	22.47	26.22	17.82	19.68	22.31	-4.01	5.33
	PLC	(32.38/49.21)	(24.14/67.78) ns	(15.62/50.74) ***	(-41.43/4.56)	(-0.52/45.47)	(2.44/50.00) *	(-5.96/41.60)	(-2.70/42.07)	(-2.52/47.15)	(-27.79/19.77)	(-18.45/29.11)

1004

1005

Table 3. Results of linear mixed effect models of size (Large versus Small) on the stress indicators and hydraulic traits for small trees (1-10 cm DBH) and large trees (>20 cm DBH) measured in dry season (Oct/2017) on the Control plot and through-fall exclusion TFE. WD - wood density; AL:ASW - leaf to sapwood area ratio; P50 - xylem embolism resistance; P88 - xylem embolism resistance; Gmin - minimum stomatal conductance; Ks - maximum hydraulic specific conductivity; Ksl - maximum hydraulic leaf -specific conductivity; Ψ_{pd} - predawn water potential; Ψ_{md} - midday water potential. HSM - branch hydraulic safety margin to P50; PLC - native dry season percentage loss of conductivity. The table shows the least square means for the Control and TFE, and the random genus effects (see analysis section in Methods for details). The first row of each trait gives the mean and second row gives one standard error for the fixed effects and the 95% confidence interval for genus-level random effects. Traits for which plot had a significant effect, and species for which the random effects were different from zero, are marked with * ($p < 0.05$), ** ($p < 0.01$) and *** ($p < 0.001$) and ns (non-significant).

Variable	Plot-level Coefficients		Genus-level Coefficients				
	Large	Small	Eschweilera	Inga	Licania	Protium	Swartzia
P ₅₀	-2.66 (-3.24/-2.08)	-4.06 (-5.20/-2.93) ***	-2.654 (-3.382/-1.926) ***	-0.824 (-1.798/0.150) ns	-1.526 (-2.540/-0.513) **	0.014 (-0.985/1.013) ns	-0.593 (-1.592/0.406) ns
P ₈₈	-4.83 (-5.87/-3.80)	-7.08 (-9.18/-5.02) ***	-4.83 (-6.16/-3.49) ***	-1.35 (-3.13/0.44) ns	-2.53 (-4.39/-0.67) **	0.21 (-1.62/2.04) ns	-1.02 (-2.85/0.81) ns
G _{min}	0.08 (0.06/0.09)	0.02 (0.007/0.06) ***	0.07482 (0.053/0.09) ***	-0.01930 (-0.049/0.010) ns	-0.02935 (-0.05941/0.00071) *	-0.03583 (-0.066/-0.005) *	0.01851 (-0.011/0.048) ns
K _s	4.60 (2.20/5.58)	2.10 (1.09/4.33) ***	3.88 (2.59/5.16) ***	1.98 (0.28/3.68) *	-2.81 (-4.69/-0.94) **	-0.90 (-2.64/0.83) ns	-0.30 (-2.11/1.52) ns
K _{sl}	6.13 (5.06/7.19)	5.00 (3.09/6.89) *	4.35 (3.42/5.28) ***	0.90 (-0.41/2.21)	1.55 (0.24/2.86) **	1.56 (0.29/2.83) **	2.98 (1.69/4.28) ***
W _D	0.70 (0.61/0.70)	0.60 (0.52/0.67) ***	0.63 (0.59/0.67) ***	0.01 (-0.04/0.06) ns	0.05 (0.00/0.11) *	-0.05 (-0.11/0.00) *	0.05 (-0.01/0.10) ns
Ψ_{pd}	-0.44 (-0.50/-0.38)	-0.44 (-0.61/-0.28) ns	-0.48 (-0.59/-0.36) ***	0.04 (-0.12/0.20) ns	0.09 (-0.07/0.25) ns	-0.05 (-0.21/0.11) ns	0.08 (-0.08/0.24) ns
Ψ_{md}	-1.75 (-2.04/-1.46)	-1.50 (-1.98/-1.02) **	-1.85 (-2.07/-1.63) ***	0.17 (-0.12 to 0.47) ns	0.54 (0.24/0.84) ***	0.41 (0.11/0.71) ***	-0.23 (-0.54/0.08) ns
HSM	0.90	2.70	0.92	0.97	1.96	0.21	0.27

1
2
3
4
5
6
7
8
9
10
11
12
13
14
15
16
17
18
19
20
21
22
23
24
25
26
27
28
29
30
31
32
33
34
35
36
37
38
39
40
41
42
43
44
45
46

	(1.09/2.32)	(1.32/3.91)***	(0.10/1.74) **	(-0.13/2.08) ns	(0.82/3.11) ***	(-0.92/1.34) ns	(-0.85/1.40) ns
PLC	19.50	42.03	19.19	-4.71	12.90(-2.14/27.94) ns	20.93	16.15
	(8.91/30.75)	(23.13/60.94)***	(8.87/29.50) ***	(-18.36/8.93) ns		(7.02/34.84) **	(1.56/ 30.74) *

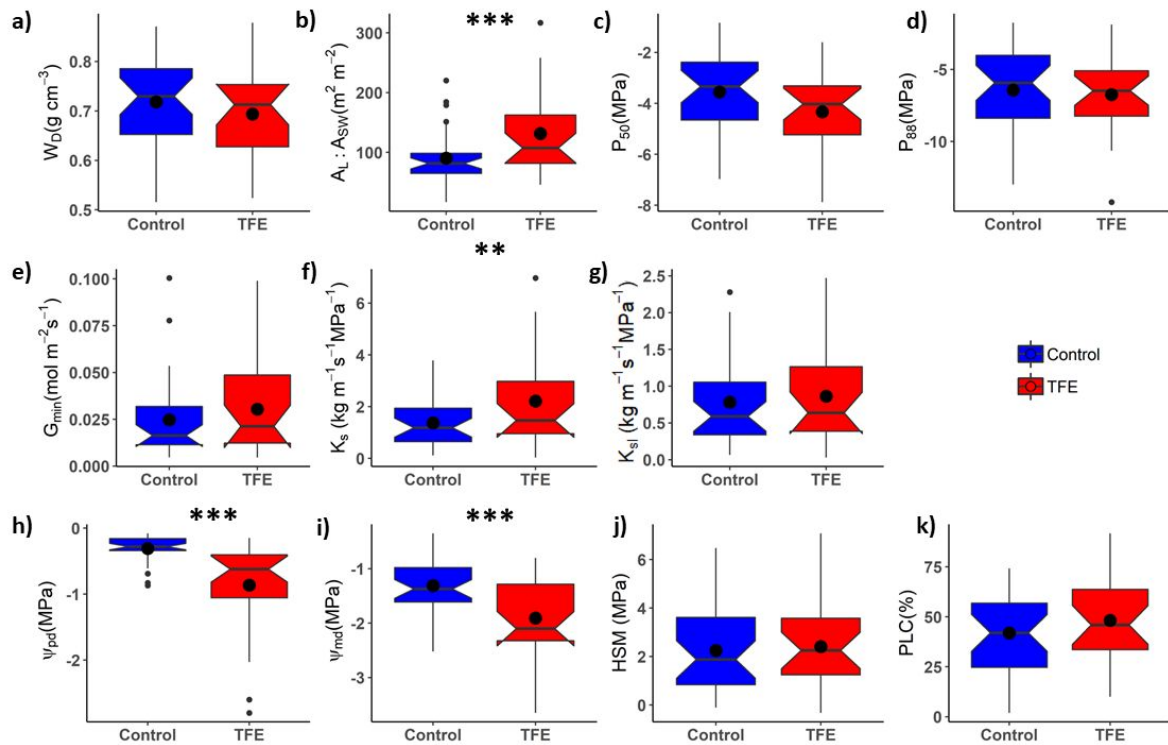
For Peer Review

1020

1021

Figures

1022



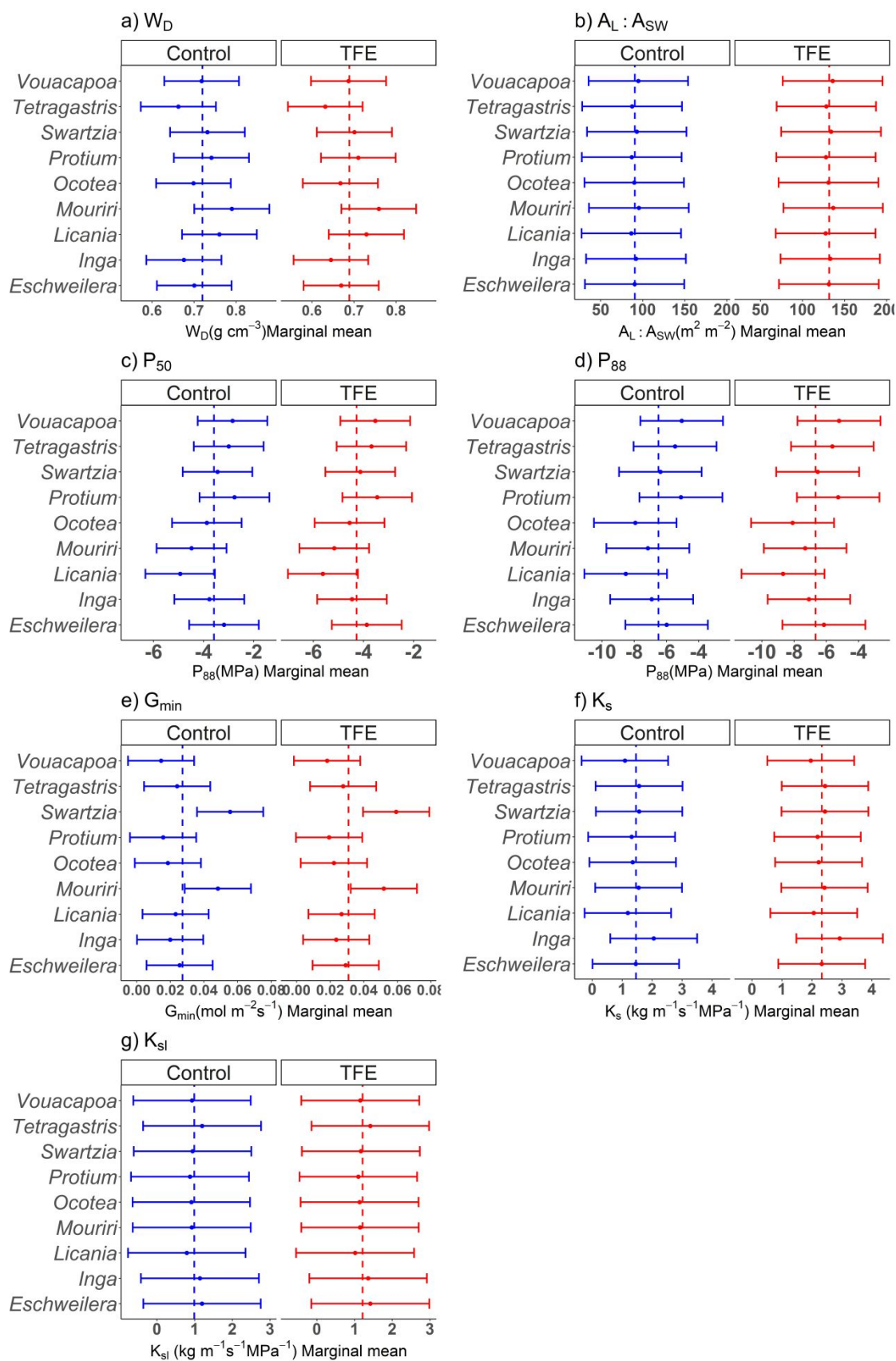
1023

1024 **Figure 1** Stress indicators and hydraulic traits for small trees (1-10 cm DBH) measured in dry season
 1025 oct/2017 on the Control plot (blue) and through-fall exclusion (TFE, red). a) W_D – wood
 1026 density b) $A_L:A_{SW}$ - leaf to sapwood area ratio c) P_{50} - xylem embolism resistance; d) P_{88} - xylem
 1027 embolism resistance; e) G_{min} – minimum stomatal conductance; f) K_s – maximum hydraulic specific
 1028 conductivity; g) K_{sl} - maximum hydraulic leaf -specific conductivity; h) Ψ_{pd} - predawn water
 1029 potential; i) Ψ_{md} - midday water potential. j) HSM – branch hydraulic safety margin to P_{50} ; l) PLC –
 1030 native dry season percentage loss of conductivity. The boxes represent quartiles 1 and 3, the
 1031 central line indicates the median and the black points the mean of each treatment. Whiskers are
 1032 either maximum value or 1.5 interquartile range above quartile 3, if outliers are present and
 1033 notches represents a confidence interval around the median represented by central line. Traits for
 1034 which plot had a significant effect are marked with * ($p < 0.05$), ** ($p < 0.01$) and *** ($p < 0.001$).
 1035 P-values are from mixed effects analysis (see Table 2 for models and analysis section in Methods

1036

1037

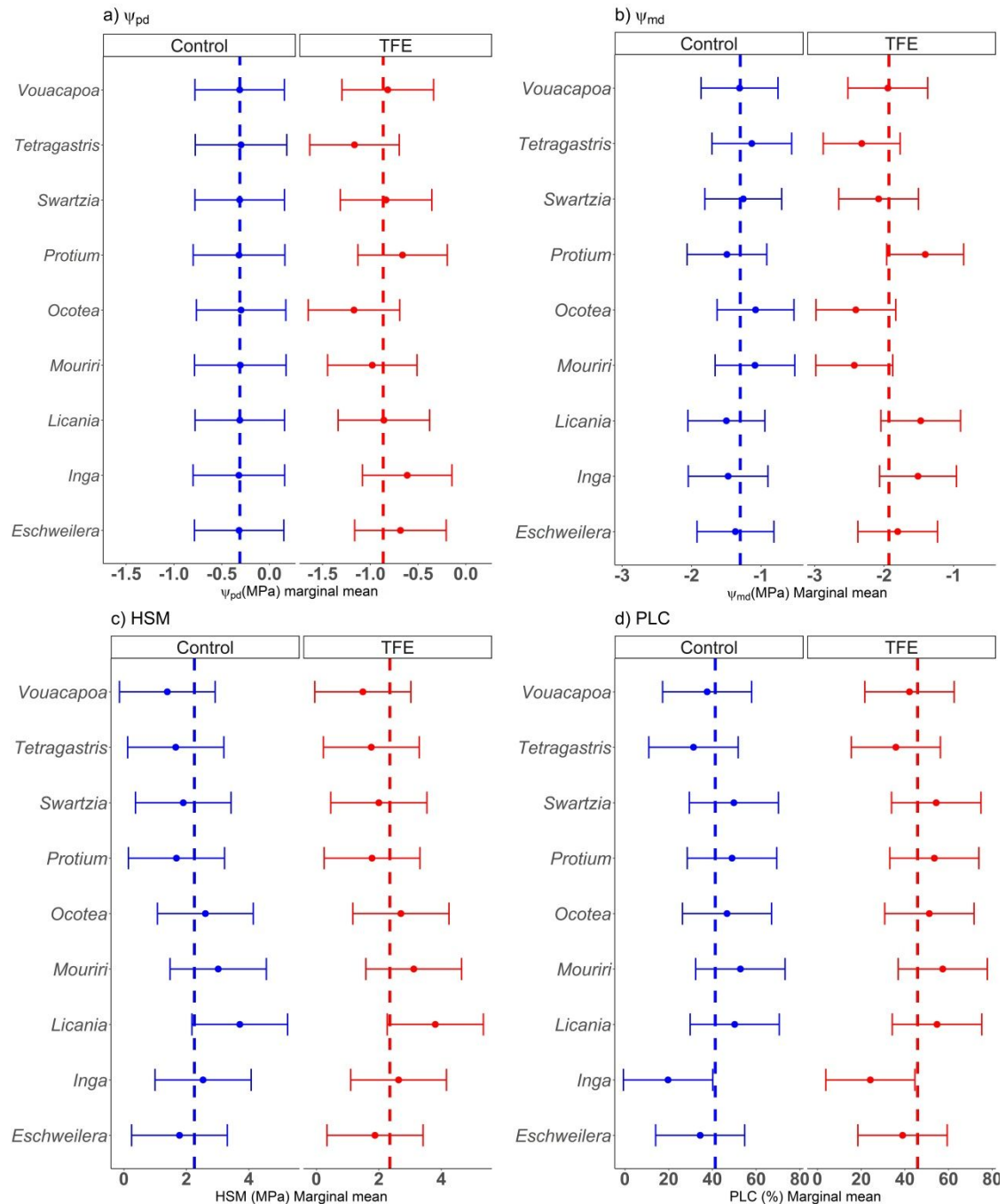
1038



1039

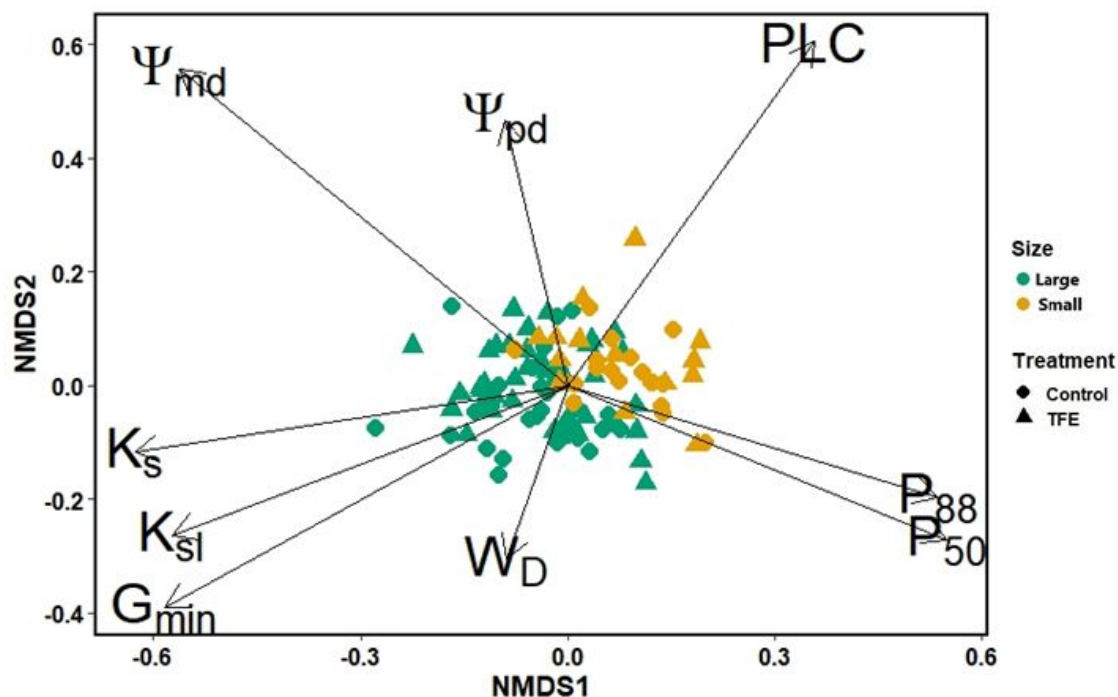
1040 **Figure 2** Hydraulic traits by genus for small trees (1-10 cm DBH) surviving after 15 years of
 1041 throughfall exclusion (TFE – red) and the Control plot (blue). a) W_D - wood density b) $A_L:A_{SW}$ - leaf
 1042 to sapwood area ratio c) P_{50} - xylem embolism resistance; d) P_{88} - xylem embolism resistance; e)

1043 G_{\min} - minimum stomatal conductance; f) K_s - maximum hydraulic specific conductivity; g) K_{sl} -
 1044 maximum hydraulic leaf -specific conductivity. The vertical dashed coloured lines represent the
 1045 marginal fixed effects for plot. The points represent random effects plus fixed effect mean by
 1046 genus and the horizontal lines represents standard error for each genus (see Table 2 for models
 1047 and analysis section in Methods).



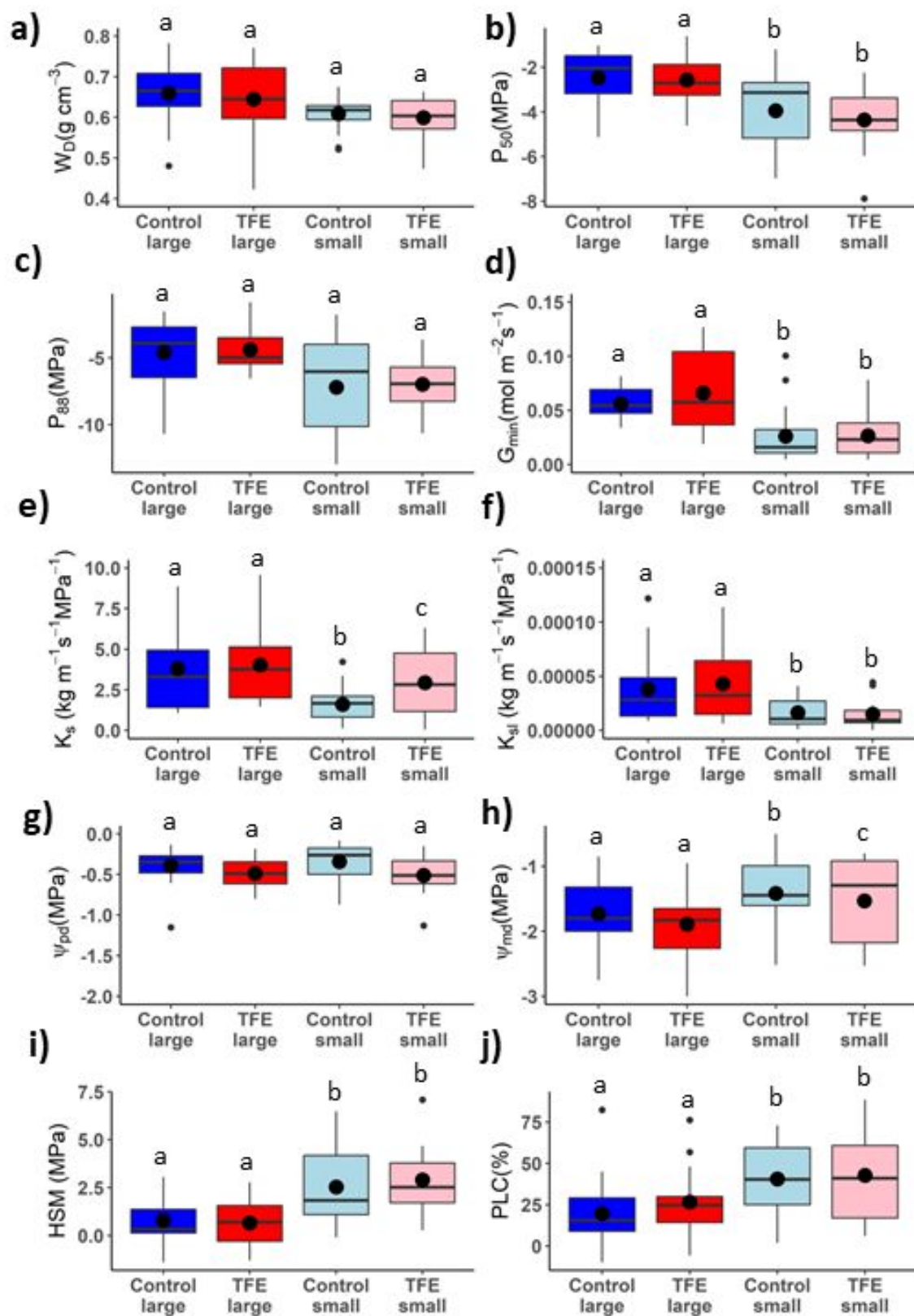
1048
 1049 **Figure 3** Drought stress indicators considered by genus for small trees (1-10 cm DBH) surviving
 1050 after 15 years of throughfall exclusion (TFE – red) and the Control plot (blue). a) Ψ_{pd} - predawn
 1051 water potential; b) Ψ_{md} - midday water potential. c) HSM – branch hydraulic safety margin to P_{50} ;
 1052 d) PLC – native dry season percentage loss of conductivity. The vertical dashed lines represents
 1053 marginal fixed effects for plot, the points represents random effects plus fixed effect mean by
 1054 genus and the horizontal lines represents standard error by genus (see Table 2 for models and
 1055 analysis section in Methods).

1056



1057

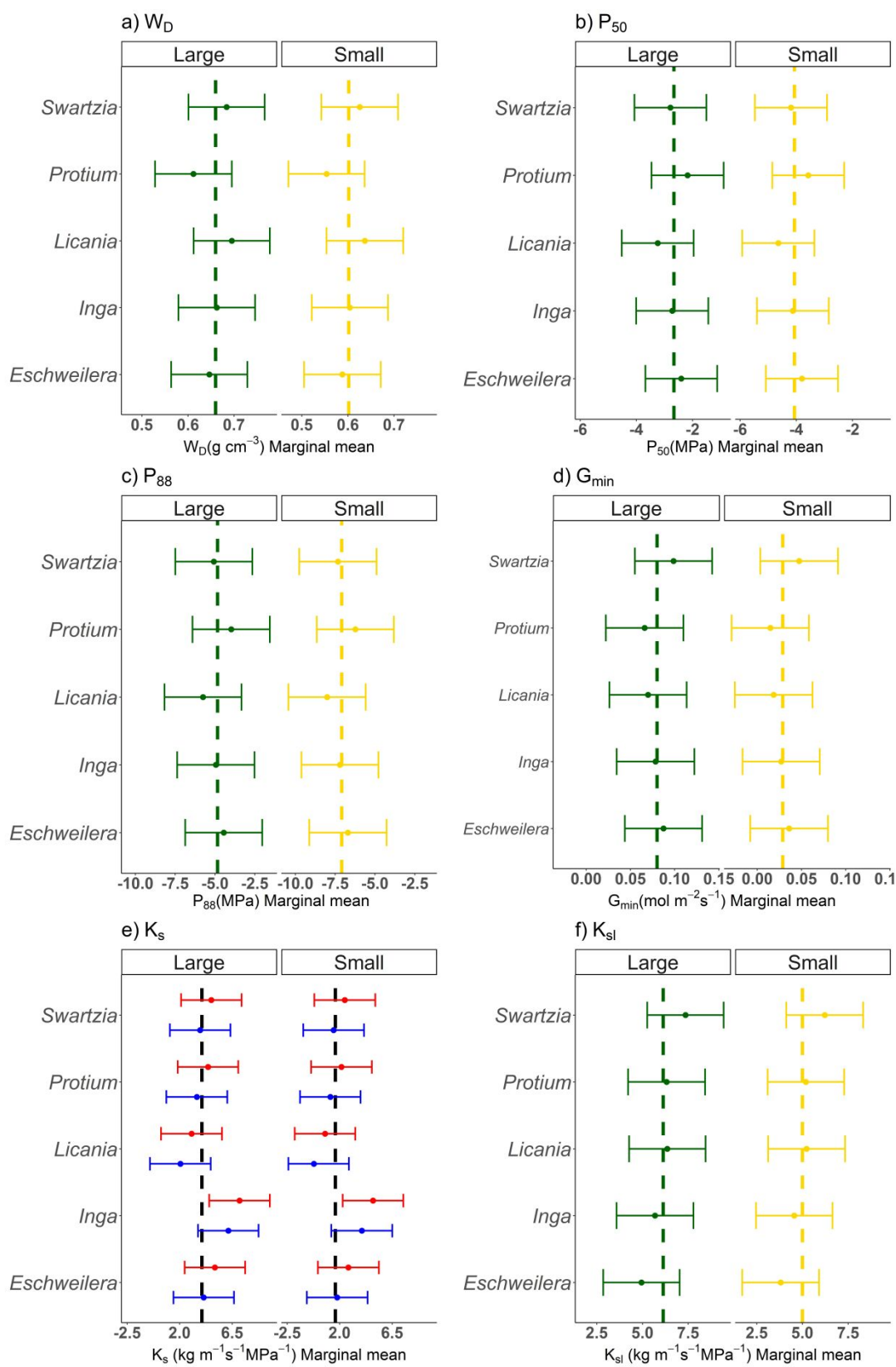
1058 **Figure 4** Non-metric multidimensional scaling (NMDS) of drought stress indicators and hydraulic
 1059 traits. Ordination showing multidimensional space filled by small (yellow) and large (green) trees
 1060 indicating distinct hydraulic ecological strategies (MANOVA; $P < 0.05$) between trees from the TFE
 1061 and Control. Hydraulic traits represented by arrows (Arrow length represent predictor “strength”).
 1062 Dots represent individuals in Control and triangles individuals in TFE treatment. The green colour
 1063 represents large trees and yellow represents small trees.



1064

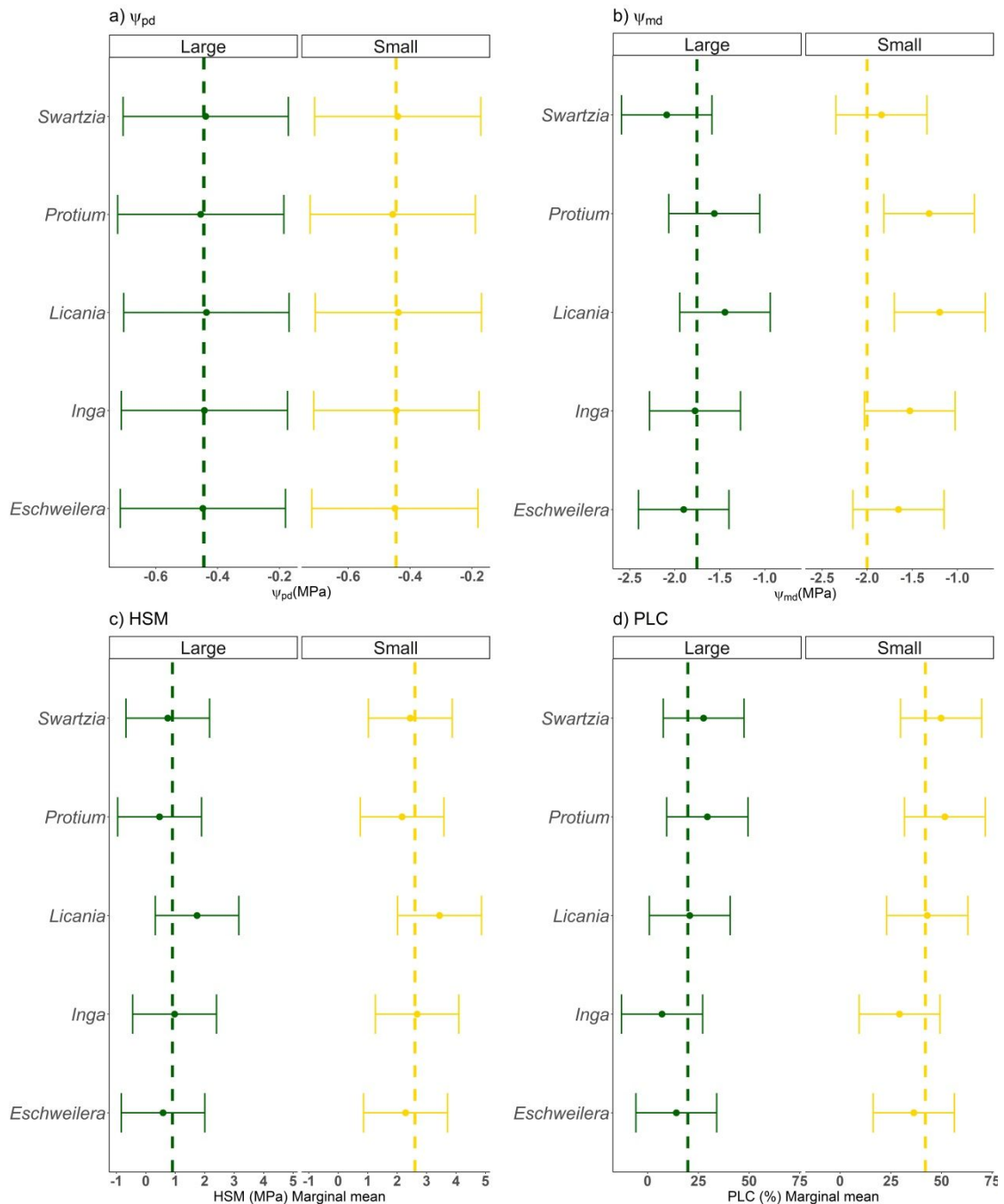
1065 **Figure 5** Comparison between small trees and large trees from the throughfall exclusion (TFE) and
 1066 Control plots. a) W_D – wood density; b) P_{50} - xylem embolism resistance; c) P_{88} - xylem embolism
 1067 resistance; d) G_{\min} – minimum stomatal conductance; e) K_s – maximum hydraulic specific
 1068 conductivity; f) K_{sl} - maximum hydraulic leaf -specific conductivity; g) Ψ_{pd} - predawn water
 1069 potential; h) Ψ_{md} midday water potential; i) HSM – branch hydraulic safety margin to P_{50} ; j) PLC –

1070 native dry season percentage loss of conductivity. The boxes represent quartiles 1 and 3, the
 1071 central line indicates the median and the black points the mean of each treatment. Whiskers are
 1072 either maximum value or 1.5 interquartile range above the quartile 3, when outliers are present.
 1073 Different letters indicate significant differences within each graph, $p < 0.05$.



1074

1
2
3 1075 **Figure 6** Hydraulic traits comparison between small trees and large trees from throughfall
4 1076 exclusion (TFE) and Control plot. a) W_D – wood density; b) P_{50} - xylem embolism resistance; c) P_{88} -
5 1077 xylem embolism resistance; d) G_{min} – minimum stomatal conductance; e) K_s – maximum hydraulic
6 1078 specific conductivity; f) K_{sl} - maximum hydraulic leaf-specific conductivity. The vertical dashed lines
7 1079 represents marginal fixed effect mean, green vertical lines represents large trees and yellow
8 1080 vertical lines, the points represents random plus fixed effect mean by each level (by genus)
9 1081 and the horizontal lines represents standard error by each random effects level. The blue and red in
10 1082 horizontal lines represents Control and TFE plot, respectively and are show when a significant plot
11 1083 effect was found. All points and lines represent genus in each treatment (see Table 3 for models
12 1084 and analysis section in Methods).



1085

1086 **Figure 7** Drought stress indicators comparison between small trees and large trees from
1087 throughfall exclusion (TFE) and Control plot. a) Ψ_{pd} - predawn water potential; b) Ψ_{md} - midday

1
2
3 1088 water potential. c) HSM – branch hydraulic safety margin to P50; d) PLC – native dry season
4 1089 percentage loss of conductivity. The vertical dashed lines represents marginal fixed effect mean,
5 1090 the points represents random effects plus fixed effect mean by each level (by genus) and the
6 1091 horizontal lines represents standard error by each random effects level. All points and lines
7 1092 represent genus in each treatment. P-values are from mixed effects analysis (see Table 3 for
8 1093 models and analysis section in Methods).
9
10
11
12
13
14
15
16
17
18
19
20
21
22
23
24
25
26
27
28
29
30
31
32
33
34
35
36
37
38
39
40
41
42
43
44
45
46
47
48
49
50
51
52
53
54
55
56
57
58
59
60

For Peer Review

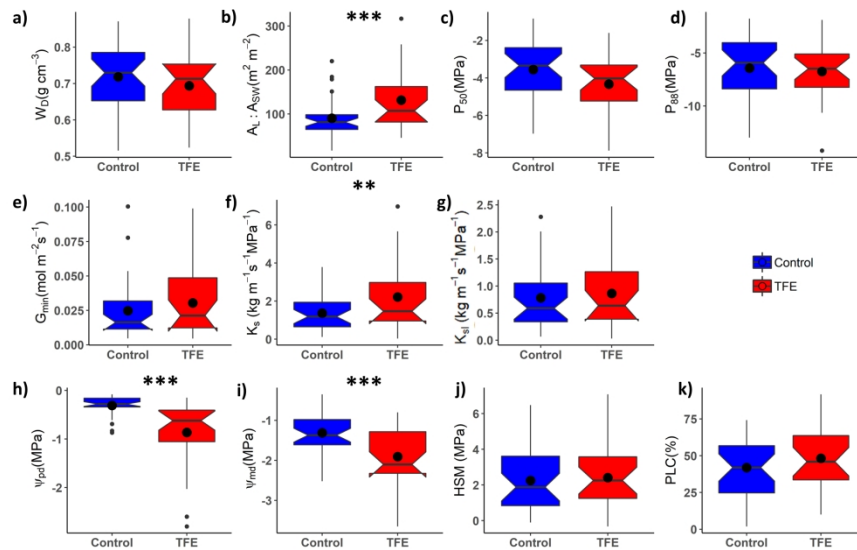


Figure 1 Stress indicators and hydraulic traits for small trees (1-10 cm DBH) measured in dry season oct/2017 on the Control plot (blue) and through-fall exclusion (TFE, red). a) WD – wood density b) AL:ASW – leaf to sapwood area ratio c) P50 – xylem embolism resistance; d) P88 – xylem embolism resistance; e) Gmin – minimum stomatal conductance; f) Ks – maximum hydraulic specific conductivity; g) Ksl – maximum hydraulic leaf -specific conductivity; h) Ψ_{pd} – predawn water potential; i) Ψ_{md} – midday water potential. j) HSM – branch hydraulic safety margin to P50; l) PLC – native dry season percentage loss of conductivity. The boxes represent quartiles 1 and 3, the central line indicates the median and the black points the mean of each treatment. Whiskers are either maximum value or 1.5 interquartile range above quartile 3, if outliers are present and notches represents a confidence interval around the median represented by central line. Traits for which plot had a significant effect are marked with * ($p < 0.05$), ** ($p < 0.01$) and *** ($p < 0.001$). P-values are from mixed effects analysis (see Table 2 for models and analysis section in Methods).

338x190mm (230 x 230 DPI)

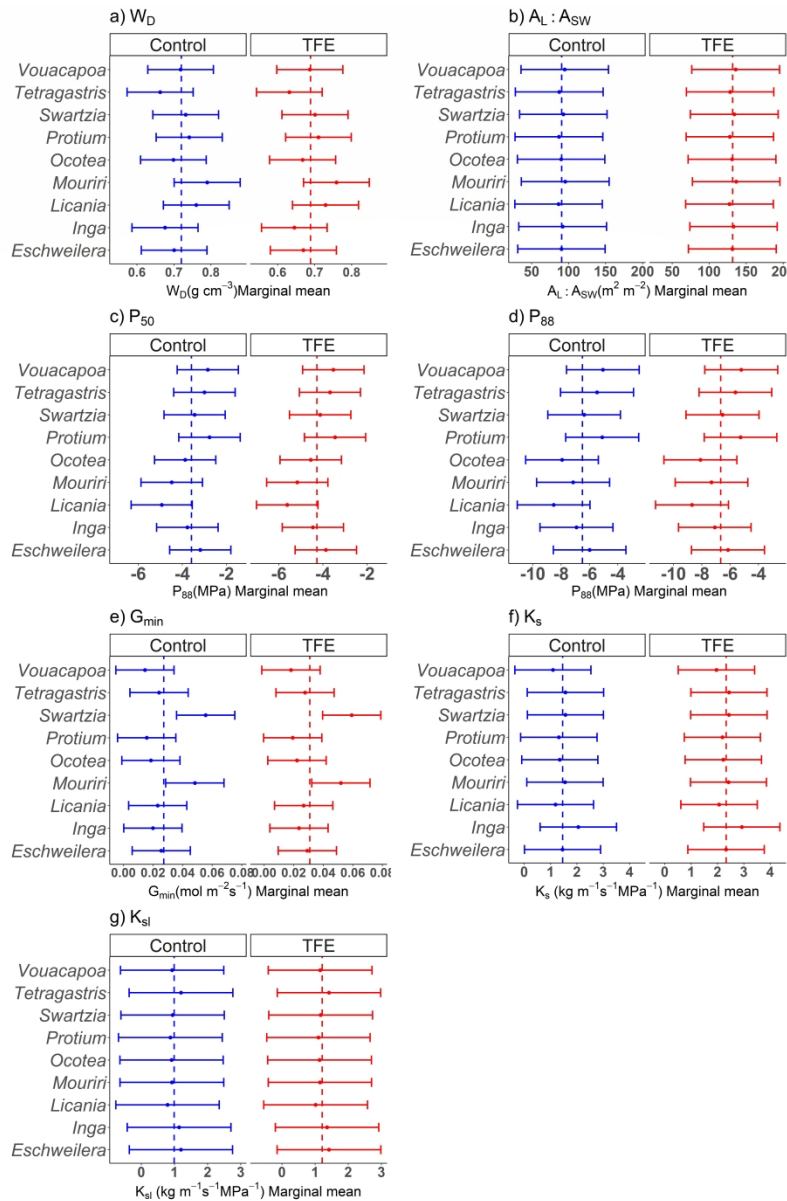


Figure 2 Hydraulic traits by genus for small trees (1-10 cm DBH) surviving after 15 years of throughfall exclusion (TFE – red) and the Control plot (blue). a) WD - wood density b) AL:ASW - leaf to sapwood area ratio c) P50 - xylem embolism resistance; d) P88 - xylem embolism resistance; e) Gmin - minimum stomatal conductance; f) Ks - maximum hydraulic specific conductivity; g) Ksl - maximum hydraulic leaf -specific conductivity. The vertical dashed coloured lines represent the marginal fixed effects for plot. The points represent random effects plus fixed effect mean by genus and the horizontal lines represents standard error for each genus (see Table 2 for models and analysis section in Methods).

1312x1969mm (96 x 96 DPI)

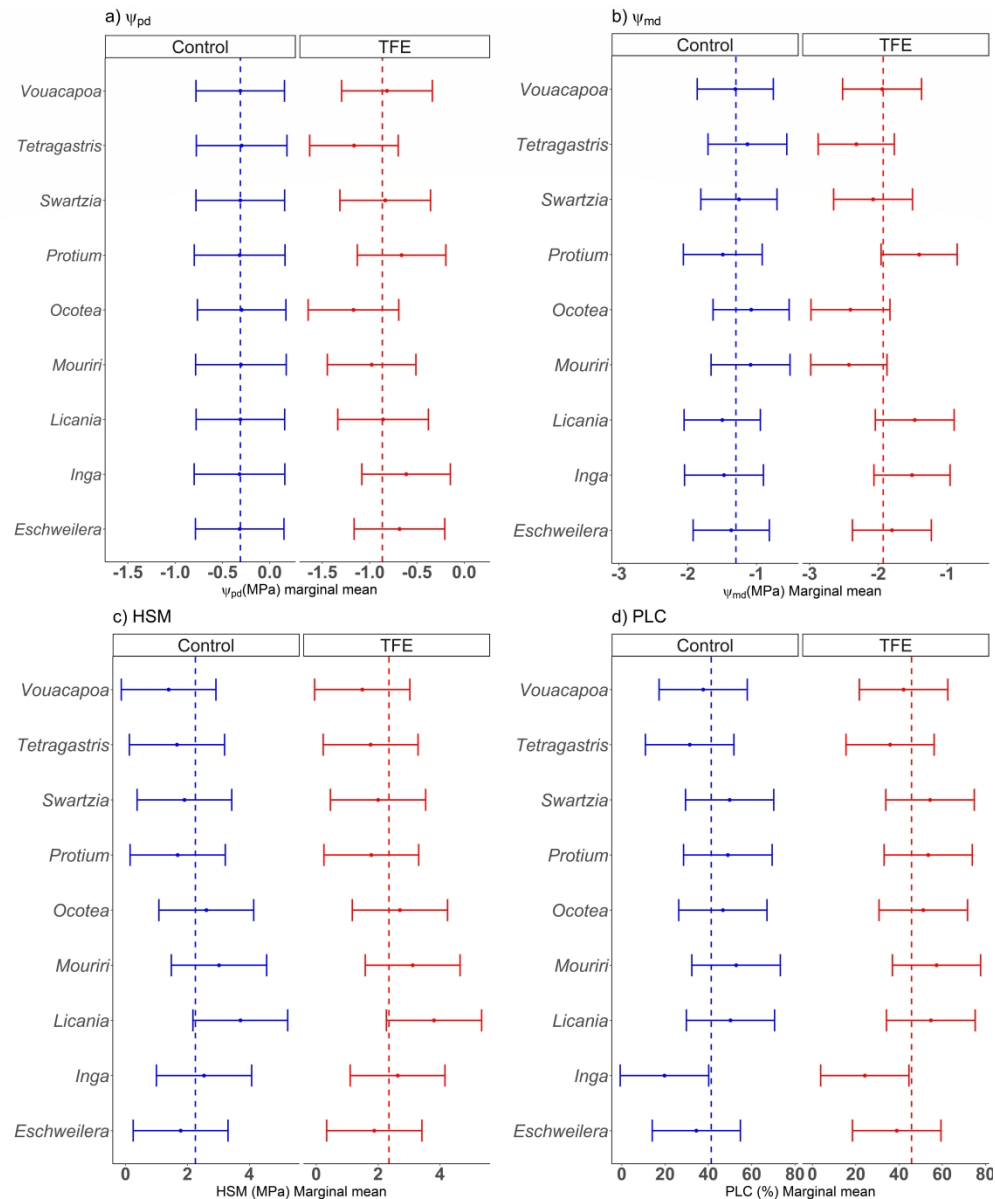


Figure 3 Drought stress indicators considered by genus for small trees (1-10 cm DBH) surviving after 15 years of throughfall exclusion (TFE – red) and the Control plot (blue). a) Ψ_{pd} - predawn water potential; b) Ψ_{md} - midday water potential. c) HSM – branch hydraulic safety margin to P50; d) PLC – native dry season percentage loss of conductivity. The vertical dashed lines represents marginal fixed effects for plot, the points represents random effects plus fixed effect mean by genus and the horizontal lines represents standard error by genus (see Table 2 for models and analysis section in Methods).

1467x1761mm (96 x 96 DPI)

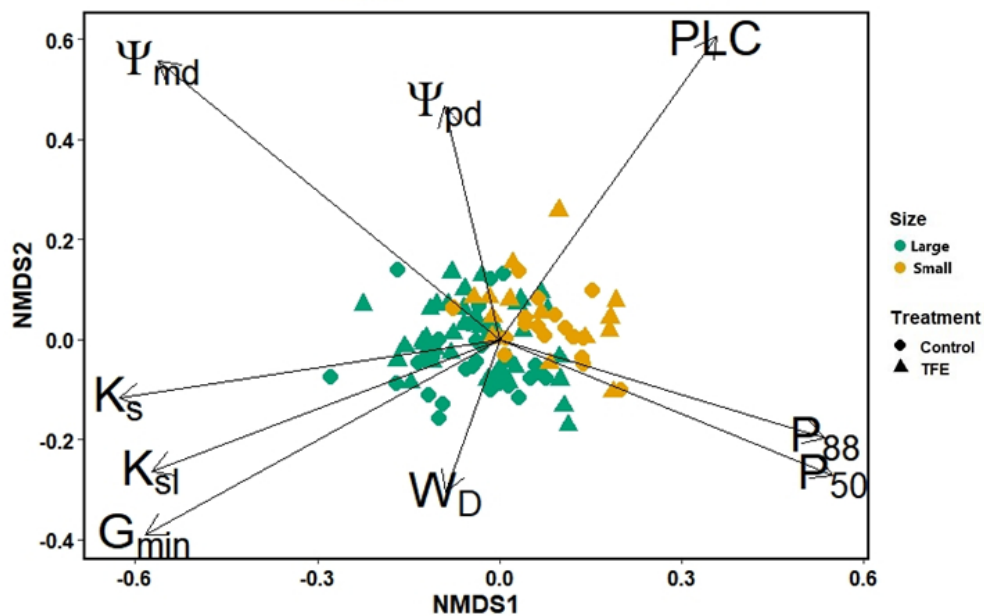


Figure 4 Non-metric multidimensional scaling (NMDS) of drought stress indicators and hydraulic traits. Ordination showing multidimensional space filled by small (yellow) and large (green) trees indicating distinct hydraulic ecological strategies (MANOVA; $P < 0.05$) between trees from the TFE and Control. Hydraulic traits represented by arrows (Arrow length represent predictor "strength"). Dots represent individuals in Control and triangles individuals in TFE treatment. The green colour represents large trees and yellow represents small trees.

190x125mm (96 x 96 DPI)

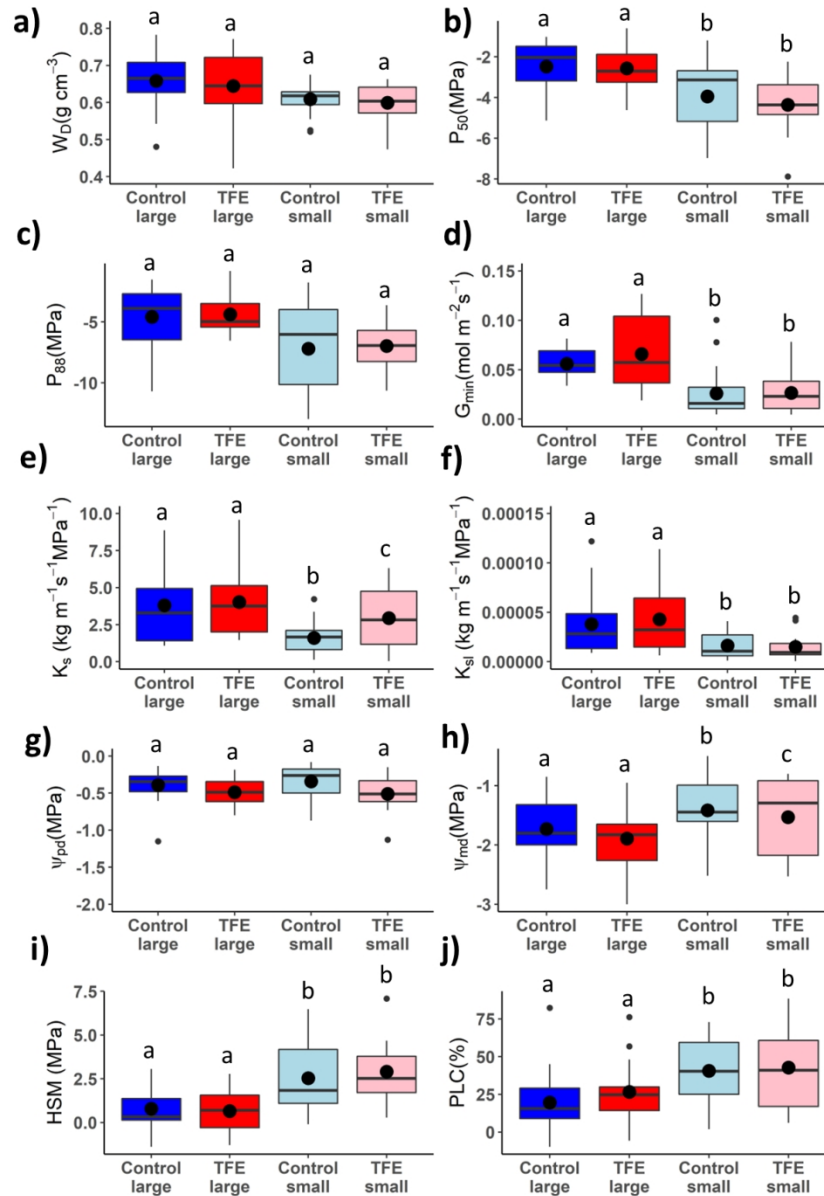


Figure 5 Comparison between small trees and large trees from the throughfall exclusion (TFE) and Control plots. a) W_d – wood density; b) P50 - xylem embolism resistance; c) P88 - xylem embolism resistance; d) G_{min} – minimum stomatal conductance; e) K_s – maximum hydraulic specific conductivity; f) K_{sl} - maximum hydraulic leaf -specific conductivity; g) Ψ_{pd} - predawn water potential; h) Ψ_{md} midday water potential; i) HSM – branch hydraulic safety margin to P50; j) PLC – native dry season percentage loss of conductivity. The boxes represent quartiles 1 and 3, the central line indicates the median and the black points the mean of each treatment. Whiskers are either maximum value or 1.5 interquartile range above the quartile 3, when outliers are present. Different letters indicate significant differences within each graph, $p < 0.05$.

321x456mm (96 x 96 DPI)

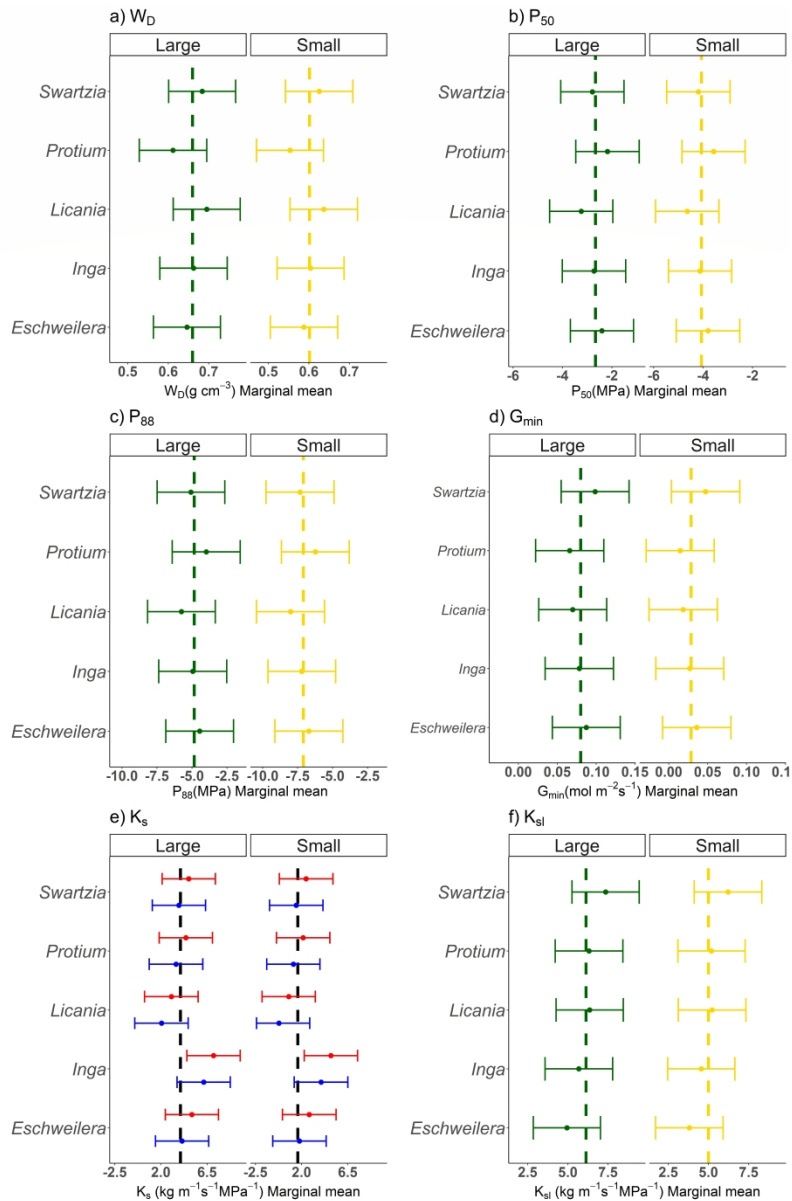


Figure 6 Hydraulic traits comparison between small trees and large trees from throughfall exclusion (TFE) and Control plot. a) W_D – wood density; b) P_{50} - xylem embolism resistance; c) P_{88} - xylem embolism resistance; d) G_{min} – minimum stomatal conductance; e) K_s – maximum hydraulic specific conductivity; f) K_{sl} - maximum hydraulic leaf-specific conductivity. The vertical dashed lines represents marginal fixed effect mean, green vertical lines represents large trees and yellow vertical lines, the points represents random plus fixed effect mean by each level (by genus) and the horizontal lines represents standard error by each random effects level. The blue and red in horizontal lines represents Control and TFE plot, respectively and are show when a significant plot effect was found. All points and lines represent genus in each treatment (see Table 3 for models and analysis section in Methods).

1312x1969mm (96 x 96 DPI)

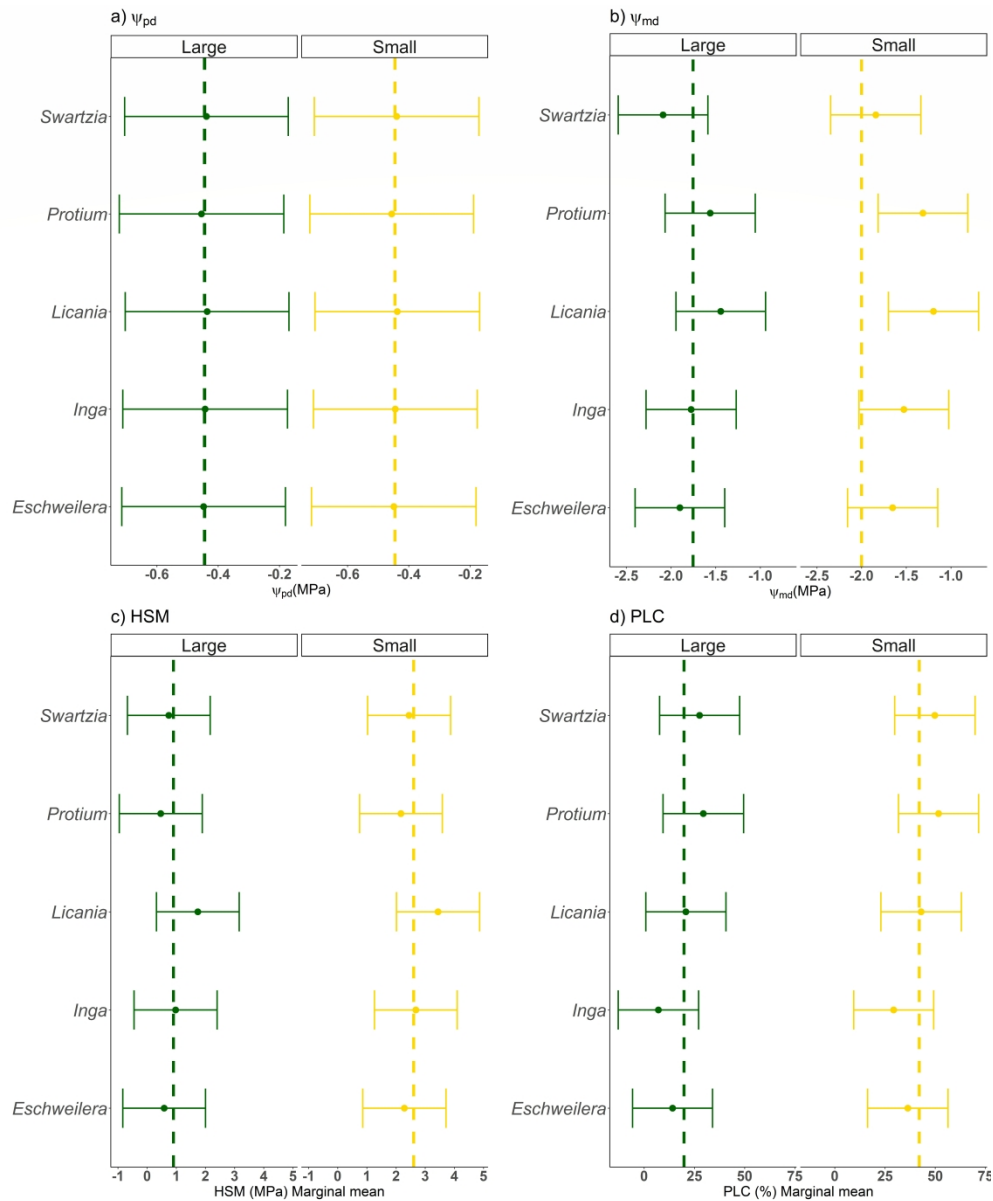


Figure 7 Drought stress indicators comparison between small trees and large trees from throughfall exclusion (TFE) and Control plot. a) Ψ_{pd} - predawn water potential; b) Ψ_{md} - midday water potential. c) HSM - branch hydraulic safety margin to P50; d) PLC - native dry season percentage loss of conductivity. The vertical dashed lines represents marginal fixed effect mean, the points represents random effects plus fixed effect mean by each level (by genus) and the horizontal lines represents standard error by each random effects level. All points and lines represent genus in each treatment. P-values are from mixed effects analysis (see Table 3 for models and analysis section in Methods).

1467x1761mm (96 x 96 DPI)

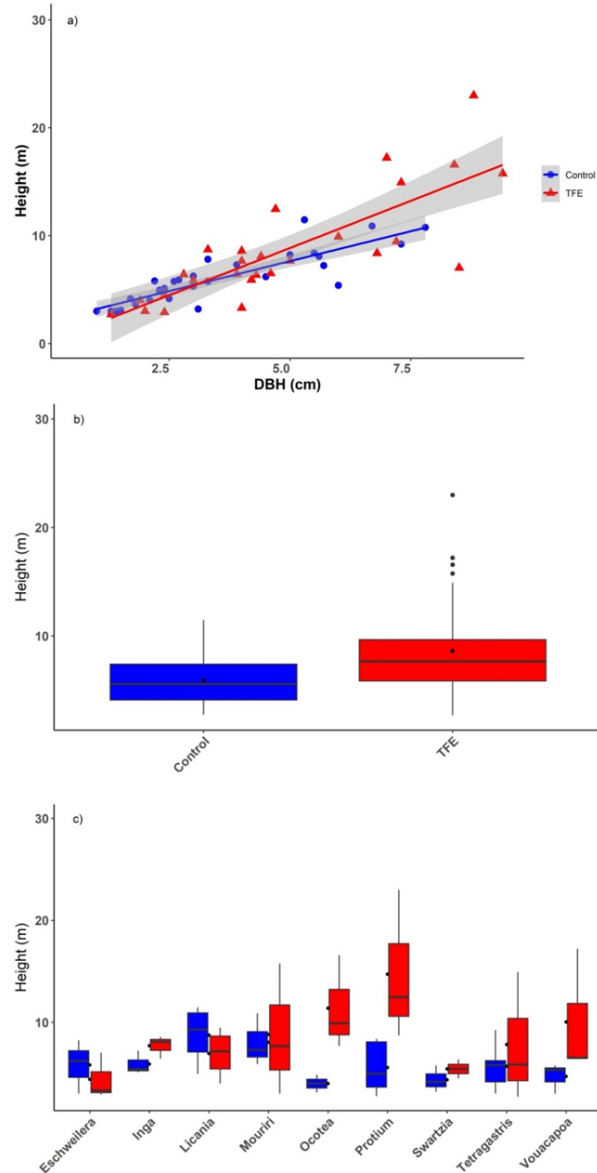


Figure S1. Height and diameter in each treatment (TFE vs. Control) and by genus for the most common small tree genera in this study (9 genera). a) The significant relationship between diameter (DBH) and Height by treatment ($F=48.61$; $R^2=0.72$; $p\text{-value}<0.001$), b) Height of Small trees by treatment c) Height of Small trees by genus. The box represents quartiles 1 and 3, with the central line indicating the median. Whiskers are either maximum value or 1.5 interquartile range above the quartile 3, when outliers are present.

228x341mm (96 x 96 DPI)

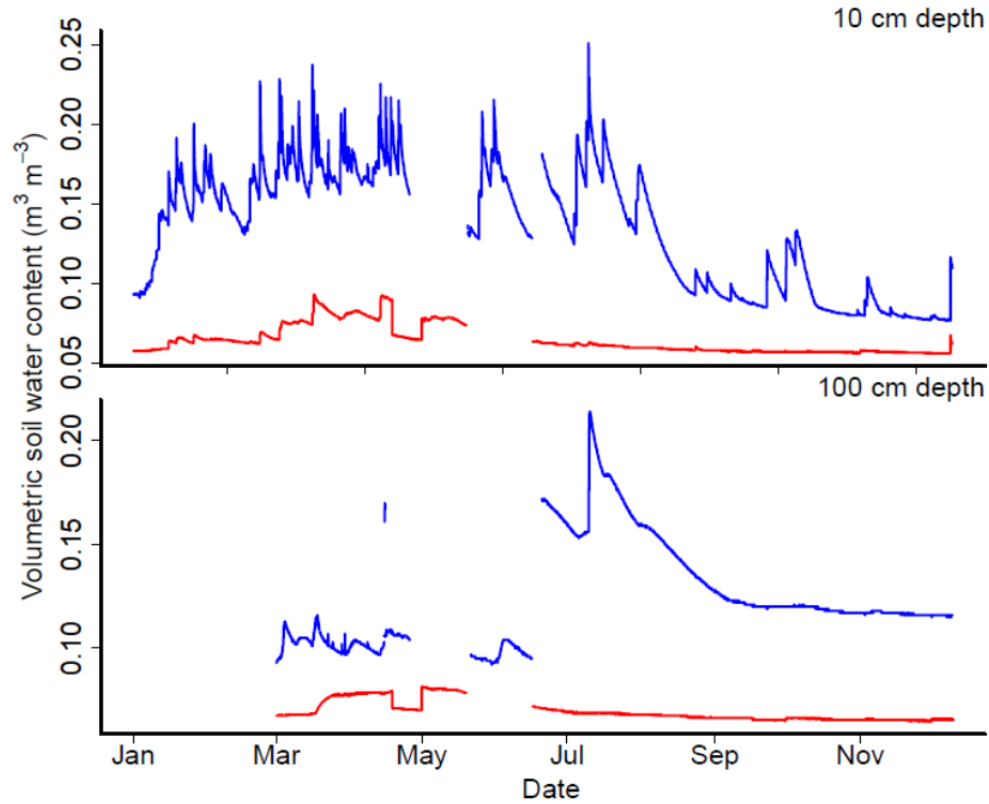


Figure S2. Soil water content during 2016 in the Throughfall Exclusion Experiment plot (red) and in the Control plot (blue) at 10 cm and at 100 cm depth adapted from Bittencourt et al. 2020. The TFE had a mean reduction, in relation to Control, of 48% and 56% in soil water content at 10 cm and 100 cm depth, respectively. Data are missing for periods when sensors failed.

247x201mm (96 x 96 DPI)

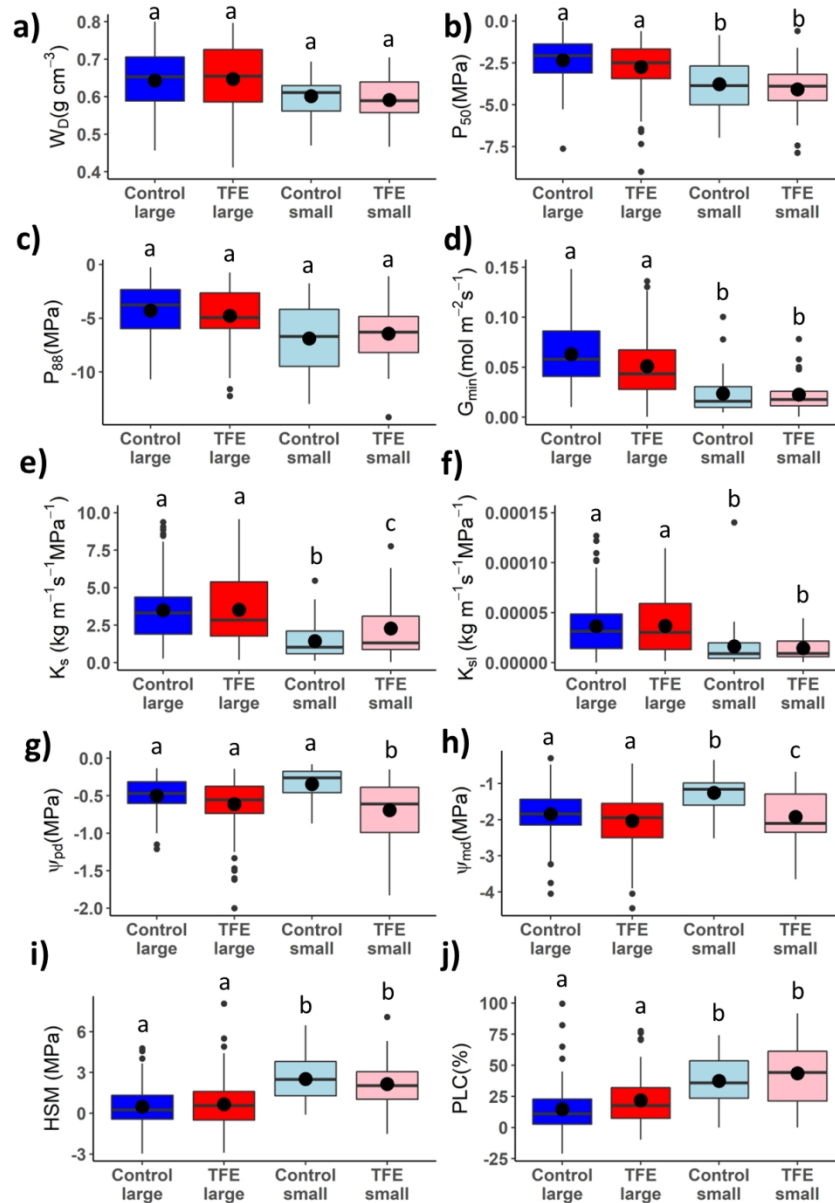


Figure S3- Comparison between the small trees and large trees from the throughfall exclusion (TFE) and Control plots from grouping all 9 genera available within the large and small tree groupings. Note that four of these genera were not present in both of the large and small tree groupings, and were thus excluded from Figure 3. a) W_D – wood density; b) P_{50} – xylem embolism resistance (MPa); c) P_{88} – xylem embolism resistance; d) G_{min} – minimum stomatal conductance; e) K_s – maximum hydraulic specific conductivity; f) K_{sl} – maximum hydraulic leaf -specific conductivity; g) Ψ_{pd} – predawn water potential; h) Ψ_{md} midday water potential; i) PLC – native dry season percentage loss of conductivity; j) HSM – hydraulic safety margin to P_{50} . The box represents quartiles 1 and 3, with the central line indicating the median. Whiskers are either maximum value or 1.5 interquartile range above the quartile 3, when outliers are present. Different letter indicant significant differences, $p < 0.001$.

325x456mm (96 x 96 DPI)